COMPUTATION OF
GROUNDWATER CONTAMINATION
BY USING MODFLOW

119651

A Thesis Submitted to the
Graduate School of Natural and Applied Sciences of
Dokuz Eylül University
In Partial Fulfillment of the Requirements for
the Degree of Master of Science in Civil Engineering,
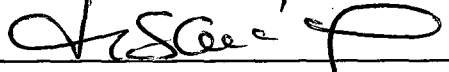**Hydraulics, Hydrology and Water Resources Program**

by
Ayşegül ÖZGENÇ

July, 2002
İZMİR

Ms.Sc. THESIS EXAMINATION RESULT FORM

We certify that we have read the thesis, entitled "COMPUTATION OF GROUNDWATER CONTAMINATION BY USING MODFLOW" completed by Ayşegül ÖZGENÇ under supervision of Prof. Dr. M. Şükrü GÜNEY and that in our opinion it is fully adequate, in scope and in quality, as a thesis for the degree of Master of Science.

Prof. Dr. M. Şükrü GÜNEY

Supervisor

Prof. Dr. Yüksel K. Birsoy

Committee Member

Doç. Dr. Sevinç ÖZKUL

Committee Member

Approved by the

Graduate School of Natural and Applied Sciences

Prof.Dr.Cahit Helvacı

Director

ACKNOWLEDGMENTS

I would like thank my supervisor Prof. Dr. M. Şükrü GÜNEY for his guidance and his support during the development of this project.

ABSTRACT

Groundwater is the source for drinking water for many people around the world. Virtually all the homes that supply their own water have wells and use groundwater. So the quality of groundwater is of paramount importance.

In such cases the groundwater has been contaminated by the acts of humans. In addition to providing for the sustenance of human life, groundwater has important ecological functions. Many freshwater habitats are supplied by the discharge of springs. If the groundwater supplying these springs is contaminated, the ecological function of the freshwater habitat can be impaired.

The wastes of industrial plants which are located near the groundwater sources are the common reason of groundwater contamination.

In this thesis groundwater contamination model is applied to the Harmandalı Sanitary Landfill Area and to a heterogeneous aquifer by using the PMWIN MODFLOW. The numerical results obtained from the computer program are discussed.

ÖZET

Dünyadaki birçok yerde yeraltısuyundan içme suyu olarak yararlanılmaktadır. Sularını kendileri temin eden insanlar kuyulara sahip olup yeraltısuyundan yararlanmaktadırlar. Bu nedenle yeraltısuyu kalitesi büyük bir öneme sahiptir.

İnsanlar kendi kullandıkları yeraltısuyunu bazı durumlarda kirletmektedirler. İnsan hayatının devamını sağlamaya ilave olarak yeraltısuyunun önemli çevre etkileşim işlevleri vardır. Birçok yerleşim yeri pınarlardan elde edilen suyla beslenmektedir. Bu pınarları besleyen yeraltısuyu kirlenirse; bu yeraltısuyunun çevresel etkileşimi zarar görecektir.

Yeraltısuyu kaynaklarına yakın yerleşmiş sanayi tesisleri yeraltısuyu kirliliğinin başta gelen sebeplerindendir.

Bu tez çalışmasında yeraltısuyu kirlilik modeli, Harmandalı Düzenli Atık Depolama Tesisi ve heterojen bir akifer için PMWIN MODFLOW programı kullanılarak uygulanmıştır. Programdan elde edilen sayısal sonuçlar tartışılmıştır.

CONTENTS

Chapter One
INTRODUCTION

Chapter Two
THEORY OF CONTAMINANT TRANSPORT

Chapter Three
NUMERICAL MODELING OF CONTAMINANT TRANSPORT

Chapter Four
PROCESSING MODFLOW FOR WINDOWS (PMWIN)

Chapter Five
RESULTS FOR HARMANDALI SANITARY LANDFILL AREA

Chapter Six
RESULTS FOR HETEREGENOUS AQUIFER WITH HIGH PERMEABILITY

Chapter Seven
COMPARISON OF RESULTS AND CONCLUSION

LIST OF TABLES

LIST OF FIGURES

CHAPTER ONE
INTRODUCTION

1.1. Groundwater Contamination

Contaminant transport modeling generally is performed to evaluate the potential impact of contaminant migration causing hazardous results which are vital in municipal areas. The results of the modeling evaluations are used to design of remedial strategies in the case of existing pollution and to assess the probable contamination in the case of new waste disposal.

The physical processes governing contaminant transport are advection, diffusion, dispersion, adsorption, biodegradation and chemical reaction.

1.2. Previous Studies in this Subject

The aim of field efforts in the mid 1980s was to quantify dispersion , adsorption and biodegradation mechanisms. These processes are the focus of a lot of studies at many hazardous-waste research sites. One of the most successful field sites for tracer studies is the Borden landfill site in Canada , from which a lot of important papers on dispersion and adsorption processes measured during a 2-year field experiment have been published (Mackay , 1986; Roberts , 1986). Le Blanc (1991) described a natural gradient tracer experiment performed at Otis Air Base on Cape Cod, Massachusetts. In this study more than 30000 samples were analyzed over a 2-year period.

Borden and Bedient (1986), Rifai (1988) and Berry-Spark and Barker (1987) have modeled the biodegradation of contaminant plumes associated with naphthalene and benzene-related compounds in ground water and obtained some success on measuring it.

The models of transport mechanisms into ground water for the prediction and evaluation of waste sites have been described in many references over the past three decays. Some of the earliest efforts are presented in Bear (1972), Bredehoeft and Pinder (1973) , Fried (1975), Anderson (1979), Bear (1979) and Freeze and Cherry (1979). Domenico and Schwartz (1990), Mercer (1990), Anderson and Woessner (1992) and Fetter (1993) provided discussion of some of the more complex flow and transport issues.

Oktay Güven (1983) presented a study involving a basis for understanding the phenomenon of scale-dependent dispersion within a deterministic framework. The results of that study are used as a basis to define a scale-dependent macro-dispersion coefficient for unidirectional flow in a stratified aquifer.

D.M. Mackay, D.L. Freyberg, and P.V. Roberts represented, for each process thought to influence significantly the transport and fate of dissolved contaminants, the key hypotheses that require field validation in 1986. They described an experiment designed to address the identified needs, they evaluated its success in creating a well-defined initial condition and in providing detailed and accurate monitoring data on solute concentration and distribution for a period of 3 years.

David L. Freyberg presented 'Spatial moments and the Advective and Dispersion of Nonreactive Tracers' in 1986. The three-dimensional movement of a tracer plume containing bromide and chloride is investigated using the data base from a large-scale natural gradient field experiment on ground water solute transport.

Paul V. Roberts, Mark N. Goltz and Douglas M. Mackay (1986) examined the long-term behavior of five organic solutes during transport over a period of 2 years in ground water under natural gradient conditions. This behavior was characterized quantitatively by means of moment estimates.

A new approach to the description of site characterization which accounts for variability in a systematic way represented by Dennis Mclaughlin, Lynn B. Reid, Shu-Guang Li and Jennifer Hyman in 1993. The site characterization procedure extracts more information from limited data by combining field measurements with prediction from a stochastic groundwater model. The model provides prior estimates of the mean and standard deviation of solute concentration throughout a contaminated site. These estimates are updated whenever new measurements of hydraulic conductivity, head, and/or concentration become available. The updated concentration standard deviation estimates may be used to guide the placement of sampling wells and to evaluate the accuracy of the site characterization. If updating and data collection are carried out sequentially, over a series of discrete sampling rounds, the sampling network can evolve in response to new information.

Neupauer and Wilson (1999) developed a formal mathematical approach for obtaining the backward probability model by using the adjoint method. The model has been developed for one- and multi-dimensional domains, homogeneous and heterogeneous aquifers, conservative and reactive solutes, and one or more observations. The multiple observations can be at one location at different times, at different locations at the same time, or at different locations at different times. The information from the additional detections reduce the variance of the probability density function; thus providing a better characterization of the source of contamination. The modeling approach was tested using data from a trichloroethylene plume at the Massachusetts Military Reservation.

How easily metals such as cobalt, copper and lead travel through the environment depends on the compounds they form in the soil and how these dissolve in water. New work by researchers at the University of California, Davis, and Olin College in 2002; showed a simple way to work out the stability and solubility of a whole class of clay-like compounds called hydrotalcites. The finding should help geochemists make much better estimates of soil contamination.

Hydrotalcites are layered compounds that form when metals combine with aluminum oxides and hydroxides in the soil. By understanding how easily hydrotalcites form from various metals, scientists can predict how much of the metal stays dissolved in groundwater and how fast it can spread.

Hydrotalctites are "garbage bags" with a layered structure that can take up many metals, nitrates and other chemicals, said William Casey, a professor of land, air and water resources at UC Davis and one of the authors of the study.

Rama Allada, a graduate student in the Nanophases in the Environment, Agriculture and Technology (NEAT) initiative at UC Davis, measured the energy needed to form three cobalt-aluminum hydrotalcites. The team then developed a simple model to predict the corresponding results for other hydrotalcites containing different metals.

With some further measurements, the model could be used to make predictions about the solubility of a wide range of environmental contaminants, such as chromium, said UC Davis professor Alexandra Navrotsky, Allada's thesis supervisor and an author on the paper. The same methods could also be used to study contamination with radioactive wastes such as carbon, iodine and technetium isotopes, Casey said.

Hillary Berbeco, an assistant professor at Olin College in Needham, Mass., conducted the difficult synthesis of the hydrotalcites used to establish the model.

1.3. Scope of This Study

Groundwater contamination is an increasing problem for the countries. Wastes which are thrown away at industrial plants cause pollution of groundwater and soil. This pollution menaces the human health.

The aim of this study is to investigate the groundwater contamination by means of the computer program based on powerful numerical solution techniques.

The rate and direction of contaminant in different case studies are examined by the Processing MODFLOW program which is a simulation system for modeling groundwater flow and pollution.

In the first chapter, definition of groundwater contamination and the previous studies about this subject are given.

Contamination transport mechanisms and basic equations of contaminant transport are presented in the second chapter.

In the third chapter, various numerical solution methods are reviewed.

The fourth chapter contains explanations about the MODFLOW software.

Data about Harmandalı Sanitary Landfill Area and numerical results of Processing MODFLOW are represented in the fifth chapter.

In the sixth chapter presents numerical results for heterogeneous aquifer with high permeability.

The comparison and interpretations of the numerical results are given in the seventh chapter also the seventh chapter include the conclusion.

CHAPTER TWO
THEORY OF CONTAMİNANT
TRANSPORT

2.1. Contaminant Transport Mechanisms

2.1.1. Advection Processes

The movement of a contaminant with the flowing groundwater according to the seepage velocity in the pore space is referred to as advection.

$$v_x = \frac{k}{n} \frac{dh}{dL} \qquad (2.1)$$

where v_x is the seepage velocity, k is the hydraulic conductivity, n is the porosity, h is the hydraulic head and L denotes the aquifer thickness.

The average linear velocity, or seepage velocity, is less than the microscopic velocities of water molecules moving along individual flow paths, because of tortuosity. The one-dimensional mass flux (F_x) due to advection is expressed as follows:

$$F_x = v_x \, n \, C \qquad (2.2)$$

Some advective models include the concept of arrival time by integration along known streamlines (Nelson,1977). Streamline models are used to solve for arrival times of particles that move along the streamlines at specified velocities , usually in a two-dimensional flow net. Others have set up an induced flow field through injection or pumping and evaluated breakthrough curves by numerical integration along flow lines. Dispersion is not directly considered in this models, but results from the variation of velocity and arrival times in the flow field   (Charbeneau,1981,1982). In cases where pumping of groundwater dominates the flow field, it may be useful to neglect dispersion processes without loss of accuracy. (Bedient, Rifai, Newell; 1994).

2.1.2.   Diffusion and Dispersion Processes

The   molecular-scale process which causes spreading due to concentration gradients and random motion is called diffusion. Solute in water is moving from an area of higher concentration to an area of lower concentration. Diffusive transport can occur when there is no velocity . Mass transport in the subsurface due to diffusion in one dimension can be described by the following equation:

$$f_x = -D_d \frac{dC}{dx} \qquad (2.3)$$

which is known as Fick's first law of diffusion.

In this equation f_x = mass flux $(M/L^2/T)$

D_d = diffusion coefficient (L^2/T)

dC/dx = concentration gradient $(M/L^3/L)$

Typical values of D_d are relatively constant and range from $1 \ast 10^{-9}$ to $2 \ast 10^{-9}$ m^2/sec at 25 ^{0}C. Typical dispersion coefficients in groundwater are several orders of magnitude larger and tend to dominate the spreading process when velocities are present. Figure 2.1 shows the resulting concentration versus time response measured at the end of a column loaded continuously with tracer at relative concentration of

C/C₀=1. This curve is called the breakthrough curve. If there were no dispersion, the shape of the breakthrough curve would be identical to the step input function. (Bedient, Rifai, Newell; 1994).
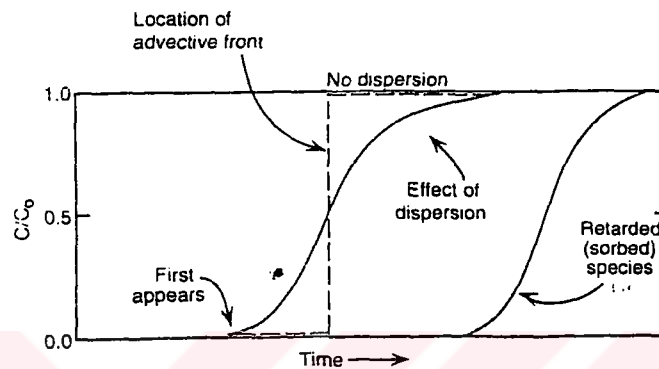
Figure 2.1 Breakthrough curves in one dimension showing effects of dispersion and retardation.

(Bedient, Rifai, Newell; 1994)

Dispersion is due to heterogeneities in the medium that create variations in flow velocities and flow paths. These variations are due to friction within a single pore channel, to velocity differences from one channel to another , or to variable path lengths. Laboratory column studies have shown that dispersion is a function of average linear velocity and a factor called dispersivity, α. Dispersivity in a soil column is on the order of centimeters, while values in field studies may be on the order of one to thousands of meters. Figure 2.2 shows the factors causing longitudinal dispersion (D_x) of a contaminant in the porous media. In most cases involving a two-dimensional plume of contamination , D_y is much less than D_x and the shape of the plume tends to be elongated in the direction of flow.

Pore Size   Path Length

Friction in Pore
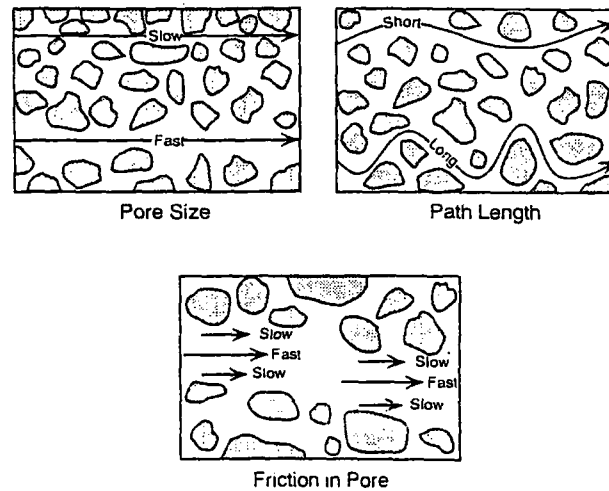
Figure 2.2   Factors causing longitudinal dispersion.

(Bedient, Rifai, Newell; 1994)

Two dimensional dispersion causes spreading in the longitudinal (x) and transverse (y) directions both ahead of and lateral to the advective front. Figure 2.3 depicts the normal shape of such a plume in two dimensions compared to advection alone. Longitudinal dispersion causes spreading and decreases concentrations near the frontal portions of the plume. The main difference with the one-dimensional soil column results described is that two-dimensional plumes have transverse spreading , which reduces concentrations everywhere behind the advective front. (Bedient, Rifai, Newell;1994).

Source

(a)

Source

(b)
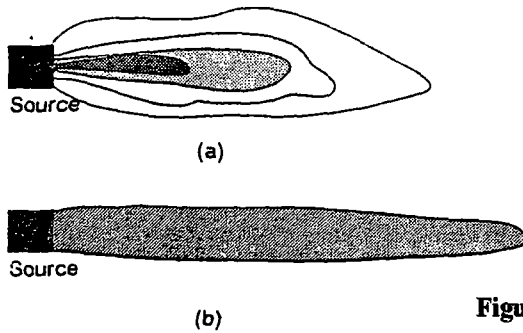
Figure 2.3 (a) Advection and dispersion.
(b) Advection only.

(Bedient, Rifai, Newell; 1994)

2.2. Basic Equations of Contaminants Transport

2.2.1. Mass-Transport Equations

If there is a uniform flow field where $v_x = \tilde{v}_x =$ constant , and $v_y = 0$, dispersive flux is assumed proportional to the concentration gradient in the x direction:

$$f_{x^*} = n \, C \, v_{x^*} = - \, n \, D_x \, \partial C/\partial x \qquad (2.4)$$

where D_x is the longitudinal dispersion coefficient , n is the effective porosity , and C is concentration of contaminant tracer. Similarly the dispersive flux f_{y^*} is expressed as:

$$f_{y^*} = n \, C \, v_{y^*} = - \, n \, D_y \, \partial C/\partial y \qquad (2.5)$$

In the case of a simple uniform flow field with average linear (seepage) velocity $\tilde{v}_x$,

$$D_x = \alpha_x \, \tilde{v}_x \qquad (2.6)$$

$$D_y = \alpha_y \, \tilde{v}_x \qquad (2.7)$$

may be written. In the last equations α_x and α_y are the longitudinal and transverse dispersivities, respectively.

2.2.2. Derivation of the Advection-Dispersion Equation for Solute Transport :

The solute transport in groundwater is based on the law of the conservation of mass. The derivation is based on those of Ogata (1970) and Bear (1972) and is presented in Freeze and Cherry(1979). The following assumptions are made: the porous medium is homogenous, isotropic and saturated; it is also assumed that the flow is steady and Darcy's law applies.

In figure 2.4, the components of specific discharge v are denoted by v_x, v_y, v_z and those of the average linear velocity $\tilde{v}$ =v/n are denoted by $\tilde{v_x}$, $\tilde{v_y}$ and $\tilde{v_z}$. The rate of advective transport corresponds to $\tilde{v}$. The concentration of the solute C represents the mass of solute per unit volume of solution. The mass of solute per unit volume of porous media is equal to nC. Homogenous medium has a constant effective porosity and $\partial(nC) / \partial x = n (\partial C/\partial x)$.
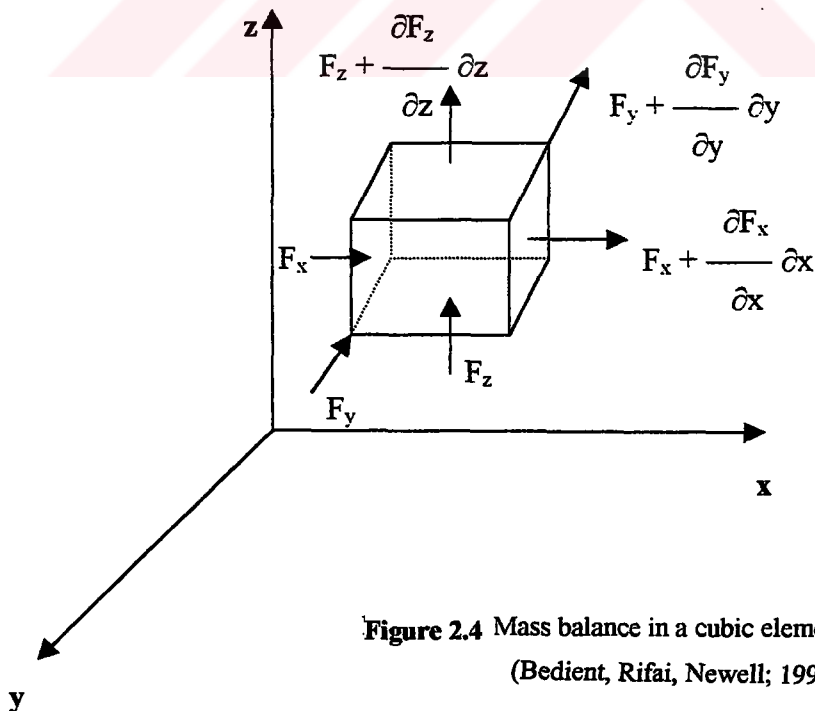
Figure 2.4 Mass balance in a cubic element in space.
(Bedient, Rifai, Newell; 1994)

The mass of solute transported in the x direction by the two mechanisms of solute transport is given by

Transport by advection $= \tilde{v}_x \, n \, C \, dA$

Transport by dispersion $= n \, D_x \, \partial C/\partial x \, dA$ \hfill (2.8)

where D_x is the hydrodynamic dispersion coefficient in the x direction and dA is the elemental cross-sectional area of the cubic element.

$$D_x = \alpha_x \, \tilde{v}_x + D_d \hfill (2.9)$$

If the total mass of solute per unit cross-sectional area transported in the x direction per unit time is denoted by F_x;

$$F_x = \tilde{v}_x \, n \, C - n \, D_x \, \partial C / \partial x \hfill (2.10)$$

The negative sign before the dispersive term indicates that the contaminant moves from high concentration area to a lower concentration area. Similarly ;

$$F_y = \tilde{v}_y \, n \, C - n \, D_y \, \partial C / \partial y \hfill (2.11)$$

$$F_z = \tilde{v}_z \, n \, C - n \, D_z \, \partial C / \partial z \hfill (2.12)$$

The total amount of solute entering the fluid element (figure 2.4) is expressed as

$$F_x \, dz \, dy + F_y \, dz \, dx + F_z \, dx \, dy$$

The total amount leaving the representative fluid element corresponds to

$$\{ F_x + (\partial F_x / \partial x)\, dx\}\, dz\, dy + \{ F_y + (\partial F_y / \partial y)\, dy\}\, dz\, dx$$
$$+ \{F_z + (\partial F_z / \partial z)\, dz\}\, dx\, dy$$

The difference in the amount entering and leaving the fluid element is equal to

$$\{ (\partial F_x / \partial x) + (\partial F_y / \partial y) + (\partial F_z / \partial z) \}\, dx\, dy\, dz \qquad (2.13)$$

The rate of mass change in the element can be written as

$$-n\, (\partial C / \partial t)\, dx\, dy\, dz$$

Hence, the complete conservation of mass expression becomes

$$(\partial F_x/\partial x) + (\partial F_y/ \partial y) + (\partial F_z/\partial z) = -n\, (\partial C/\partial t) \qquad (2.14)$$

After some algebra, this equation becomes

$$\{ \partial/\partial x\, (D_x \partial C/\partial x) + \partial/\partial y\, (D_y \partial C/\partial y) + \partial/\partial z\, (D_z\, \partial C/\partial z) \}$$

$$- \{ (\partial/\partial x)\, \tilde{v}_x C + (\partial/\partial y)\, \tilde{v}_y C + (\partial/\partial z)\tilde{v}_z C\} = \partial C/\partial t \qquad (2.15)$$

The assumptions of steady and uniform velocity and uniform dispersion coefficients yield

$$\{ D_x\, (\partial^2 C/\partial x^2) + D_y\, (\partial^2 C/\partial y^2) + D_z\, (\partial^2 C/\partial z^2) \}$$
$$- \{ \tilde{v}_x\, (\partial C/\partial x) + \tilde{v}_y\, (\partial C/\partial y) + \tilde{v}_z\, (\partial C/\partial z) \} = \partial C/\partial t \qquad (2.16)$$

In the case of two dimensional flow and one- dimensional velocity, this equation becomes

$$\{ D_x (\partial^2 C/\partial x^2) + D_y (\partial^2 C/\partial y^2) \} - \tilde{v}_x (\partial C/\partial x) = \partial C/\partial t \qquad (2.17)$$

In one dimension such as for a soil column , the governing equation reduces to the common advective – dispersive equation ;

$$D_x (\partial^2 C/\partial x^2) - \tilde{v}_x (\partial C/\partial x) = \partial C/\partial t \qquad (2.18)$$

2.2.3. Adsorption Effects:

While there exist many reactions that can alter contaminant concentrations in ground water, adsorption onto the soil matrix appears to be one of the dominant mechanisms. The concept of the isotherm is used to relate the amount of contaminant adsorbed by the solids S to the concentration in solution, C. One of the most commonly used isotherms is the Freundlich isotherm.

$$S = K_d C^b \qquad (2.19)$$

where S is the mass of solute adsorbed per unit bulk dry mass of porous media, K_d is the distribution coefficient , and b is an experimentally derived coefficient. If b=1 eq (2.19) is known as the linear isotherm and is incorporated into the one-dimensional advective-dispersive equation in the following way:

$$D_x \frac{\partial^2 C}{\partial x^2} - v_x \frac{\partial C}{\partial x} - \frac{\rho_b}{n} \frac{\partial S}{\partial t} = \frac{\partial C}{\partial t} \qquad (2.20)$$

where ρ_b is the bulk dry mass density, n is porosity, and

$$- \frac{\rho_b}{n} \frac{\partial S}{\partial t} = \frac{\rho_b}{n} \frac{dS}{dC} \frac{\partial C}{\partial t}$$

For the case of the linear isotherm, $(dS/dC) = K_d$, and

$$D_x \frac{\partial^2 C}{\partial x^2} - v_x \frac{\partial C}{\partial x} = \frac{\partial C}{\partial t} \left(1 + \frac{\rho_b}{n} K_d \right)$$

or finally,

$$\frac{D_x}{R} \frac{\partial^2 C}{\partial x^2} - \frac{v_x}{R} \frac{\partial C}{\partial x} = \frac{\partial C}{\partial t} \qquad (2.21)$$

where $R = [\, 1 + (\rho_b / n)\, K_d] =$ retardation factor, which has the effect of retarding the adsorbed species relative to the advective velocity of the ground water (Figure 2.1). The retardation factor is equivalent to the ratio of velocity of the sorbing contaminant and the ground water and ranges from 1 to several thousand. (Bedient, Rifai, Newell; 1994).

2.2.4. One Dimensional Transport with First-Order Decay

This case is encountered where there is radioactive decay, biodegradation , or hydroloysis, and it is generally represented in the transport equation by adding the term $-\lambda C$, where λ is the first-order decay rate in units of t^{-1}. Eq (2.18) becomes

$$D_x \frac{\partial^2 C}{\partial x^2} - v_x \frac{\partial C}{\partial x} - \lambda\, C = \frac{\partial C}{\partial t} \qquad (2.22)$$

2.2.5. Governing Flow and Transport Equations in Two Dimensions

The differential equation for two dimensional groundwater flow is usually written as

$$\frac{\partial}{\partial x}\left(T_x \frac{\partial h}{\partial x}\right) + \frac{\partial}{\partial y}\left(T_y \frac{\partial h}{\partial y}\right) = S\frac{\partial h}{\partial t} + W \qquad (2.23)$$

where $T_x = K_x b$ = transmissivity in the x direction (L^2/T)

$T_y = K_y b$ = transmissivity in the y direction (L^2/T)

b = aquifer thickness (L)

S = storage coefficient

W = source or sink term (L/T)

h = hydraulic head (L)

This two dimensional flow equation must be solved before the transport equation can be solved.

The governing transport equation in two dimensions is usually written

$$\frac{\partial}{\partial x}\left(D_x \frac{\partial C}{\partial x}\right) + \frac{\partial}{\partial y}\left(D_y \frac{\partial C}{\partial y}\right) - \frac{\partial}{\partial x}(Cv_x) - \frac{\partial}{\partial y}(Cv_y) - \frac{C_0 W}{nb} + \Sigma R_k$$

$$= \frac{\partial C}{\partial t} \qquad (2.24)$$

where C = concentration of solute (M/L^3)

v_x, v_y = seepage velocity (L/T) averaged in the vertical direction

D_x, D_y = coefficient of dispersion (L^2/T) in x and y directions

C_0 = solute concentration in source or sink fluid (M/L^3)

R_k = rate of addition or removal of solute (+,-) ($M/L^3 T$)

n = effective porosity

W = source or sink term

Equation (2.24) can only be solved analytically under the most simplifying conditions where velocities are constant , dispersion coefficients are constant, and source terms are simple functions. There are difficulties in attempting to use the mass-transport equation to describe an actual field site in two dimensions, since dispersivities in the x and y directions are difficult to estimate from tracer tests due to the presence of spatial heterogeneities and other reactions in the porous media. Estimation of hydraulic conductivity and associated velocities can be very difficult due to the presence of field heterogeneities that are often unknown. The source and sink concentrations that drive the model are usually assumed constant in time , but may actually have varied significantly. A particular serious problem appears to be the reaction term , which may represent adsorption , ion exchange or biodegradation. The assumption of equilibrium conditions and the selection of rate coefficients are both subject to some error and may create difficult prediction problems at many field sites. (Bedient, Rifai, Newell; 1994).

CHAPTER THREE

NUMERICAL MODELING OF CONTAMINANT TRANSPORT

3.1. Introduction to Numerical Modeling

Anderson and Woessner (1992) propose a modeling protocol that can be summarized as follows:

1. Establish the purpose of the model.

2. Develop a conceptual model of the system.

3. Select the governing equation and a computer code. Both the governing equation and code should be verified. Verification of the governing equation demonstrates that it describes the physical, chemical and biological processes occurring. Code verification can be accomplished by comparing the model results to an analytical solution of a known problem.

4. Design the model. This step includes selection of a grid design , the parameters , initial and boundary conditions and developing estimates of model parameters.

5. Calibrate the designed model. Calibration refers to the process of determining a set of model input parameters that approximates field measured heads, flows, and/or concentrations. The purpose of calibration is to establish that the model can reproduce field-measured values of the unknown variable.

6. Determine the effects of uncertainty on model results . This is sometimes referred to as a sensitivity analysis. The model parameters are varied individually within a range of possible values , and the effect on model results is evaluated.

7. Verify the designed and calibrated model. This step involves testing the model's ability to reproduce another set of field measurements using the model parameters that were developed in the calibration process.

8. Predict results based on the calibrated model.

9. Determine the effects of uncertainty on model predictions.

10. Present modeling design and results.

11. Redesign the model as necessary. As more data are collected beyond model development , it is possible to compare the model predictions against the new field data. This may lead to further modifications and refinements of the site model. (Bedient, Rifai, Newell; 1994).

3.1.1. Conceptual Models

When a conceptual model is formulated, the following features are to be defined (1) hydrogeologic features of the aquifers to be modeled. (2) the flow system and sources and sinks of water in the system when there exists recharge from infiltration , baseflow to streams , evapotranspiration and pumping. (3) the transport system of chemicals and also sources and sinks of chemicals in the system.

3.1.2. Discretization

In numerical models , the physical layout of the studied area is replaced with a discretized model domain named a grid and it consists of cells , blocks or elements depending on whether finite difference or finite element methods are used.

Time parameter also needs to be discretized. Most of numerical models calculate results at time T by subdividing the total time into time steps, Δt. Generally smaller time steps are preferable because some models suffer from numerical instabilities that cause unrealistic oscillating solutions.

3.1.3. Boundary and Initial Conditions

Generally , boundary conditions are the relations which specify the value of the dependent variable or the value of the first derivative of the dependent variable, at the boundaries of the system being modeled.

Boundary conditions are described by physical and /or hydraulic boundaries of ground water flow system , such as the presence of an impermeable body of rock or a river in connection with the ground water aquifer. Hydrogeologic boundaries are represented by three types of mathematical formulations: specified head , specified flux and head-dependent flux boundaries.

3.1.4. Sources and Sinks

Both water and chemicals may enter the grid in one of two ways:
1. Through the boundaries as defined by the boundary conditions   or
2. Through sources and sinks in the interior grids.

For example specified head nodes may be placed within the grid to represent lakes and rivers or some other type of source.

An injection or pumping well is a point source or sink and is described by specifying an injection or pumping rate at a designated node or cell. In a two-dimensional model it is assumed that well is fully penetrated over the aquifer thickness.

3.1.5. Sources and Types of Errors: Accuracy of Numerical Models

There are two types of errors during numerical modelling:

1. Computational Errors: These errors are due to numerical approximation procedures that are used to solve the governing equations subject to the given boundary and initial conditions.

2. Calibration Errors: These errors occur because of assumptions and limitations in parameter estimation.

3.2. Numerical Methods

Numerical solutions are generally more flexible than analytical solutions because the user can approximate complex geometries and combinations of recharge and withdrawal wells. The general method of solution is to divide the flow field into small cells , approximate the governing partial differential equations by differences among the values of parameters over the network of time t and then predict new values for time t+Δt.

The most common numerical methods are:

- Finite difference methods
- Finite element methods
- Collocation methods
- Method of characteristics

The finite difference method is the most popular method for simulating problems of ground water flow and transport. Finite difference methods are conceptually straightforward and easily understood. The primary disadvantage of these methods is that the truncation error in approximating the partial differential equations can be significant (Anderson , 1979).

The finite element method also operates by breaking the flow field into elements but in this case the elements may vary in size and shape. A disadvantage of the finite element method is the need for formal mathematical training to understand the

procedures properly. Finite element methods generally have higher computing costs (Pinder and Gray , 1977 ; Wang and Anderson, 1982).

The method of characteristics (MOC) is a variant of the finite difference method and is particularly suitable for solving hyperbolic equations. The MOC was developed to simulate advection-dominated transport by Garder (1964). In ground water hydrology Pinder and Cooper (1970) and Reddell and Sunada (1970) used the method to solve the density-dependent transport equations. Later MOC was used widely to simulate the movement of contaminants in the subsurface (Bredehoeft and Pinder , 1973). The MOC is most useful where solute transport is dominated by advective transport. (Bedient, Rifai, Newell;1994).

In Collocation Method; the function satisfying the boundary conditions is substituted in the differential equation to give an expression termed the residual, which includes the space variable or variables and the arbitrary coefficients. If the function were the exact solution, it would satisfy the equation at all points in the domain. Since it is not, it can be made to satisfy the differential equation at as many points in the field problem as there are unknown coefficients.

3.2.1. Finite Difference Methods

In the finite difference method , nodes may be placed inside cells (block centered, Figure 3.1) or at the intersection of grid lines (mesh centered, Figure 3.2). Aquifer properties and head values are taken constant within each cell in a block-centered finite difference model. An equation is written in terms of each nodal point in finite difference models because the area surrounding a node is not directly involved in the development of the finite difference equations(Wang and Anderson, 1982).
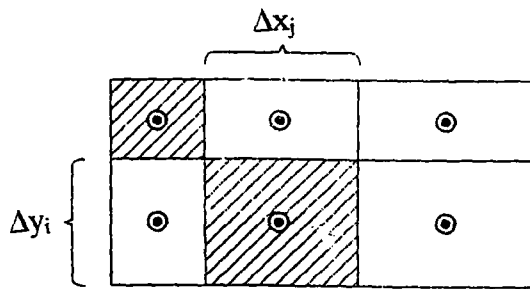
Figure 3.1 Block-centered grid system.
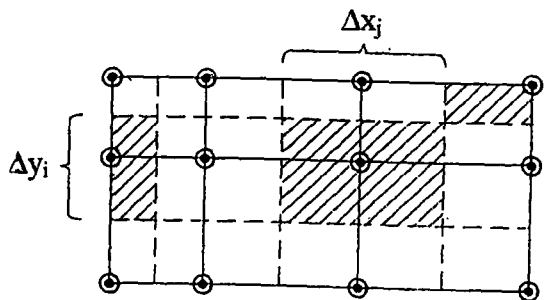
Figure 3.2 Point or mesh-centered grid system.

Figure 3.3 shows a regularly spaced grid. The derivatives are taken equal to the differences between nodal points. When a central approximation is used to the second derivative of the dependent variable h (x,y), one can write;

$$\frac{\partial^2 h}{\partial x^2} \approx \frac{\dfrac{h_{i+1,j} - h_{i,j}}{\Delta x} - \dfrac{h_{i,j} - h_{i-1,j}}{\Delta x}}{\Delta x} \tag{3.1}$$

which simplifies to

$$\frac{\partial^2 h}{\partial x^2} \approx \frac{h_{i-1,j} - 2h_{i,j} + h_{i+1,j}}{\Delta x^2} \tag{3.2}$$
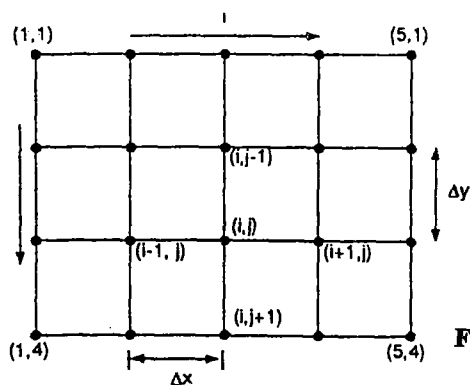
Figure 3.3 Finite difference grid system.

Similarly,

$$\frac{\partial^2 h}{\partial y^2} \approx \frac{h_{i,j-1} - 2h_{i,j} + h_{i,j+1}}{\Delta y^2} \tag{3.3}$$

3.2.1.1. Explicit Finite Difference Approximation

A forward or explicit difference approximation for $\partial h/\partial t$ is given by

$$\frac{\partial h}{\partial t} \approx \frac{h^{n+1}_{i,j} - h^{n}_{i,j}}{\Delta t} \tag{3.4}$$

where n and n+1 represent two consecutive time levels. Similarly a backward difference approximation is given by

$$\frac{\partial h}{\partial t} \approx \frac{h^{n}_{i,j} - h^{n-1}_{i,j}}{\Delta t} \tag{3.5}$$

and a central difference approximation in time is given by

$$\frac{\partial h}{\partial t} \approx \frac{h^{n+1}_{i,j} - h^{n-1}_{i,j}}{2\Delta t} \qquad (3.6)$$

For the case of transient flow given by

$$\frac{\partial^2 h}{\partial x^2} + \frac{\partial^2 h}{\partial y^2} = \frac{S}{T} \frac{\partial h}{\partial t} \qquad (3.7)$$

(where S is the storage coefficient and T is the transmissivity.).

The explicit approximation yields a stable solution if the value of the ratio $(T\Delta t)/[S(\Delta x)^2]$ is kept sufficiently small. In the one-dimensional case, where flow occurs only in the x direction the parameter $(T\Delta t)/[S(\Delta x)^2]$ must be ≤ 0.5 (Remson et al.,1971) to ensure numerical stability. For the two-dimensional case, where $\Delta x = \Delta y$, $(T\Delta t)/[S(\Delta x)^2]$ must be ≤ 0.25 (Rushton and Resshaw,1979).

3.2.1.2. Implicit Finite Difference Approximation

Weighted average of the approximations at n and n+1 is used. The weighting parameter is represented by α and its value is between 0 and 1. If the time step n+1 is weighted by α and time step n is weighted by $(1-\alpha)$, then

$$\frac{\partial^2 h}{\partial x^2} \approx \alpha \frac{h^{n+1}_{i+1,j} - 2h^{n+1}_{i,j} + h^{n+1}_{i-1,j}}{(\Delta x)^2} +(1-\alpha) \frac{h^{n}_{i+1,j} - 2h^{n}_{i,j} + h^{n}_{i-1,j}}{(\Delta x)^2} \qquad (3.8)$$

A similar expression is written for $\partial^2 h/\partial y^2$. The parameter α is selected by the model user. For $\alpha=1$, the space derivatives are approximated at n+1 and the finite difference scheme is named fully implicit. If a value of 0.5 is selected for α then the scheme is called the Crank-Nicolson method.

3.2.1.3. Alternating Direction Implicit (ADI)

The derivation and solution of the finite difference equation and the use of the iterative ADI have been discussed extensively by Pinder and Bredehoeft (1968), Prickett and Lonnquist (1971) and Trescott et al.(1976). In general the basis of the ADI method is to obtain a solution to the flow equation by alternately writing the finite difference equation, first implicitly along columns and explicitly along rows, and then vice versa. To reduce the errors that may result from the ADI method, an iterative procedure is added so that, within a single step, the solution will converge within a specified error tolerance. The ADI method may be illustrated by approximating the two-dimensional transient equation for a confined aquifer:

$$\frac{\partial^2 h}{\partial x^2} + \frac{\partial^2 h}{\partial y^2} = \frac{S}{T}\frac{\partial h}{\partial t} \tag{3.9}$$

Assuming $\Delta x = \Delta y = a$ the fully implicit finite difference approximation is

$$h^{n+1}{}_{i+1,j} + h^{n+1}{}_{i-1,j} + h^{n+1}{}_{i,j+1} + h^{n+1}{}_{i,j-1} - 4h^{n+1}{}_{i,j} = \frac{Sa^2}{T}\frac{h^{n+1}{}_{i,j} - h^n{}_{i,j}}{\Delta t} \tag{3.10}$$

In the first step of ADI , eq(3.27) is rewritten such that heads along columns are on one side of the equation and heads along rows are on the other side (also referred to as rewriting the equation first implicitly along columns and explicitly along rows), which results in

$$h^{n+1}{}_{i,j-1} + (-4 - \frac{Sa^2}{T\Delta t})\, h^{n+1}{}_{i,j} + h^{n+1}{}_{i,j+1} = -\frac{Sa^2}{T\Delta t}\, h^n{}_{i,j} - h^{n+1}{}_{i+1,j} - h^{n+1}{}_{i-1,j} \tag{3.11}$$

Equation (3.28) will yield a tridiagonal coefficient matrix (one that has non zero entries only along the three center diagonals) along any column. The second step of ADI involves rewriting eq(3.27) implicitly along rows and explicitly along columns:

$$h^{n+1}_{i-1,j} + (-4 - \frac{S\,a^2}{T\,\Delta t})\,h^{n+1}_{i,j} + h^{n+1}_{i+1,j} = - \frac{S\,a^2}{T\,\Delta t}\,h^{n}_{i,j} - h^{n+1}_{i,j+1} - h^{n+1}_{i,j-1} \qquad (3.12)$$

The explicit approximation along columns uncouples one row from another. Therefore eq(3.29) will also generate a set of matrix equations (one for each interior row) with tridiagonal coefficient matrices. Alternating the explicit approximation between column and rows is an attempt to compensate for errors generated in either direction. (Bedient, Rifai, Newell; 1994).

3.2.2. Finite Element Methods

A difficult problem in flow through porous media involves sharp fronts. A sharp front refers to a large change in a dependent variable over a small distance. Sharp front problems are encountered in both miscible (advective-dispersive flow) and immiscible (multifluid and multiphase flow) problems. The most common complaint about low order finite difference methods applied to sharp-front problems is that the computed front is 'smeared-out' (Mercer and Faust, 1977). The process by which the front becomes smeared is referred to as numerical dispersion.

In general for linear problems, the finite element method can track sharp fronts more accurately , which reduces considerably the numerical diffusion problem. The finite element method, however, has several numerical problems, which include numerical oscillation, instability, and large computation time requirements. The finite element analysis of a physical problem can be described as follows (Huyakorn and Pinder, 1983):

1. The physical system is subdivided into a series of finite elements that are connected at a number of nodal points. Each element is identified by its element number and the lines connecting the nodal points situated on the boundaries of the element.

2. A matrix expression , known as the element matrix, is developed to relate the nodal variables of each element. The element matrix may be obtained via a

mathematical formulation that makes use of either a variational or weighted residual method.

3.   The element matrices are combined or assembled to form a set of algebraic equations that describe the entire system. The coefficient matrix of this final set of equations is called the global matrix.

4.   Boundary conditions are incorporated into the global matrix equation.

5.   The resulting set of simultaneous equations is solved using a variety of techniques, such as Gauss elimination. (Bedient, Rifai, Newell; 1994).

3.2.3. Method of Characteristics

The method of characteristics (MOC) may be illustrated using the following one-dimensional form of the transport equation for a conservative tracer:

$$D_x \frac{\partial^2 C}{\partial x^2} - V \frac{\partial C}{\partial x} = \frac{\partial C}{\partial t} \qquad (3.13)$$

where C is the tracer concentration, V is the velocity, D_x is the coefficient of hydrodynamic dispersion and t is the time.

This equation can be simplified into the following system of ordinary differential equations by using the common characteristics method:

$$\frac{dx}{dt} = V \qquad (3.14)$$

$$\frac{dC}{dt} = D_x \frac{\partial^2 C}{\partial x^2} \qquad (3.15)$$

Equation (3.15) is valid along the characteristics defined by equation (3.14).

CHAPTER FOUR

PROCESSING MODFLOW
FOR WINDOWS (PMWIN)

[User Guide of PMWIN]

4.1. Features of PMWIN

• Processing Modflow for Windows (PMWIN) is one of the most complete simulation systems in the world. PMWIN comes complete with a professional graphical pre and postprocessor, the 3-D finite difference groundwater flow models MODFLOW-88 and MODFLOW-96, the solute transport models MT3D, MT3DMS and MOC3D, the particle tracking model PMPATH for Windows and the inverse models UCODE and PEST(-LITE) for automatic calibration.

• PMWIN is capable of using all available memory. It can handle models with up to 1000 stress periods, 80 layers and 250000 cells in each layer. The model grid can be shifted, rotated, refined. Model data can be specified for each finite difference cell individually, in the form of zones or even automatically interpolated by the built in Digitizer and the Field Interpolator.

• It imports geo-referenced raster graphics (bitmap) and vector graphics (DXF or Line Map) as background sitemaps.

• It imports any kind of existing standard MODFLOW models.

• It imports SURFER grid files; Exports SURFER data files.

• The telescopic mesh refinement feature allows to create higher resolution local-scale flow models from a steady-state or transient regional flow model.

PMWIN automatically transfers the results of the regional model as the boundary condition for the local-scaled submodel.

- It involves check models for potential problems prior to running the simulation.

4.2. Advanced Modeling Capability with the Full-Supported Models

- MODFLOW-PMWIN supports the simulation of the effects of wells, rivers, reservoirs, drains, head-dependent boundaries, time-dependent fixed-head boundaries, cut-off walls, compaction and subsidence, recharge and evapotranspiration. In addition to these standard packages of MODFLOW-96, PMWIN includes the unique density package for taking account the density driven flow rates into flow models.

- PMPATH for Windows allows to perform particle tracking. Both forward and backward particle tracking schemes are allowed for steady-state and transient flow fields. PMPATH calculates and animates the particle tracking processes, and simultaneously provides various on-screen graphical options including head contours, draw down contours and velocity vectors.

- MT3D/MT3D96 can be used to simulate changes in concentration of single species miscible contaminants in groundwater considering advection, dispersion and simple chemical reaction.

- MT3DMS is the next generation of MT3D; MS stands for Multi-Species. PMWIN provides full support for MT3DMS and can take advantages by using new solution schemes of MT3DMS. Up to 30 different species can be simulated with PMWIN.

- MOC3D is a new development of the popular 2-D MOC model. It features advection, dispersion and simple chemical reaction.

- PEST and UCODE simply specify the observation data and define zones of parameters with the powerful data editor of PMWIN. The following model parameters can be automatically calibrated: (1) horizontal hydraulic conductivity or transmissivity; (2) vertical leakance; (3) specific yield or confined storage coefficient; (4) pumping rate of wells; (5) conductance of drain, river, stream or

head-dependent cells; (6) recharge flux; (7) maximum evapotranspiration rate and (8) inelastic storage factor.

4.3. Sophisticated Modeling Tools

- Using the Presentation tool, one can create labeled and color filled contour maps of any kind of data, including input data and simulation results. Report-quality graphics may be printed or saved to several file formats, including SURFER, DXF, HPGL and BMP (Windows Bitmap). The Presentation tool can even create and display two dimensional animation sequences using the simulation results.

- Result Extractor allows to extract simulation results from any period to a spread sheet.

- Field Interpolator takes point-wise measurement data and interpolates the data to model grid. The model grid can be irregularly spaced.

- Field Generator generates fields with heterogeneously distributed transmissivity or hydraulic conductivity values. It allows the user to statistically simulate effects and influences of unknown small-scale heterogeneities.

- Water Budget Calculator not only calculates the budget of user-specified zones but also the exchange of flows between such zones. The facility is very useful in many practical cases. It allows the user to determine the flow through a particular boundary.

- Graph Viewer displays scatter diagrams to aid in model calibration and temporal development curves of simulation results including hydraulic heads, drawdowns, subsidence, compaction and concentrations.

A toolbar with buttons representing PMWIN operations or commands is displayed below the menus. The toolbar is a shortcut for the pull-down menus. To execute one of these shortcuts, one moves the mouse cursor over the toolbar button and click on it. PMWIN contains the menus File, Grid, Parameters, Models, Tools, Value, Options and Help. The Value and Options menus are available only in the Grid Editor and Data Editor.

4.4. System Requirements

4.4.1. Hardware

The following equipments are required to use PMWIN;

- Personal computer running Microsoft Windows 95/98 or Windows NT 4.0 or above.
- 16 MB of available memory (32MB or more highly recommended).
- A CD-ROM drive and a hard disk.
- VGA or higher-resolution monitor.
- Microsoft mouse or compatible pointing device.

4.4.2. Software

A Fortran compiler is required to modify and compile the models MODFLOW-88, MODFLOW-96, MOC3D, MT3D or MT3DMS. For the reason of compability, the models must be compiled by a Lahey Fortran compiler.

4.5. Input of Required Data

The geologic and hydraulic characteristics of the studied area are given in the following order:

1. The model grid.
2. The type of layers.
3. The boundary condition to the flow model.
4. The elevation of the top of model layers.
5. The elevation of the bottom of model layers.
6. The time parameter.
7. The initial hydraulic head.
8. The horizontal hydraulic conductivity.

9. The vertical hydraulic conductivity.

10. The effective porosity.

11. The recharge rate.

12. The pumping well and the pumping rate.

13. The observation boreholes.

14. The boundary condition to MT3D.

15. The initial concentration.

16. The input rate of contaminants.

17. The transport parameters to the Advection Package.

18. The dispersion parameters.

19. The chemical reaction parameters.

20. The output times.

CHAPTER FIVE
RESULTS FOR HARMANDALI
SANITARY LANDFILL AREA

5.1. The Studied Area [Öztuna, 1993]

Harmandalı Region is located between 27^0 05' – 27^0 10' north latitude and 38^0 32' – 38^0 33' east longitude. It is 2.5 km. far from the village of Harmandalı which is in the border of Karşıyaka. The area is approximately 900000 m^2. Contact between İzmir and Harmandalı Sanitary Landfill Area is supplied by a road which cuts the state highway, İzmir-Menemen, at the 12th km.(figure 5.1)

In Harmandalı Sanitary Landfill Area, the annular mean of temperature and precipitation is 17.6 ^0C and 700 mm. , respectively. Hydraulic conductivity varies between 10^{-7} to 10^{-10} m/sec. The highest value of hydraulic conductivity is 4.7 $*10^{-7}$. According to these data, the ground is classified as very little drainaged and generally impermeable.
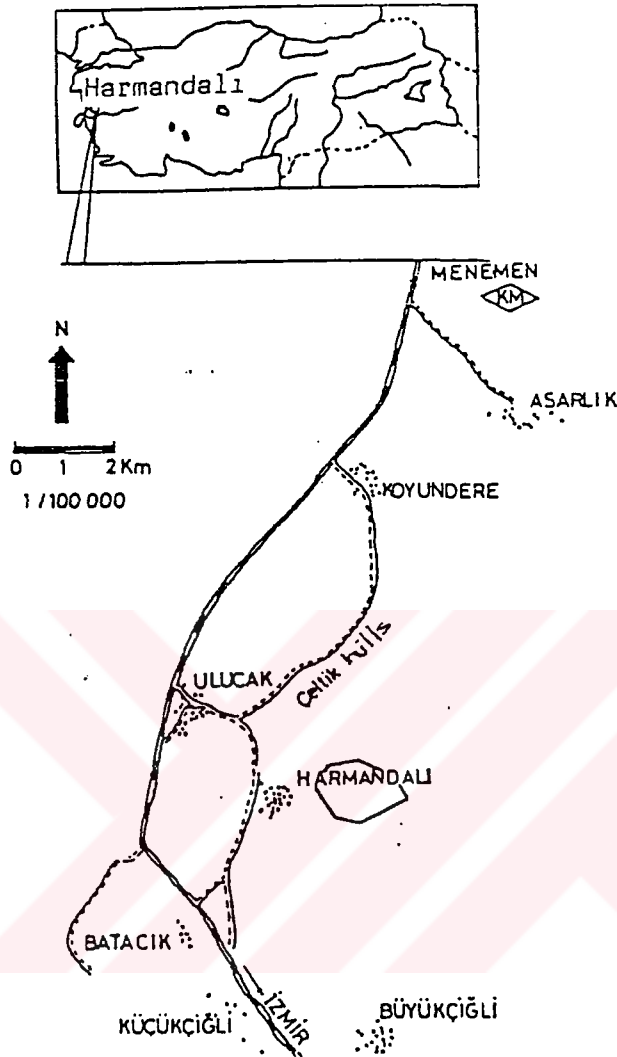
Figure 5.1 Map of the Harmandalı Sanitary Landfill Area.

After the laboratory studies the results were as follows;

1. Groundwater table is not close to surface level.

2. Geological structures include impermeable layer.

3. The Harmandalı Sanitary Landfill Area is not located on drinking water supply region of villages.

In the area to observe the concentration distribution, 4 observation wells were located. The pumping well is at the right bottom corner of the studied area. The

observation wells are marked by (1), (2), (3), (4) in the first layer and (5), (6), (7), (8) in the second layer.

At Harmandalı Sanitary Landfill Area; Harmandalı flish has been determined after studies of the geological institute. Harmandalı flish lies from the elevation 200m.

In the Harmandalı Sanitary Landfill Area, treatment sludges are being stored in two ways:

- Storing of sludge with water into the treatment sludge region,
- Storing of sludge without water into the industrial wastes.

5.1.1. Application of the Model to the Harmandalı Sanitary Landfill Area

Four different models with various contaminant areas have been considered. Harmandalı Sanitary Landfill Area is studied by dividing in two layers as shown in Figure 5.2.
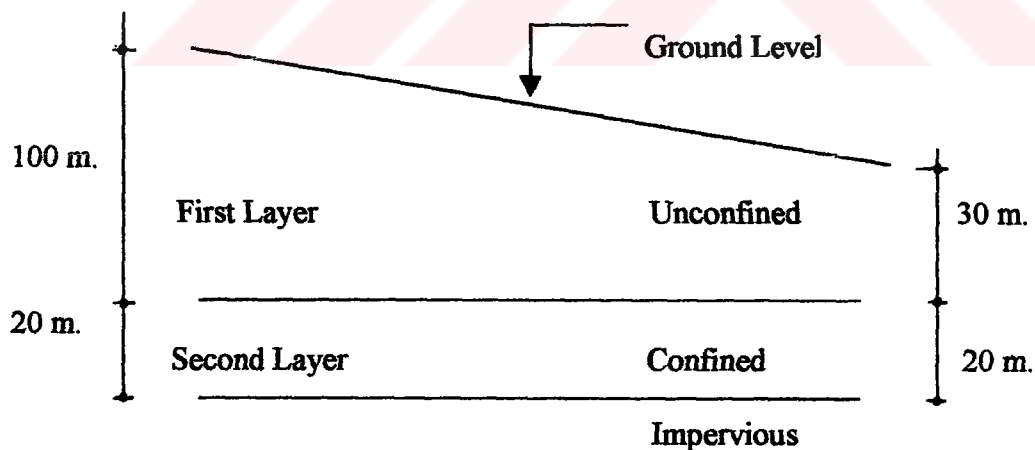
Figure 5.2   The Elevations of Layers.

The model A (figure 5.3) and the model B (figure 5.4) are located near the landfill area. The model C (figure 5.5) and the model D (figure 5.6) are located near the observation wells. The A and B models areas have been established on 16*19 grids. C and D models areas established on 16*11 grids. All   models contain four observations wells and a pumping well.

The aquifer is assumed to be homogenous and isotropic. Flow is assumed to be at steady-state.

A, B, C and D models areas are all simulated for two different periods; $T_1 = 400$ years and $T_2 = 40$ years.

The numerical solution is performed with the following data:

The aquifer system is unconfined and isotropic. The horizontal and vertical hydraulic conductivities are assumed to be equal and $4.2*10^{-7}$m/s. The effective porosity is 20 percent. A constant recharge rate of $1*10^{-9}$ m/s is applied to the aquifer. The hydraulic heads on the north and south boundaries are 65 m. and 25 m., respectively.

The pumping rate is $2.89*10^{-6}$ m^3/s. The concentration associated with the recharge flux is 70000 μg/m^3. The ratio of the transverse dispersivity to longitudinal dispersivity is 0.3 and the longitudinal dispersivity is 100. The bulk density of the porous medium is 2240 kg/m^3 and the distribution coefficient is 0.000125.
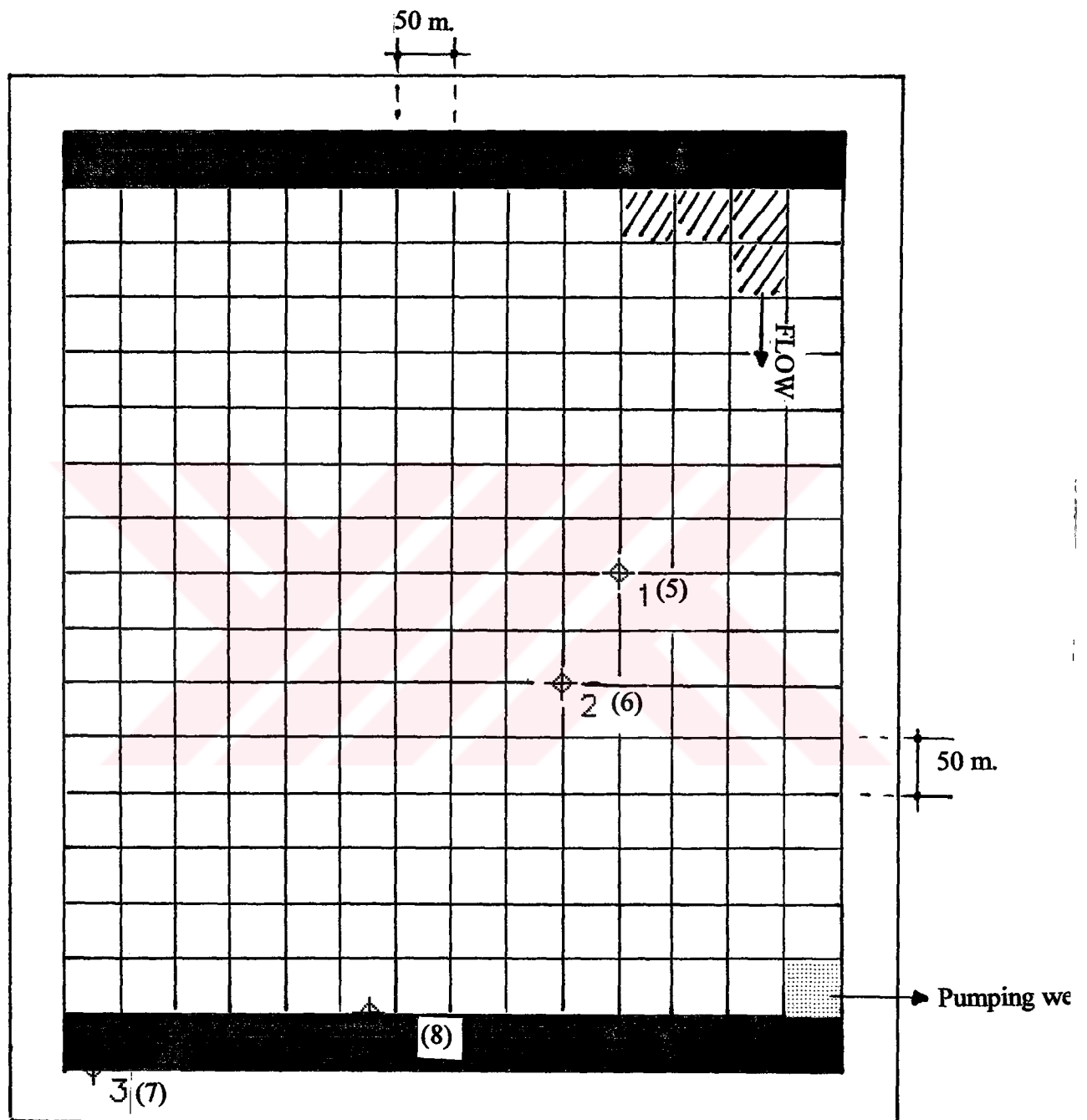
Figure 5.3 Studied area in the case of Model A
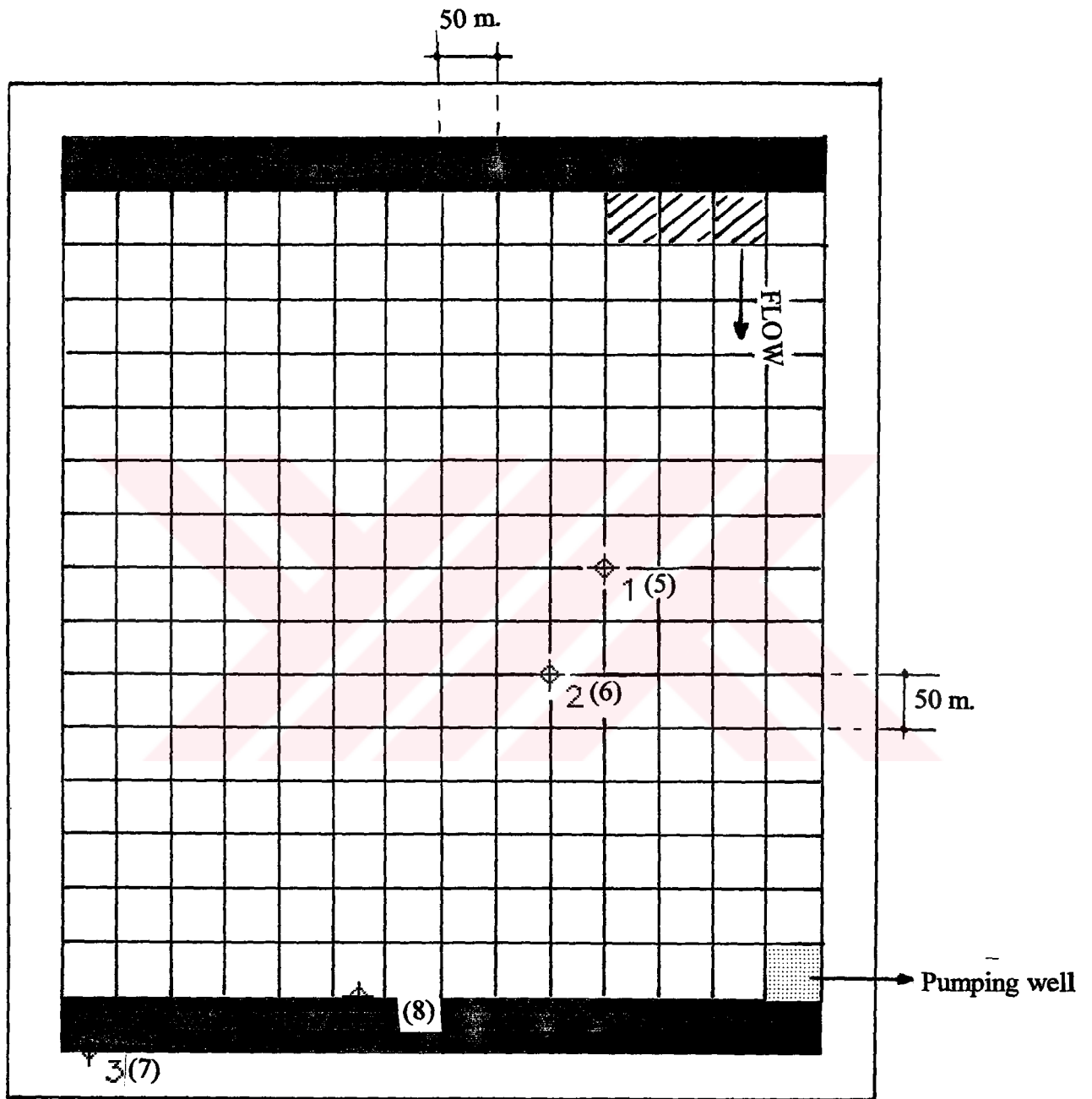
Figure 5.4 Studied area in the case of Model B

50 m.

(5)

2 (6)

FLOW

50 m.

(8)

3 (7)

Pumping well

φ observation well
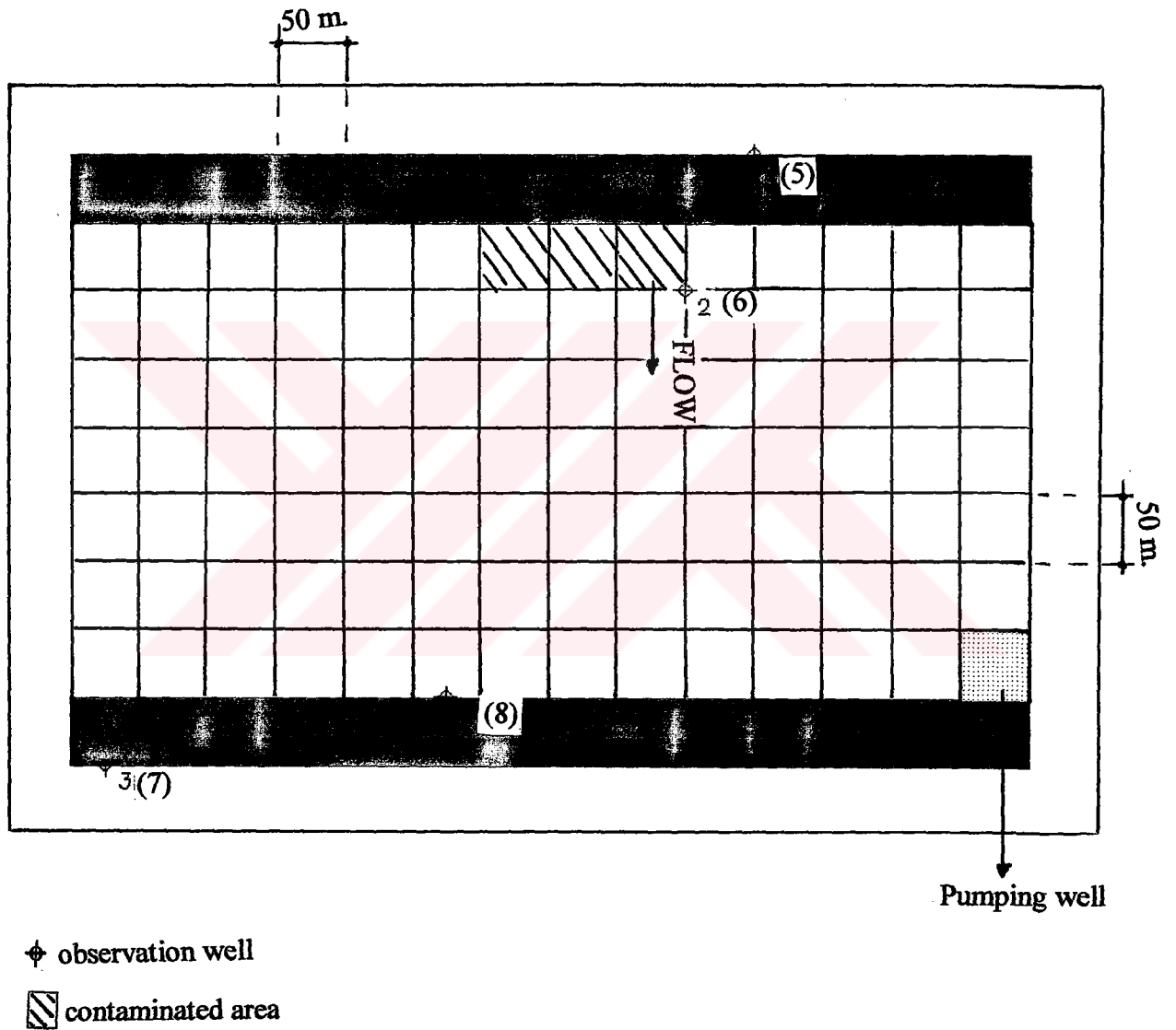
contaminated area

Figure 5.5 Studied area in the case of Model C

50 m.

FLOW

(5)

2 (6)

(8)

3 (7)

Pumping well
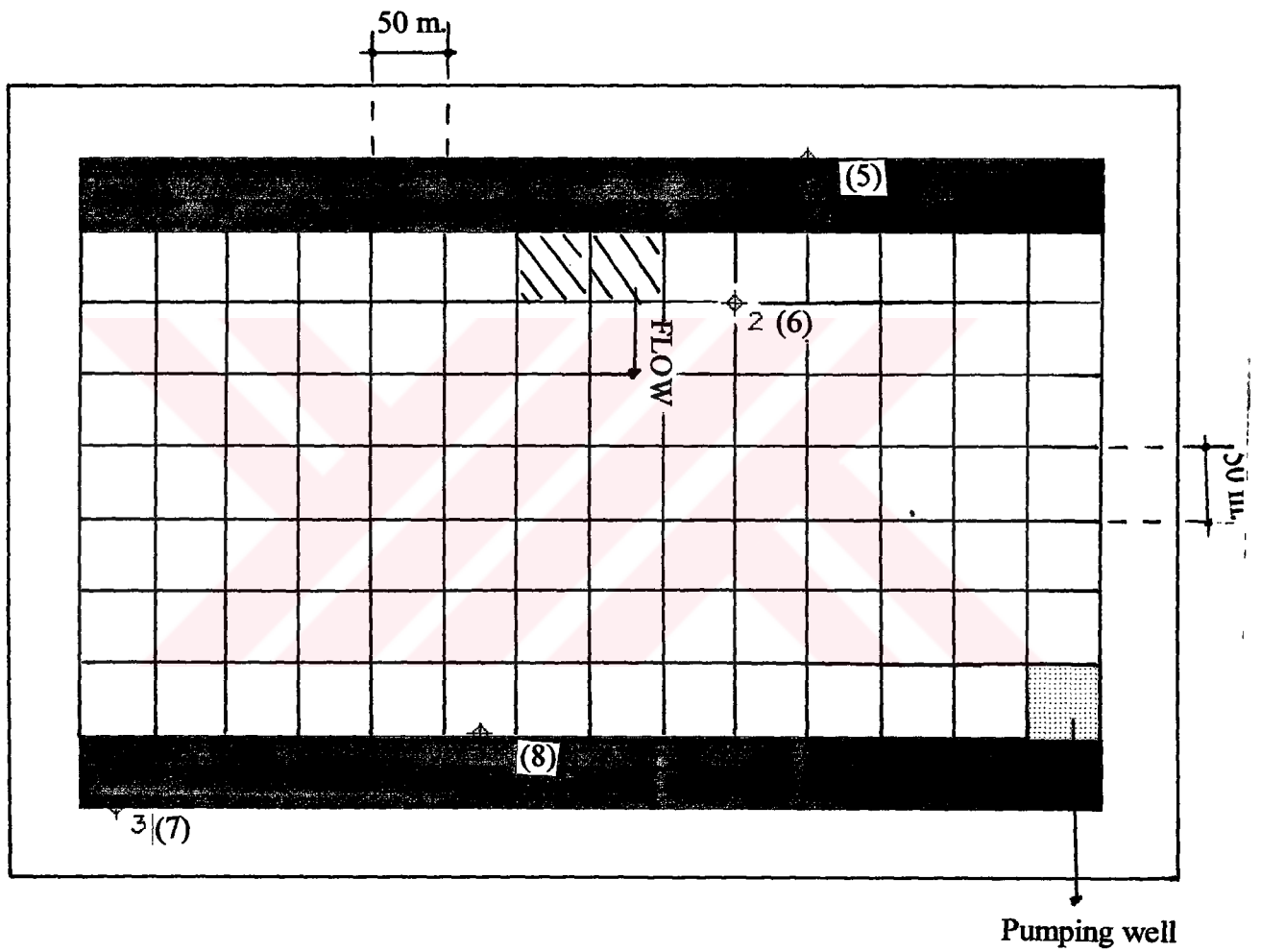
φ observation well

▨ contaminated area

Figure 5.6 Studied area in the case of Model D

5.2. Numerical Results with the Time Parameter 400 years

The following results are obtained for a period of 400 years ($=T_1$).

Water table elevations are in (m).

Concentrations in $\mu g/m^3$ are given in terms of time expressed in second.

The sign ϕ denotes the location of relevant observation well.

5.2.1. Results obtained with Model A

Figure 5.7 represents the calculated water table elevations.

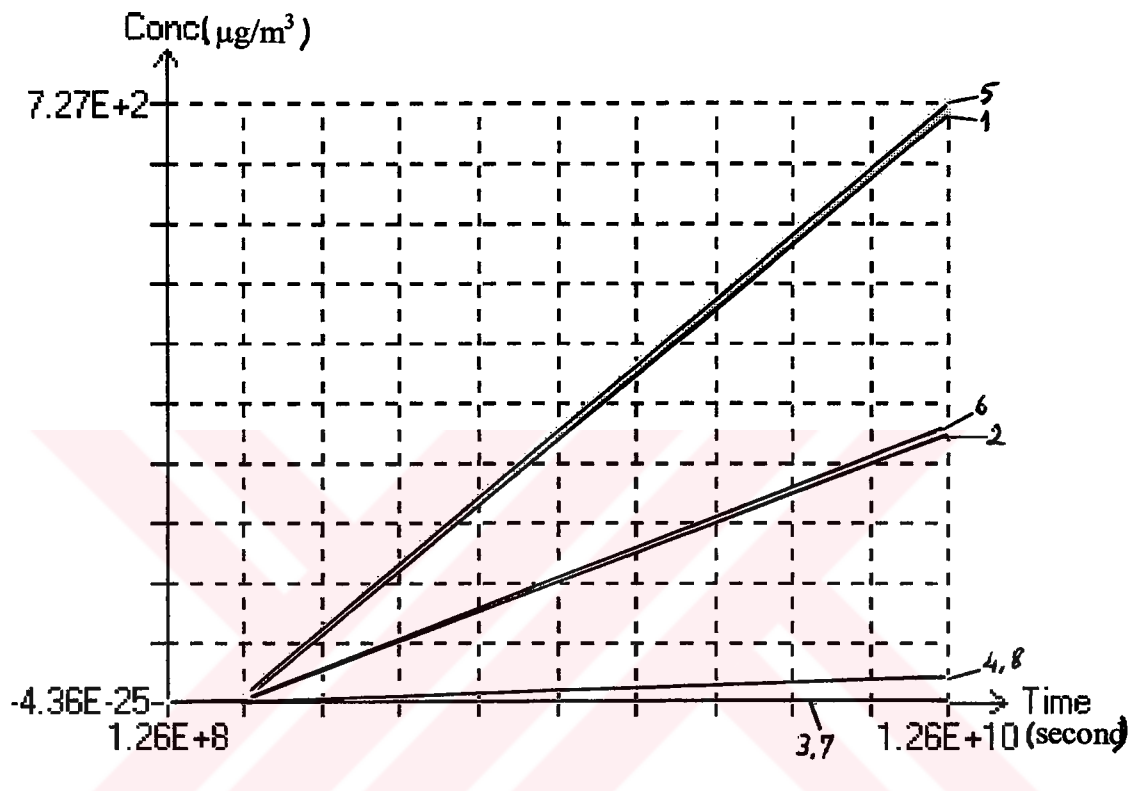The concentration variations at different observation wells are given in figure 5.8.

The curves of equal concentration in the first layer are shown in figure 5.9.

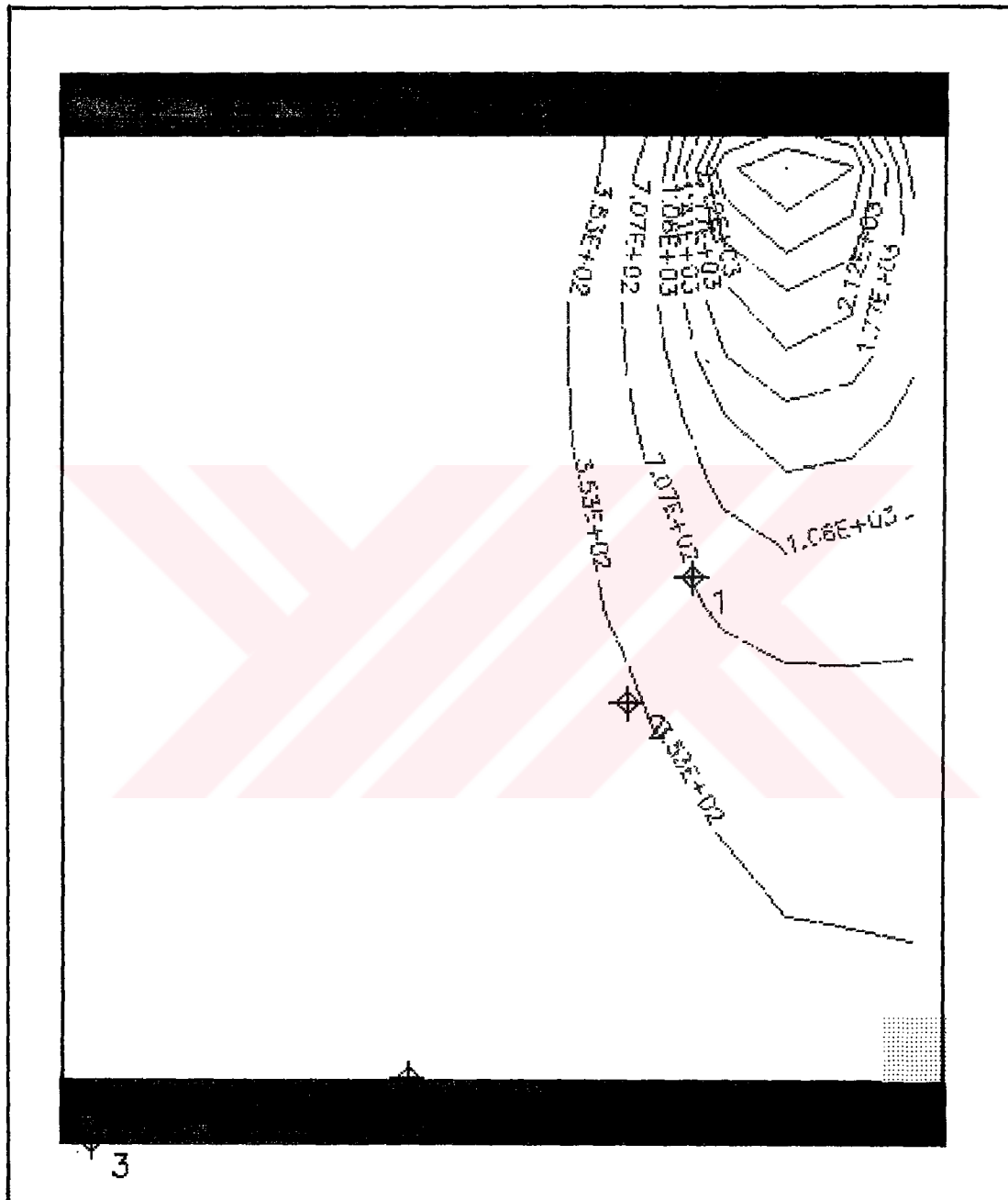Figure 5.10 represents the curves of equal concentration in the second layer.

6.10E+01 _____ 6.10E+01 _____ 6. 0E+01 ____

5.70E+01 _____ 5.70E+01 _____ 5.70E+01 ____

5.30E+01 _____ 5.30E+01 _____ 5.30E+01 ____

4.90E+01 _____ 4.90E+01 _____ 4.90E+01 ____
2

4.50E+01 _____ 4.50E+01 _____ 4.50E+01 ____

4.10E+01 _____ 4.10E+01 _____ 4. 0E+01

3.70E+01 _____ 3.70E+01 _____ 3.70E+01 ____

3.30E+01 _____ 3.30E+01 _____ 3.30E+01 __

2.90E+01 _____ 2.90E+01 _____ 2.90E+01 __

3
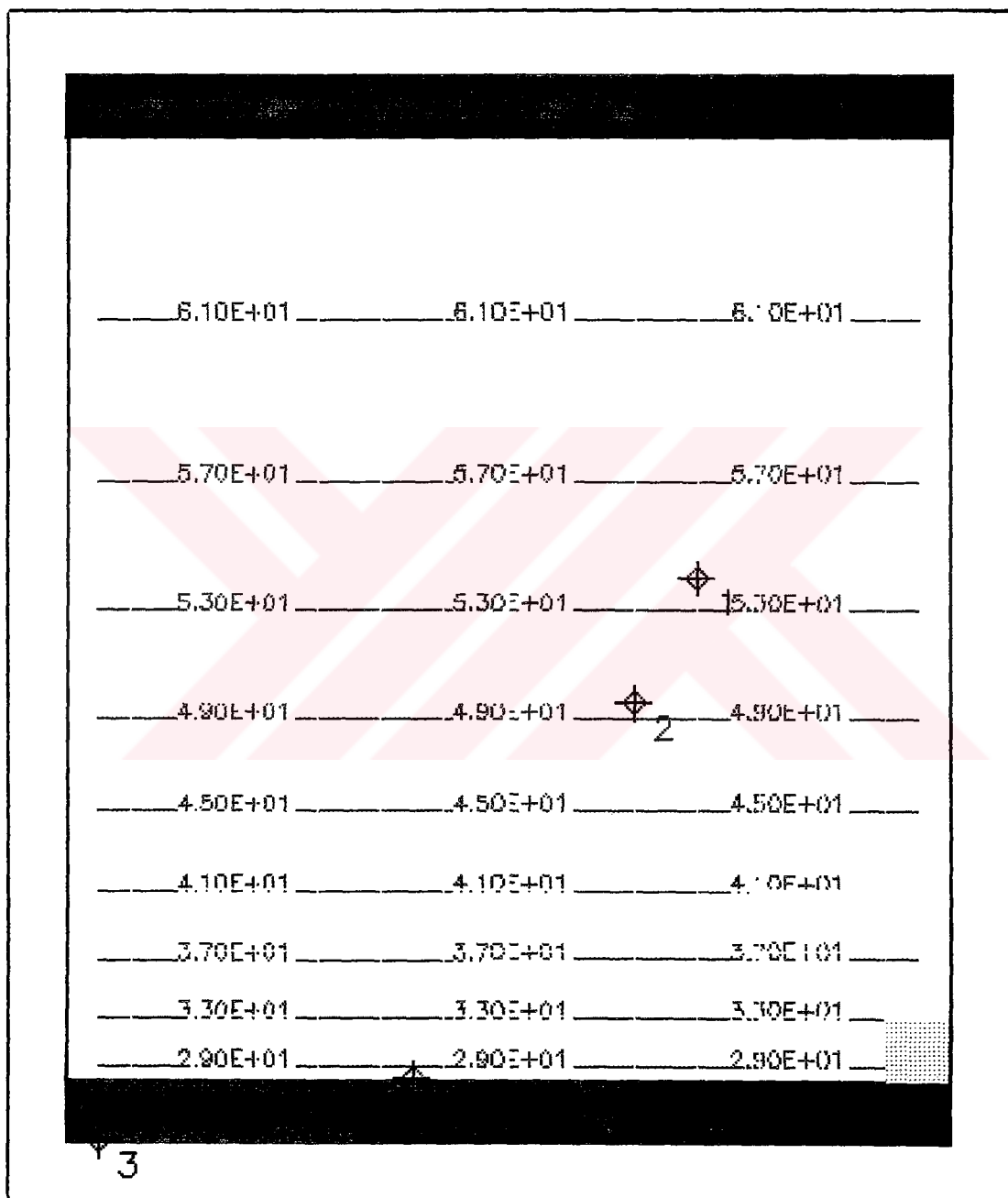
Figure 5.7 The calculated water table elevations in the case of Model A
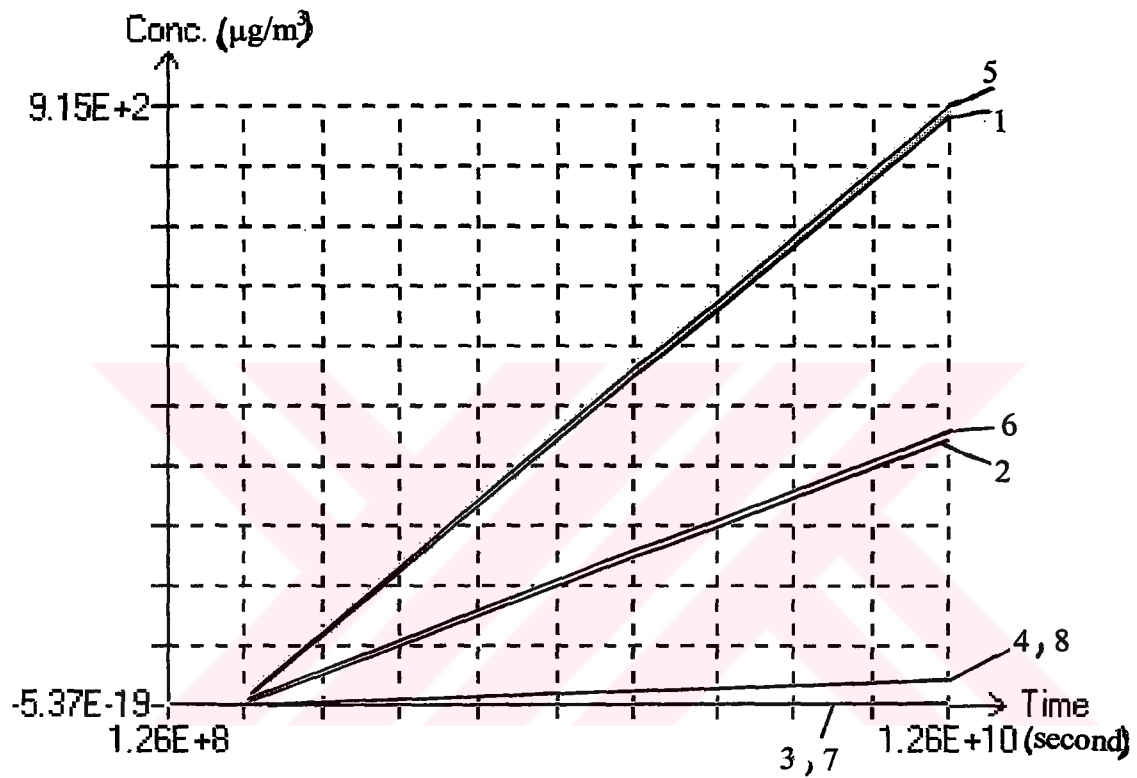
1, 2, 3, 4, 5, 6, 7 and 8 are numbers of observation wells.

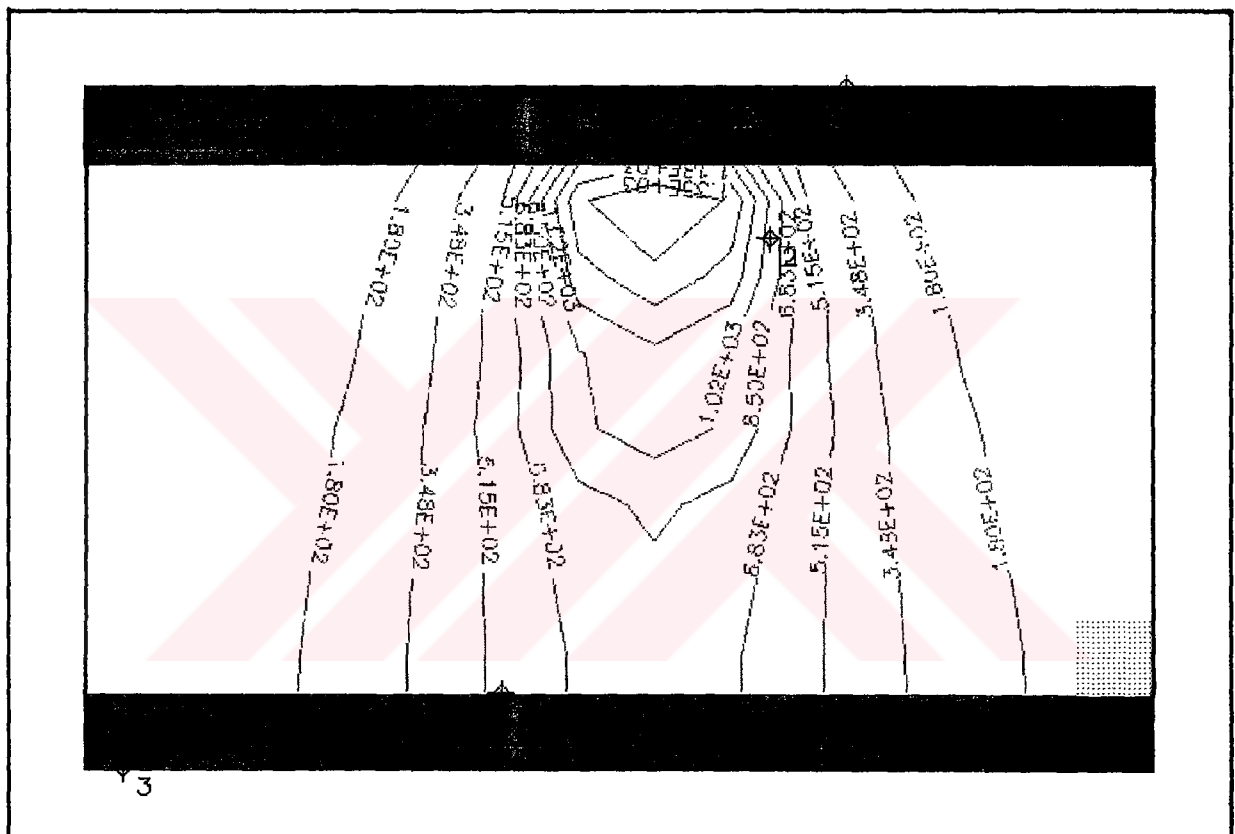**Figure 5.8** The concentration variations at different observation wells in the case of Model A
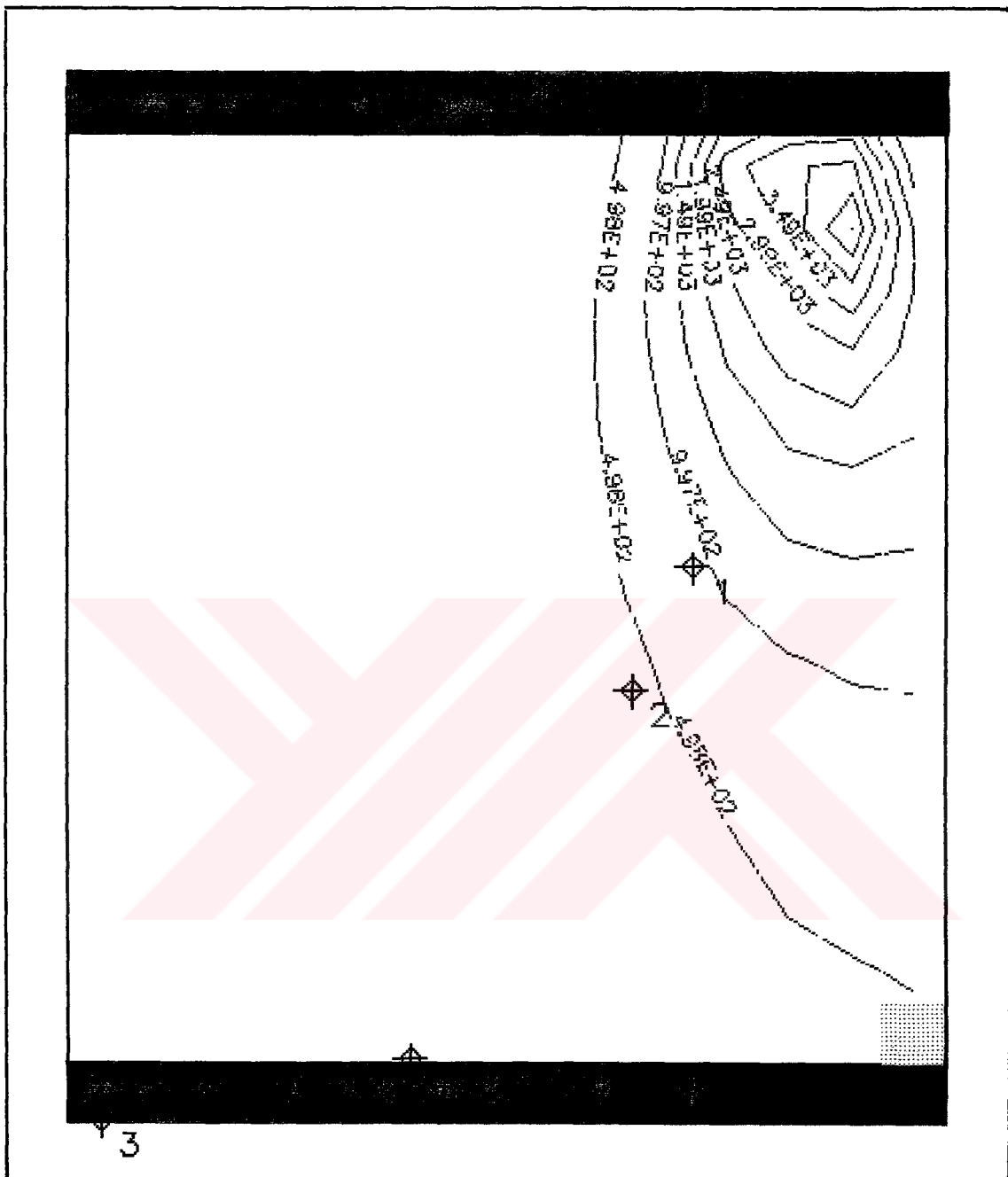
Figure 5.9 The curves of equal concentration in the first layer for Model A
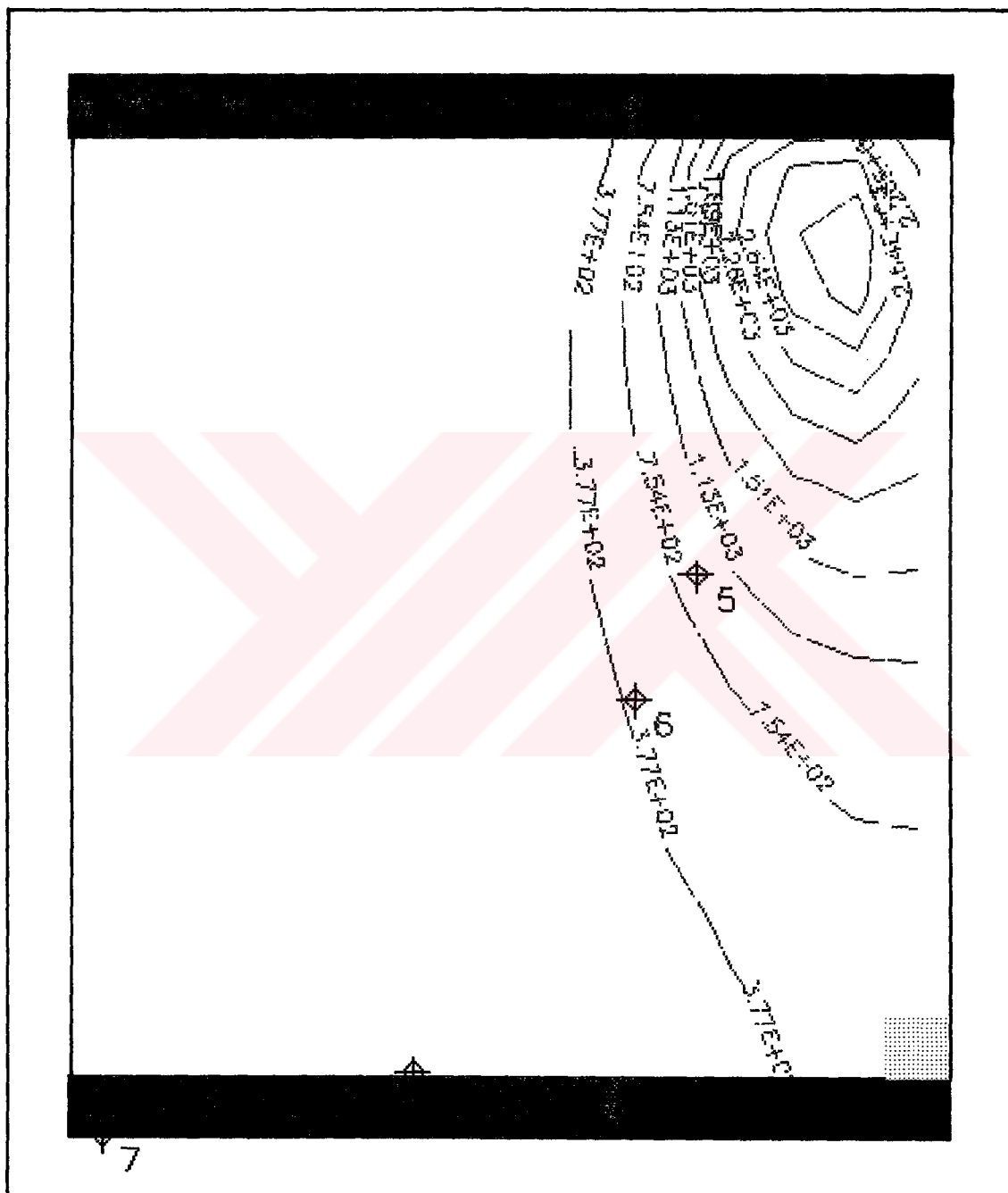
Figure 5.10 The curves of equal concentration in the second layer for Model A

5.2.2. Results obtained with Model B

The calculated water table elevations are represented in Figure 5.11.

Figure 5.12 shows the concentration variations at different observation wells.

The curves of equal concentration in the first layer are represented in figure 5.13.

Figure 5.14 represents the curves of equal concentration in the second layer.
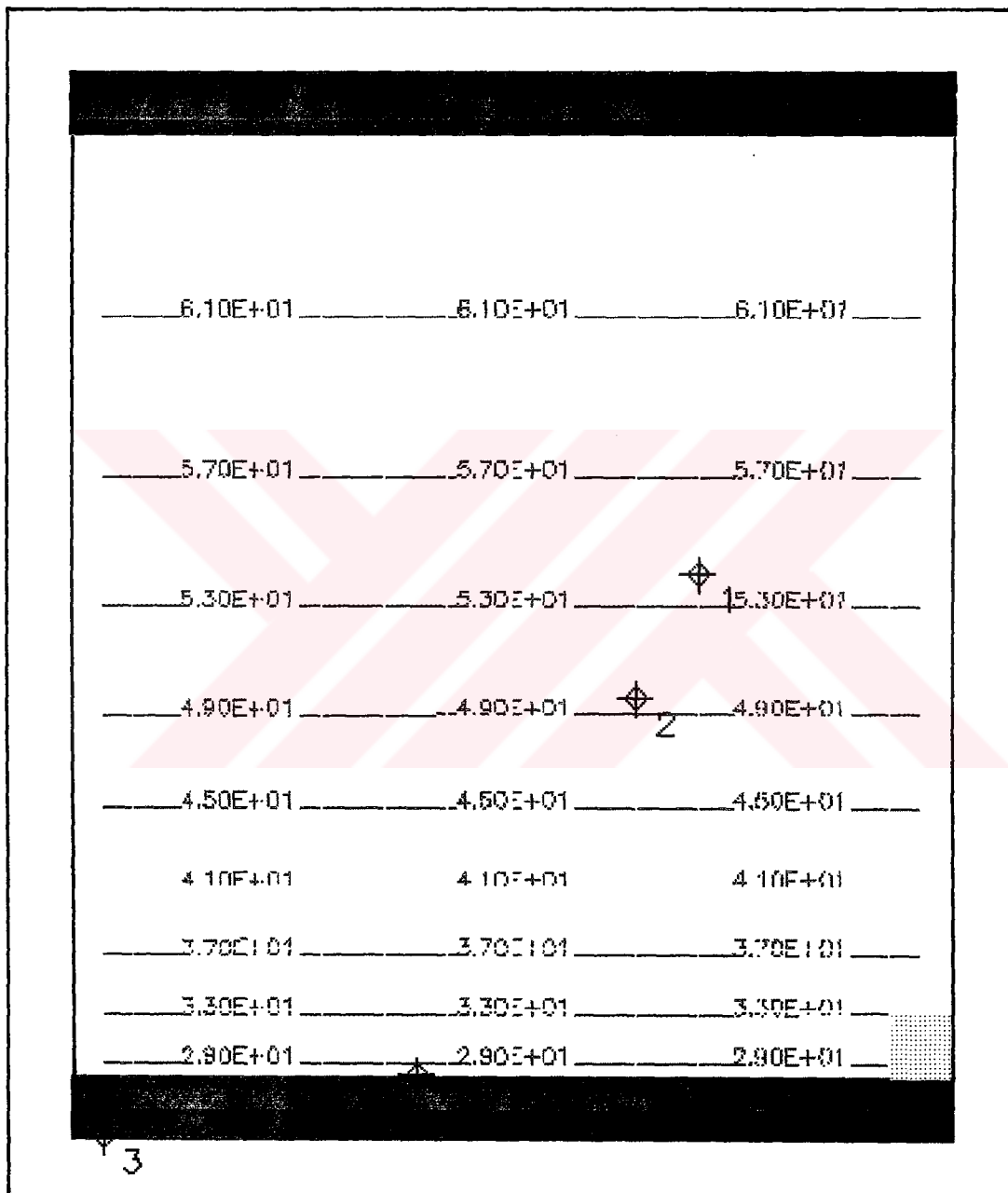
Figure 5.11 The calculated water table elevations in the case of Model B

1, 2, 3, 4, 5, 6, 7 and 8 are numbers of observation wells.

Figure 5.12 The concentration variations at different observation wells in the case of Model B

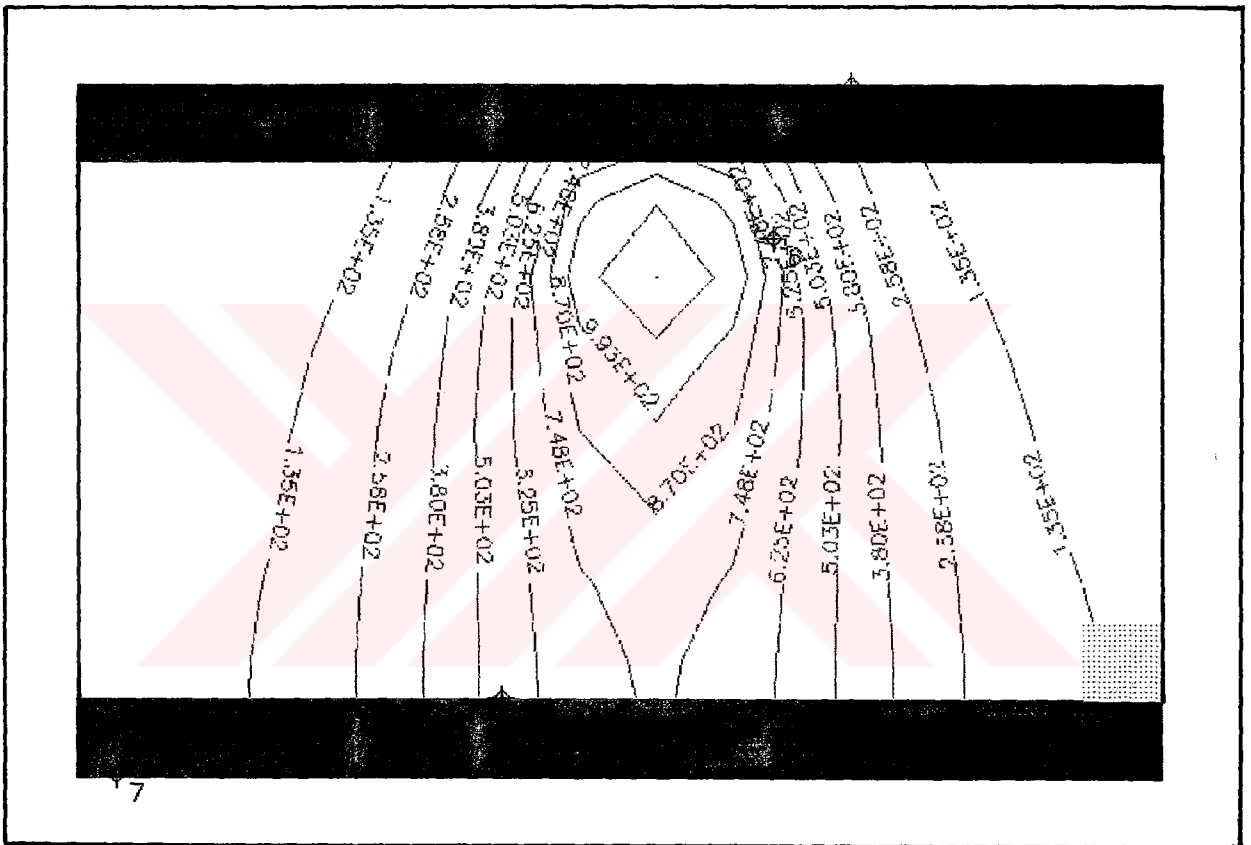**Figure 5.13** The curves of equal concentration in the first layer for Model B

Figure 5.14 The curves of equal concentration in the second layer for Model B
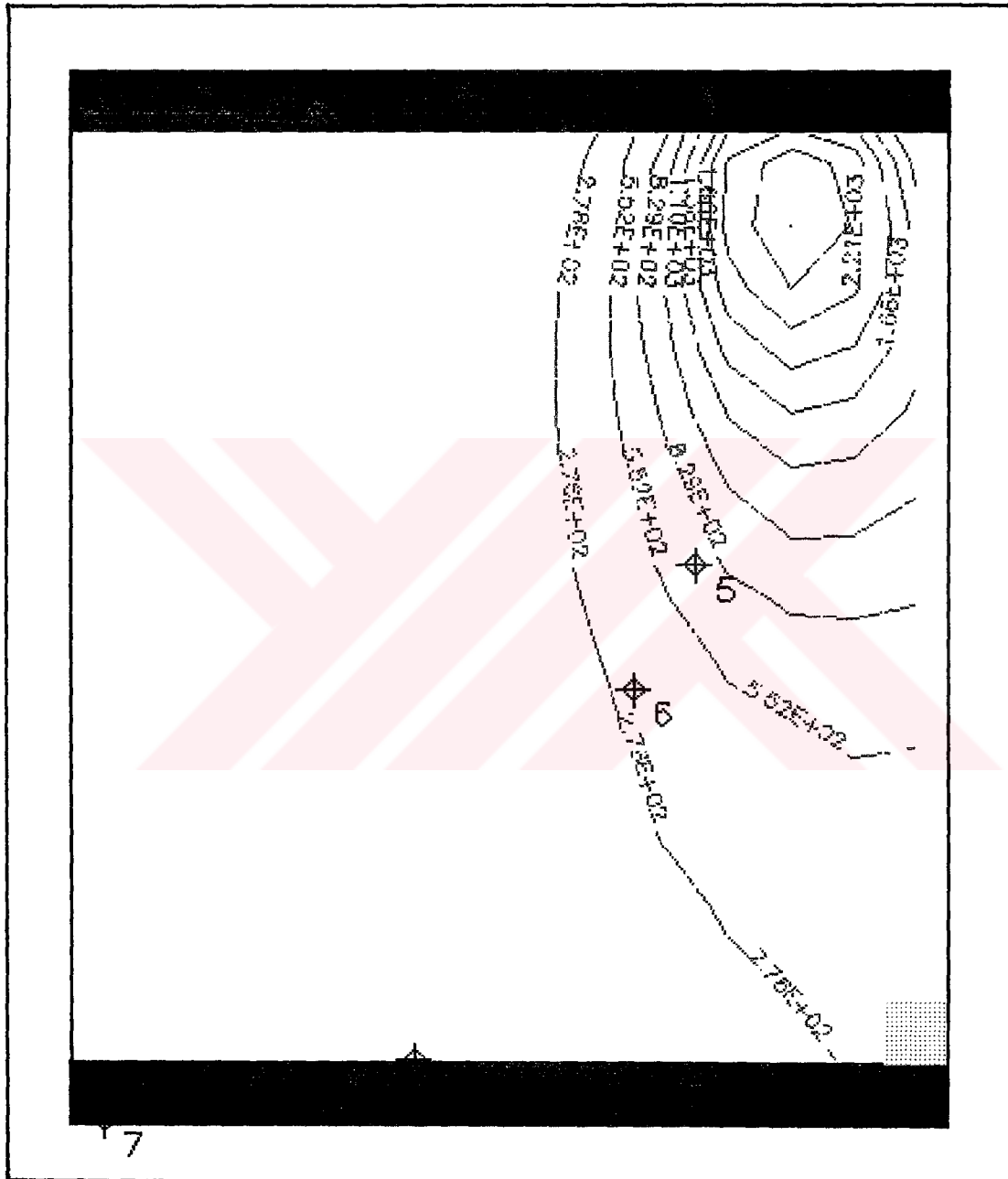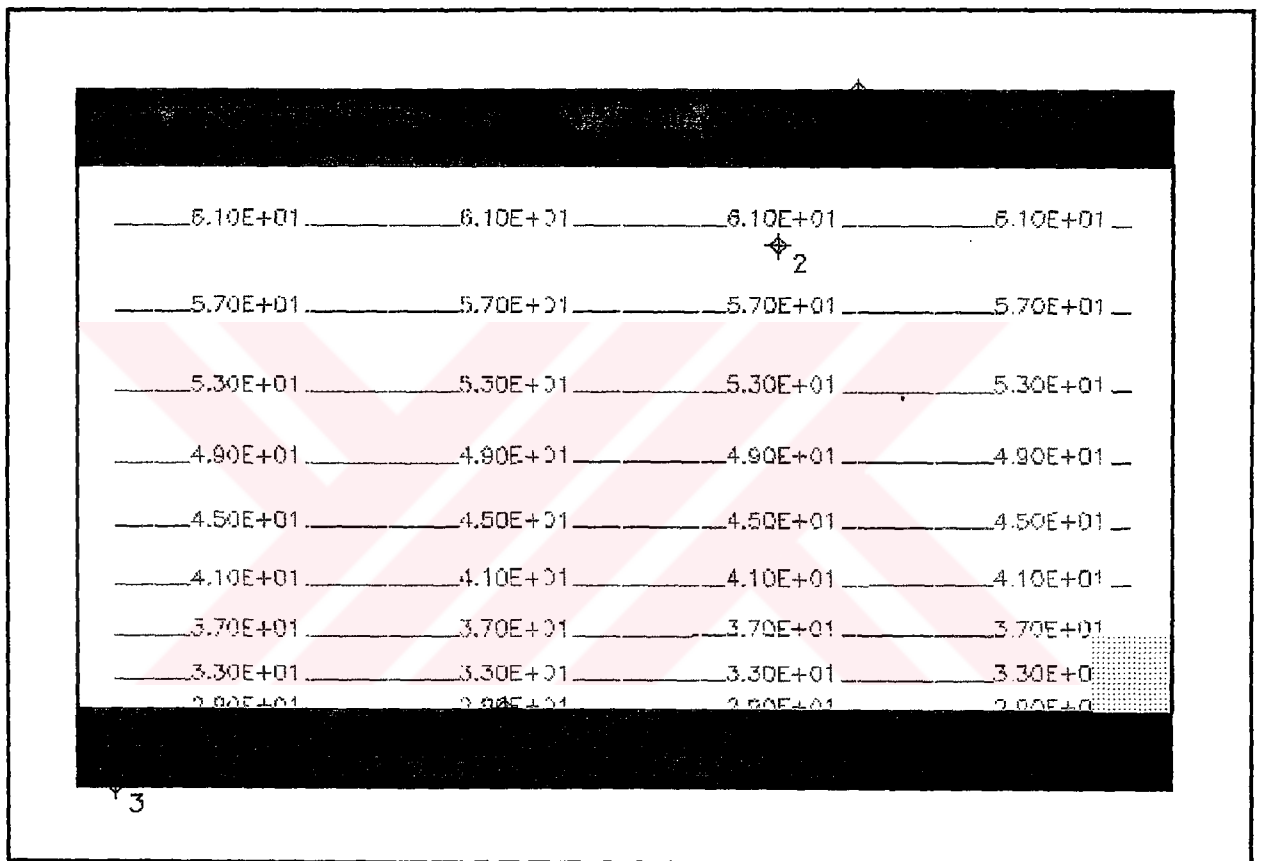
5.2.3. Results obtained with Model C

Figure 5.15 represents the calculated water table elevations.

The concentration variations at different observation wells are given in figure 5.16.

Figure 5.17 shows the curves of equal concentration in the first layer.

The curves of equal concentration in the second layer are represented in figure 5.18.
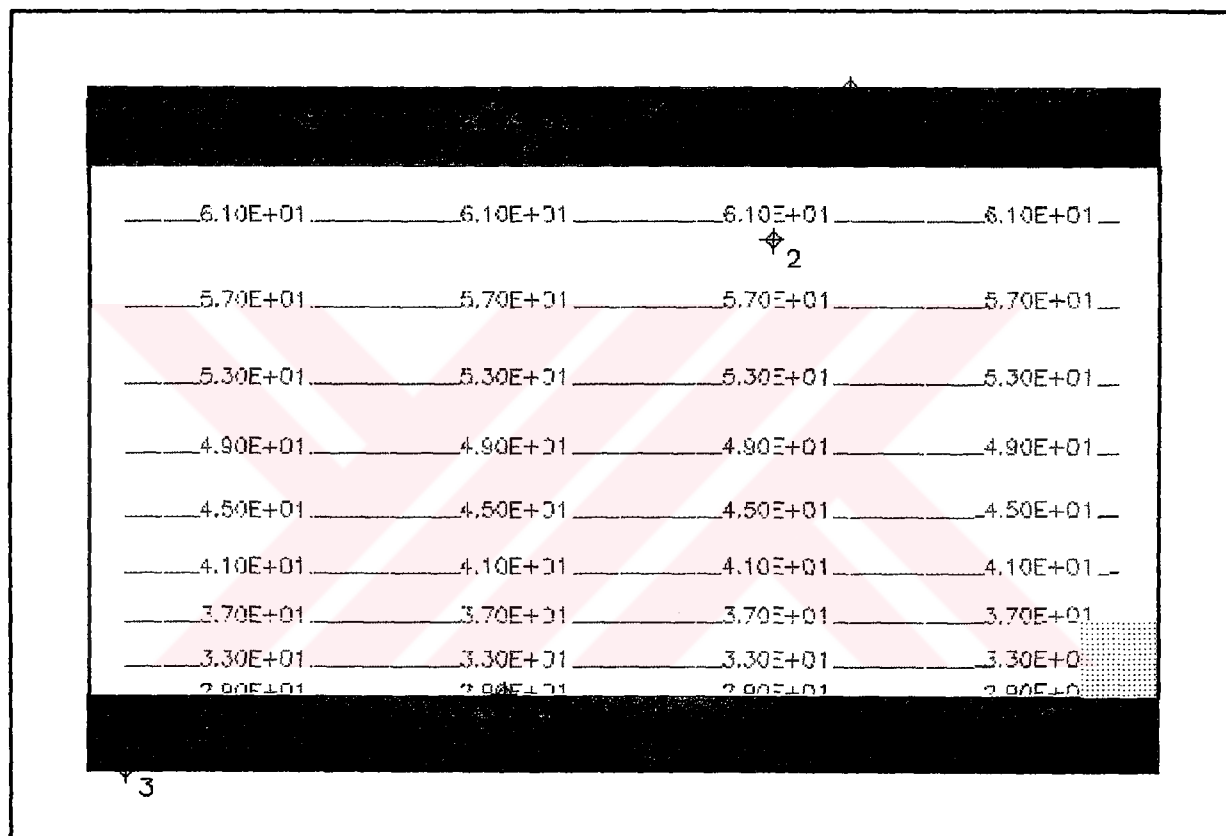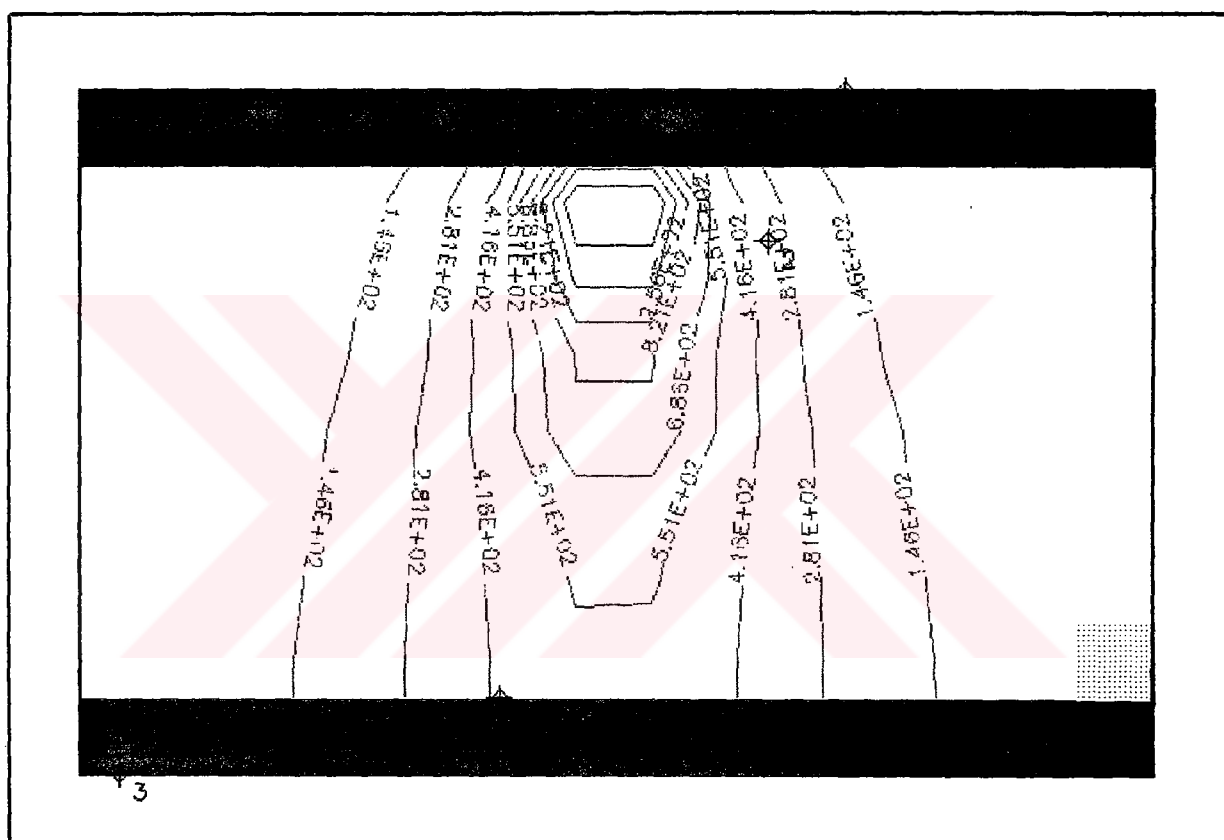
Figure 5.15 The calculated water table elevations in the case of Model C
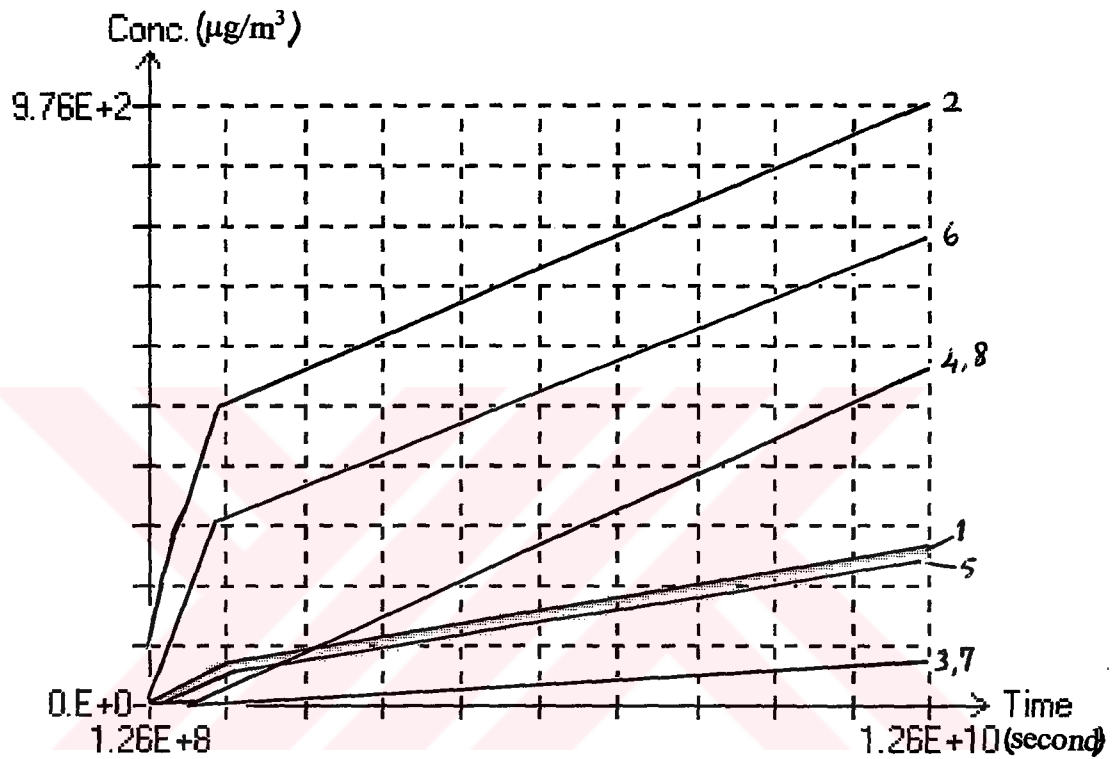
1, 2, 3, 4, 5, 6, 7 and 8 are numbers of observation wells.

Figure 5.16 The concentration variations at different observation wells in the case of Model C

Figure 5.17 The curves of equal concentration in the first layer for Model C
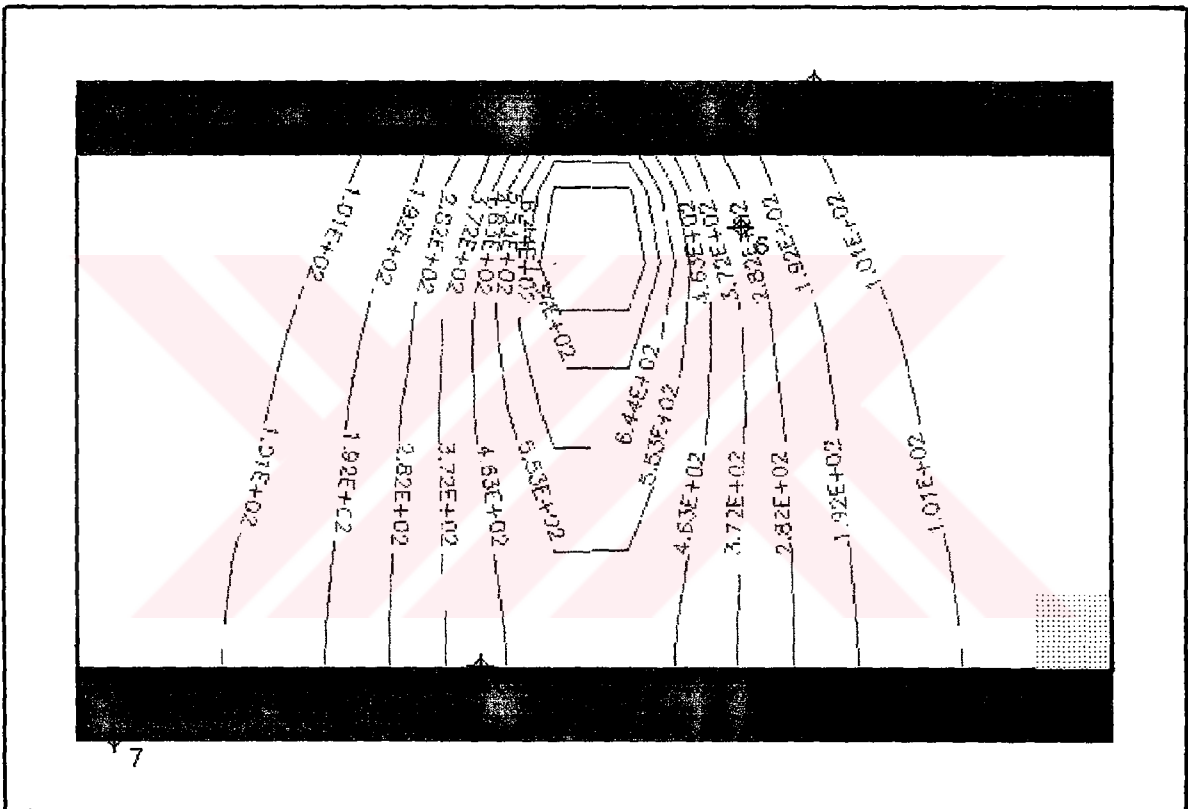
Figure 5.18 The curves of equal concentration in the second layer for Model C

5.2.4. Results obtained with Model D

The calculated water table elevations are shown in figure 5.19.

Figure 5.20 represents the concentration variations at different observation wells.

The curves of equal concentration in the first layer are shown in figure 5.21.

Figure 5.22 shows the curves of equal concentration in the second layer.

Figure 5.19 The calculated water table elevations in the case of Model D
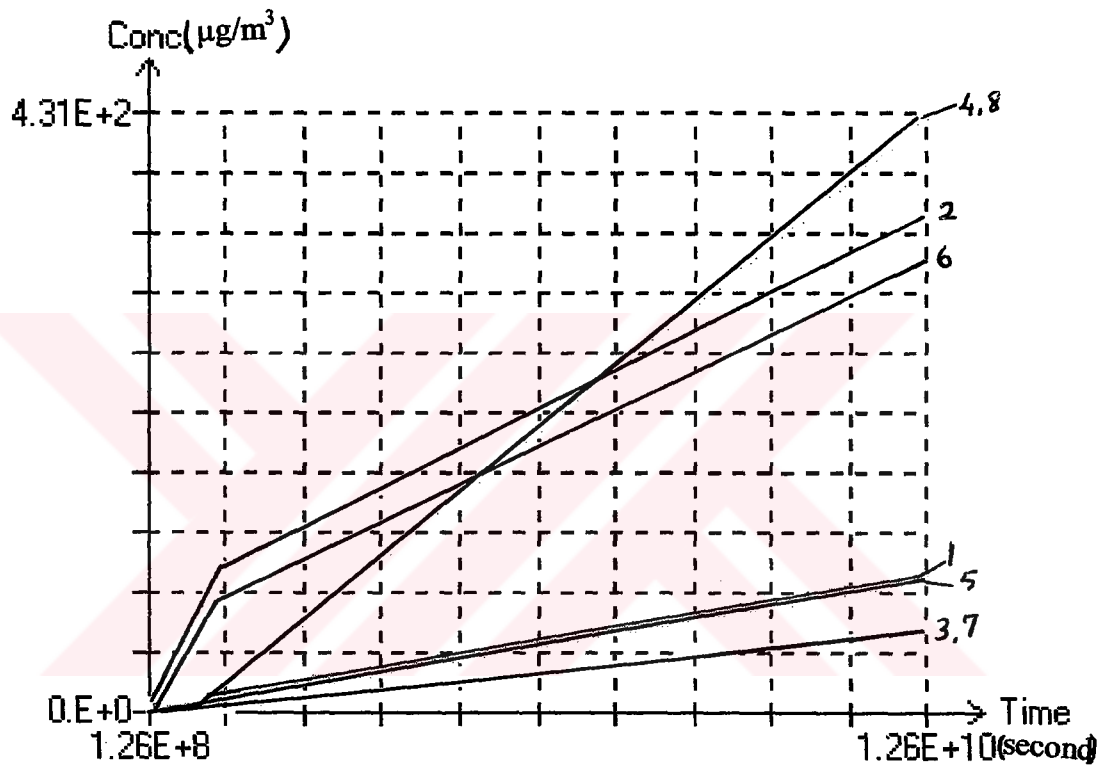
1, 2, 3, 4, 5, 6, 7 and 8 are numbers of observation wells.

Figure 5.20   The concentration variations at different observation wells
in the case of Model D

Figure 5.21 The curves of equal concentration in the first layer for Model D

Figure 5.22 The curves of equal concentration in the second layer for Model D

5.3. Numerical Results with the Time Parameter 40 years

The following results are obtained for a period of 40 years $(=T_2)$.

Water table elevations are in (m).

Concentrations in $\mu g/m^3$ are given in terms of time expressed in second.

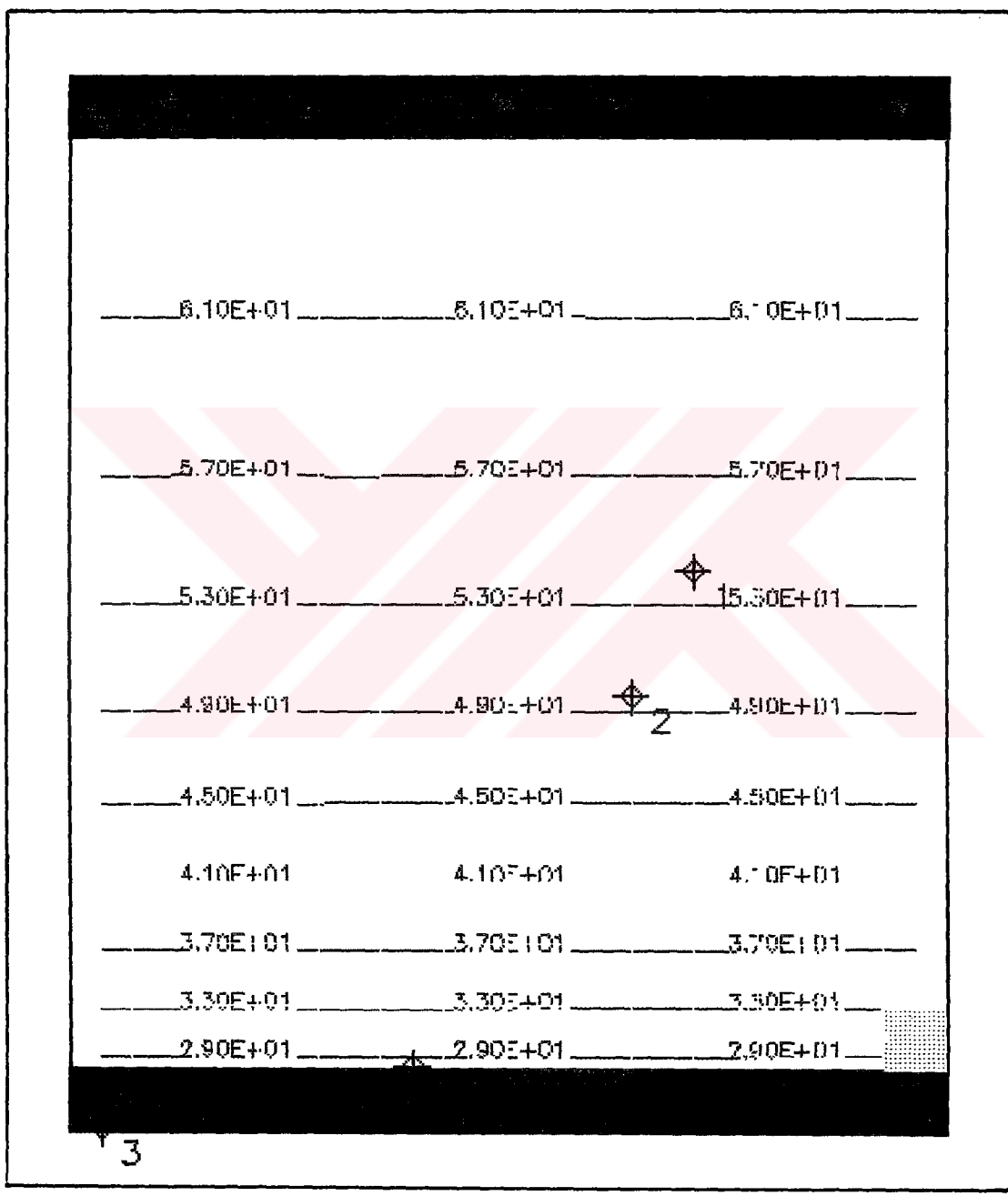The sign ϕ denotes the location of relevant observation well.

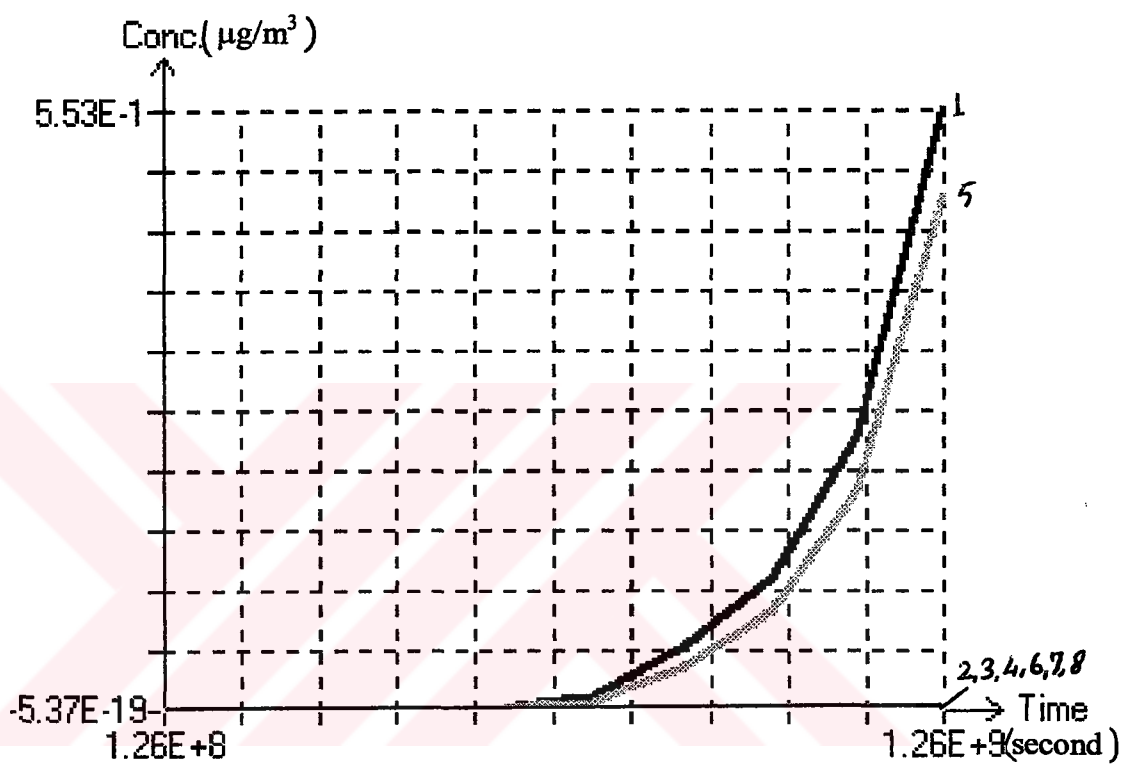### 5.3.1. Results obtained with Model A

The calculated water table elevations are shown in figure 5.23.

Figure 5.24 represents the concentration variations at different observation wells.

The curves of equal concentration in the first layer are shown in figure 5.25.

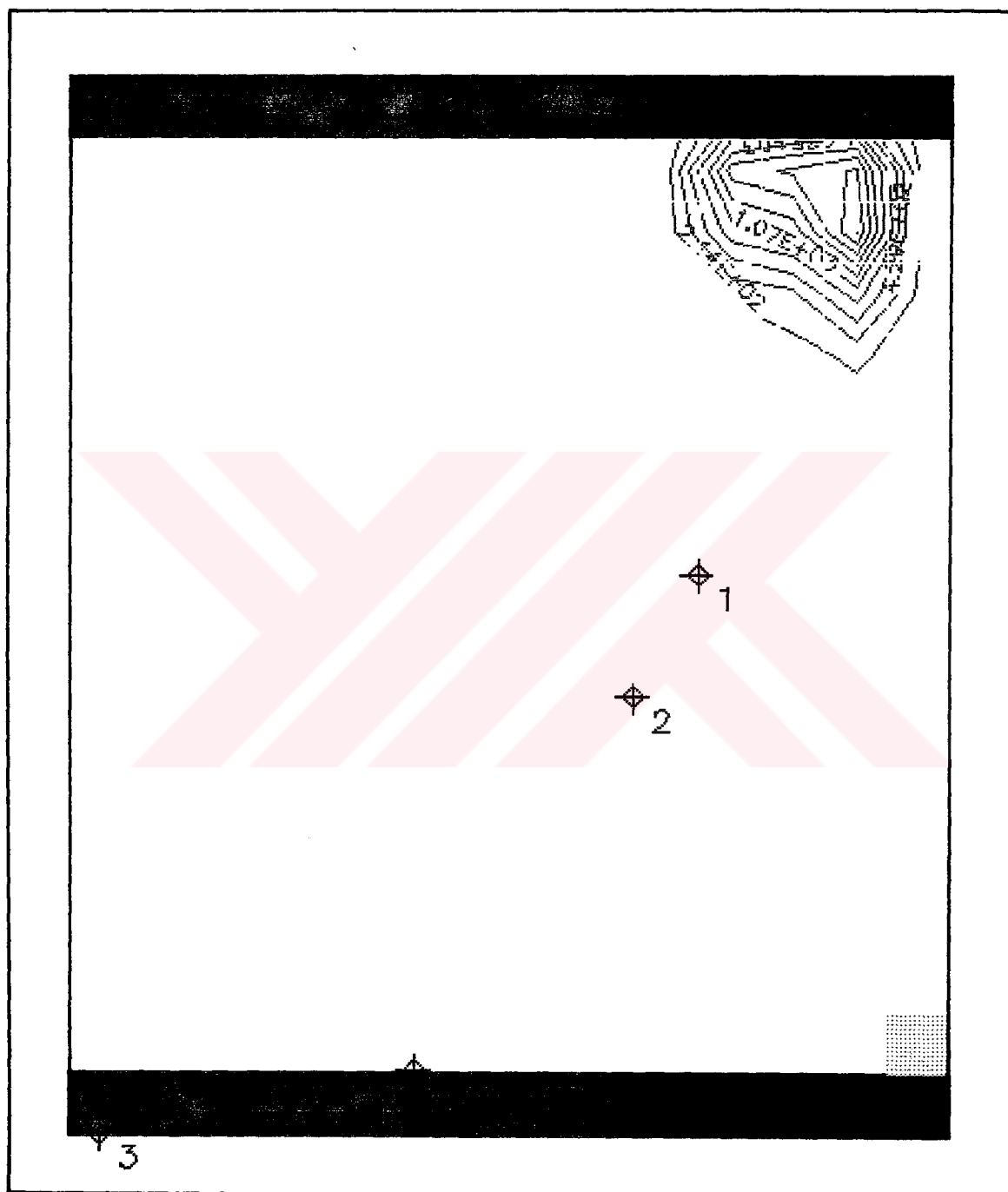Figure 5.26 shows the curves of equal concentration in the second layer.

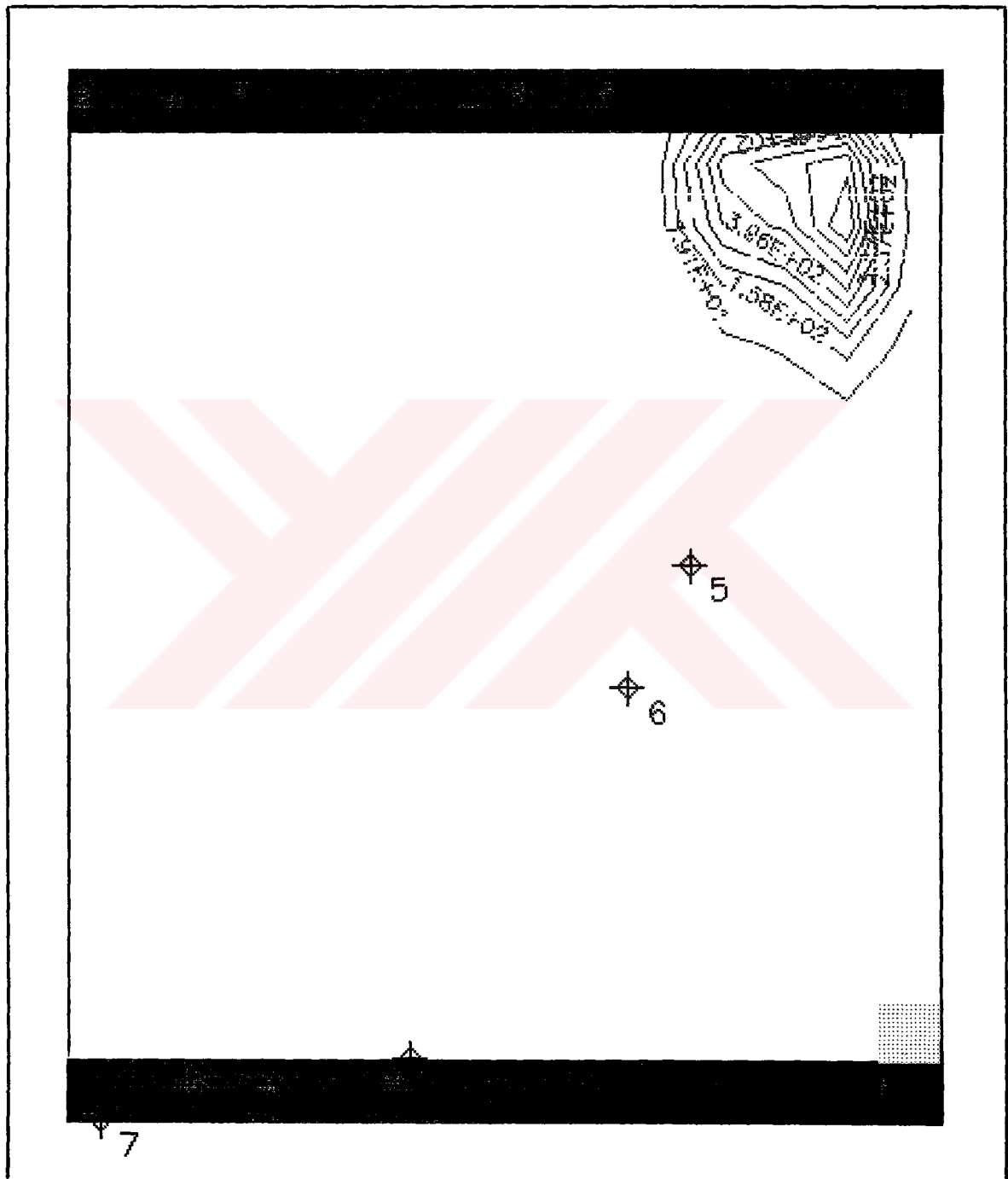**Figure 5.23** The calculated water table elevations in the case of Model A

1, 2, 3, 4, 5, 6, 7 and 8 are numbers of observation wells.

Figure 5.24 The concentration variations at different observation wells in the case of Model A

Figure 5.25 The curves of equal concentration in the first layer for Model A

Figure 5.26 The curves of equal concentration in the second layer for Model A

5.3.2. Results obtained with Model B

The calculated water table elevations are shown in figure 5.27.

Figure 5.28 represents the concentration variations at different observation wells.

The curves of equal concentration in the first layer are shown in figure 5.29.

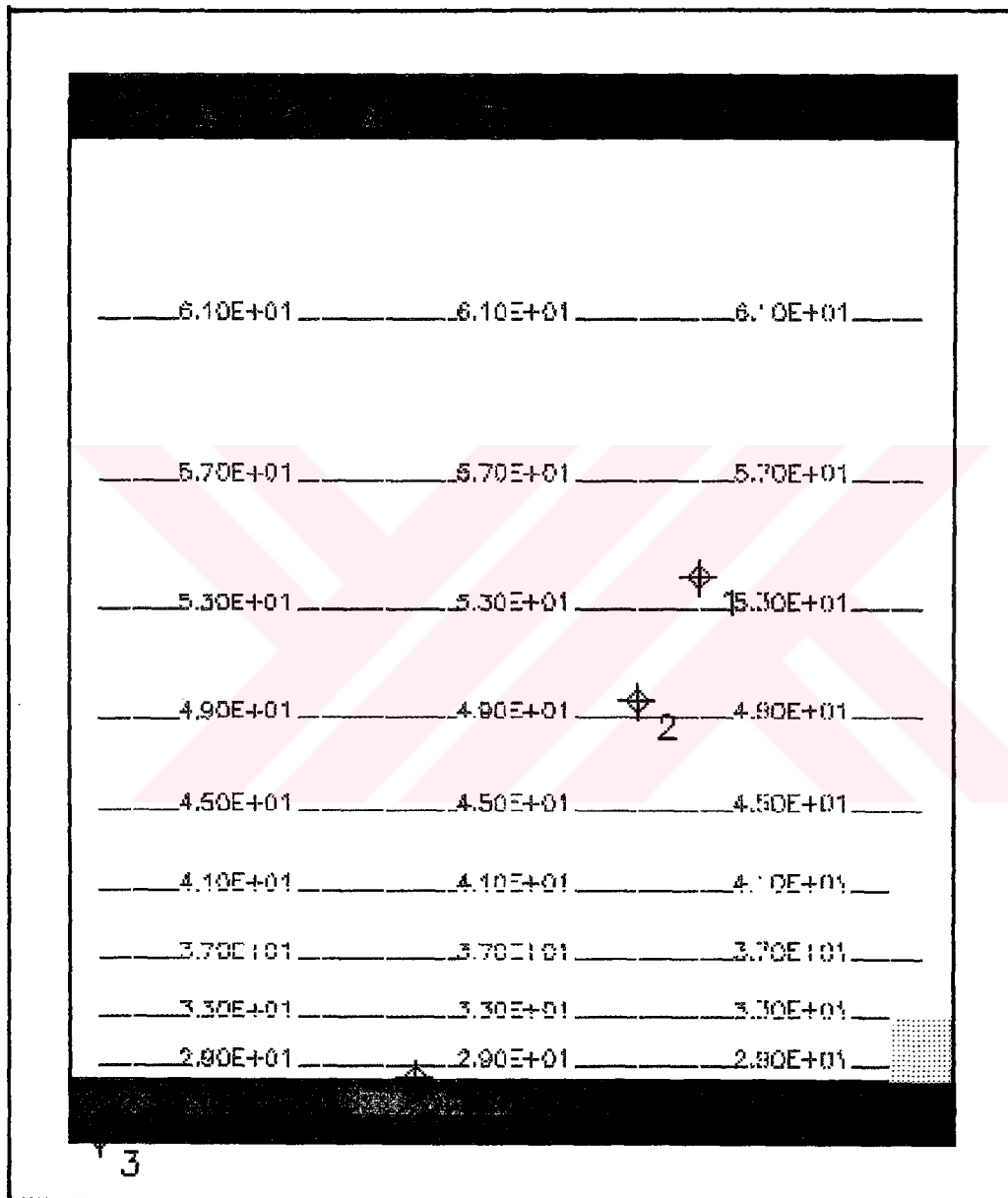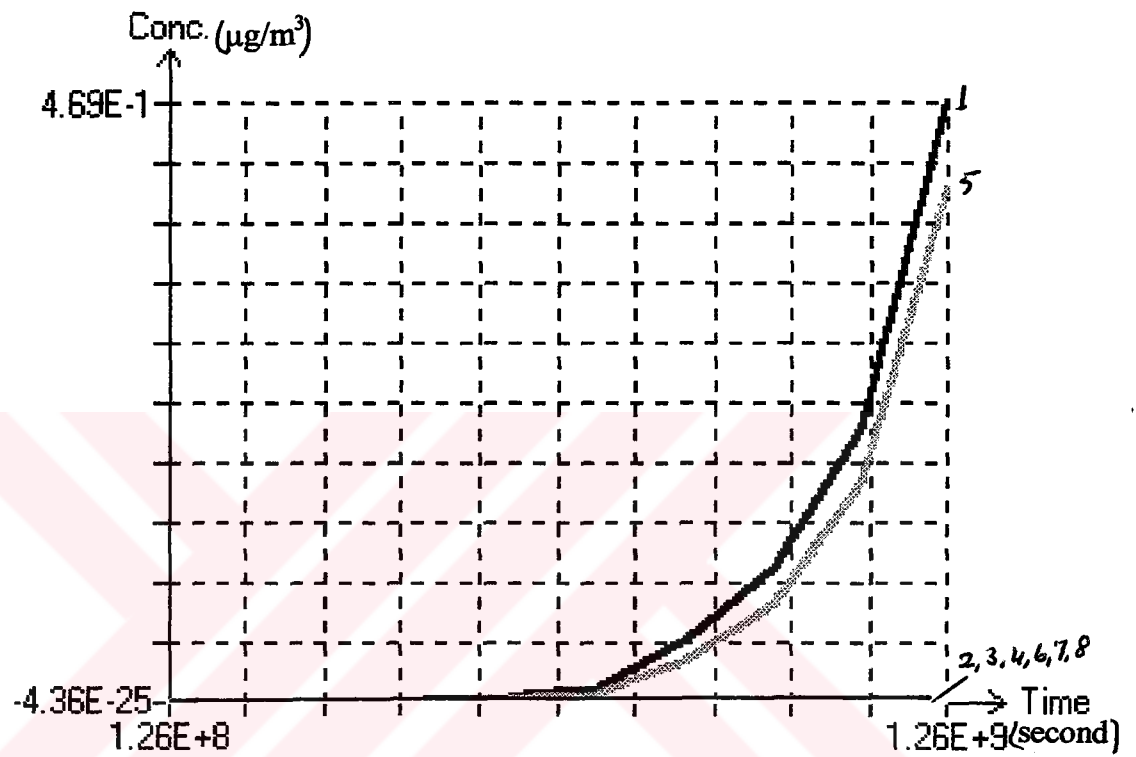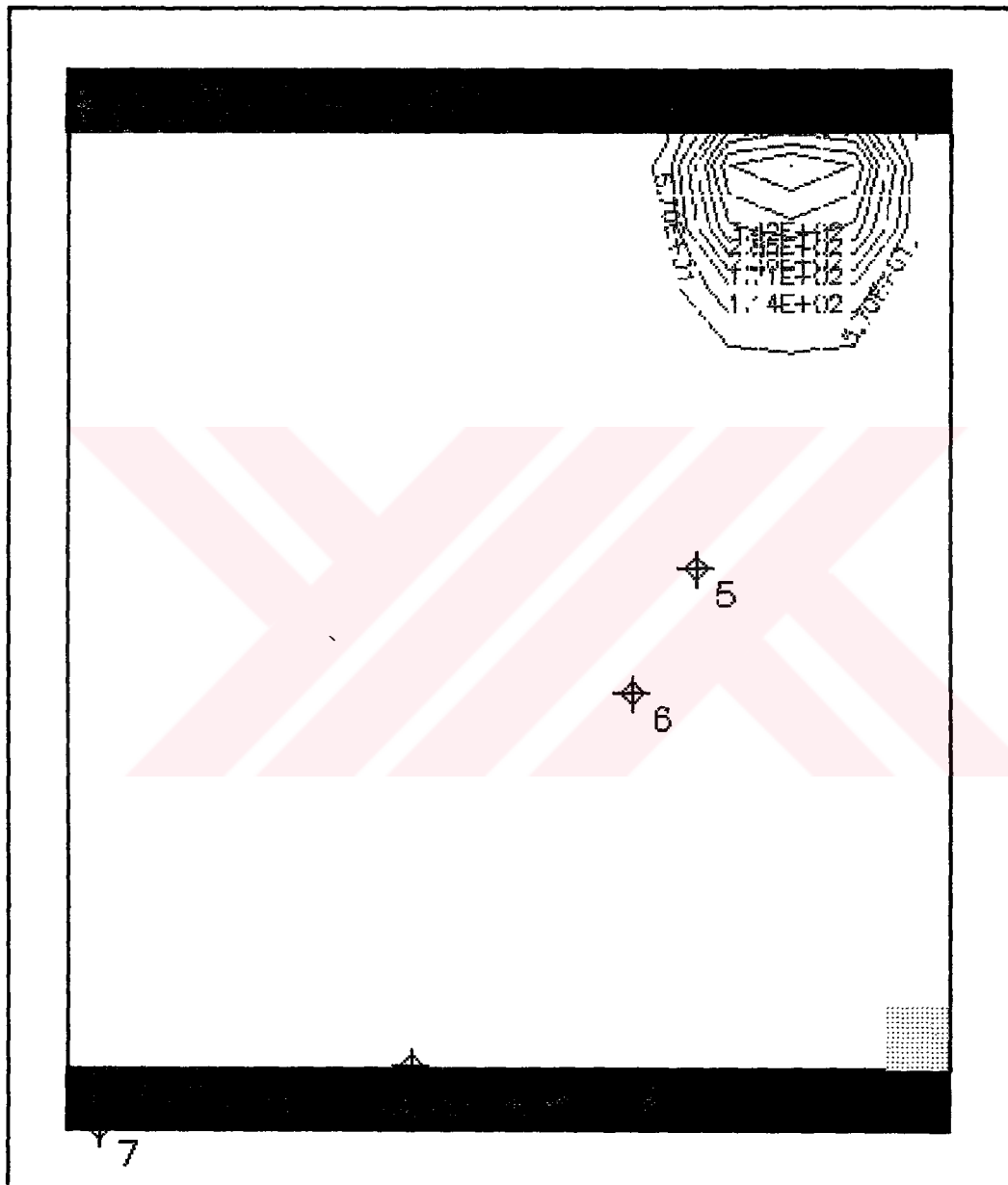Figure 5.30 shows the curves of equal concentration in the second layer.

Figure 5.27   The calculated water table elevations in the case of Model B

Figure 5.28 The concentration variations at different observation wells in the case of Model B

Figure 5.29 The curves of equal concentration in the first layer for Model B

Figure 5.30 The curves of equal concentration in the second layer for Model B
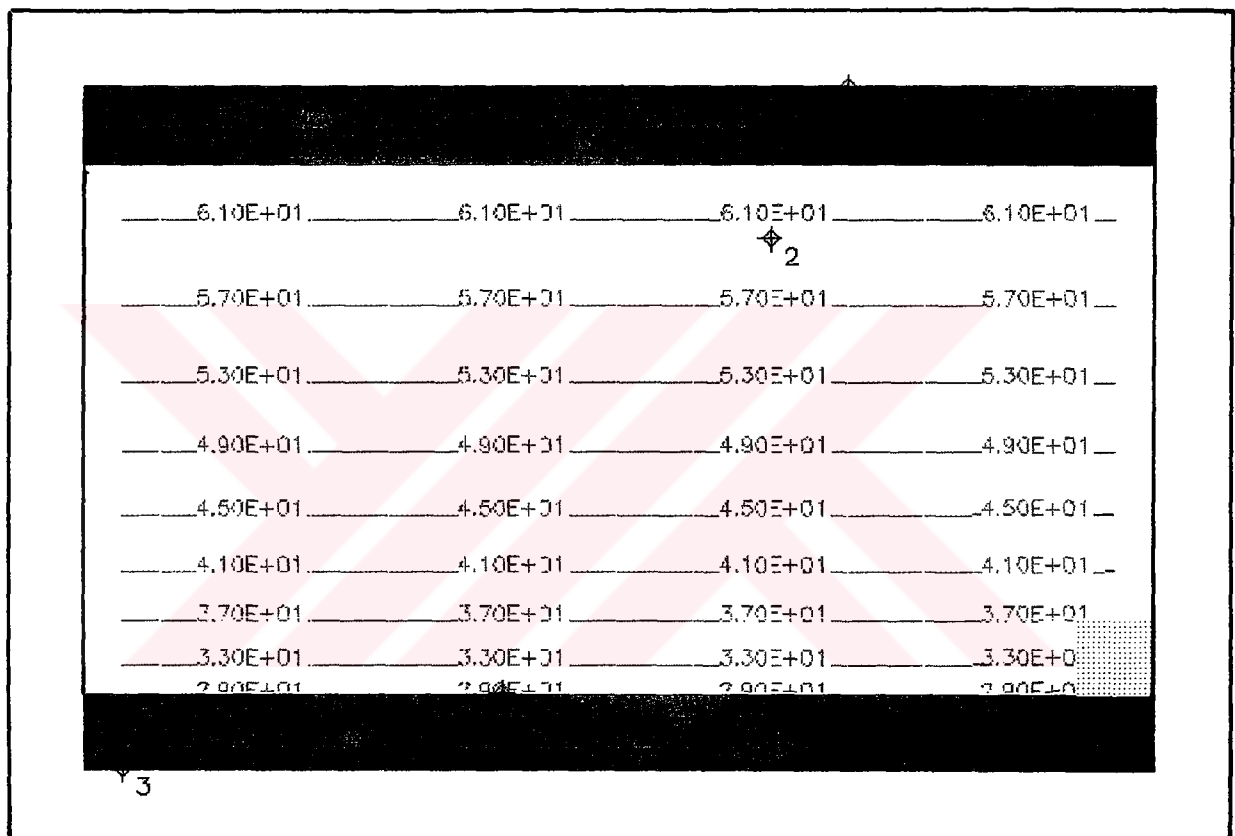
5.3.3. Results obtained with the Model C

The calculated water table elevations are shown in figure 5.31.

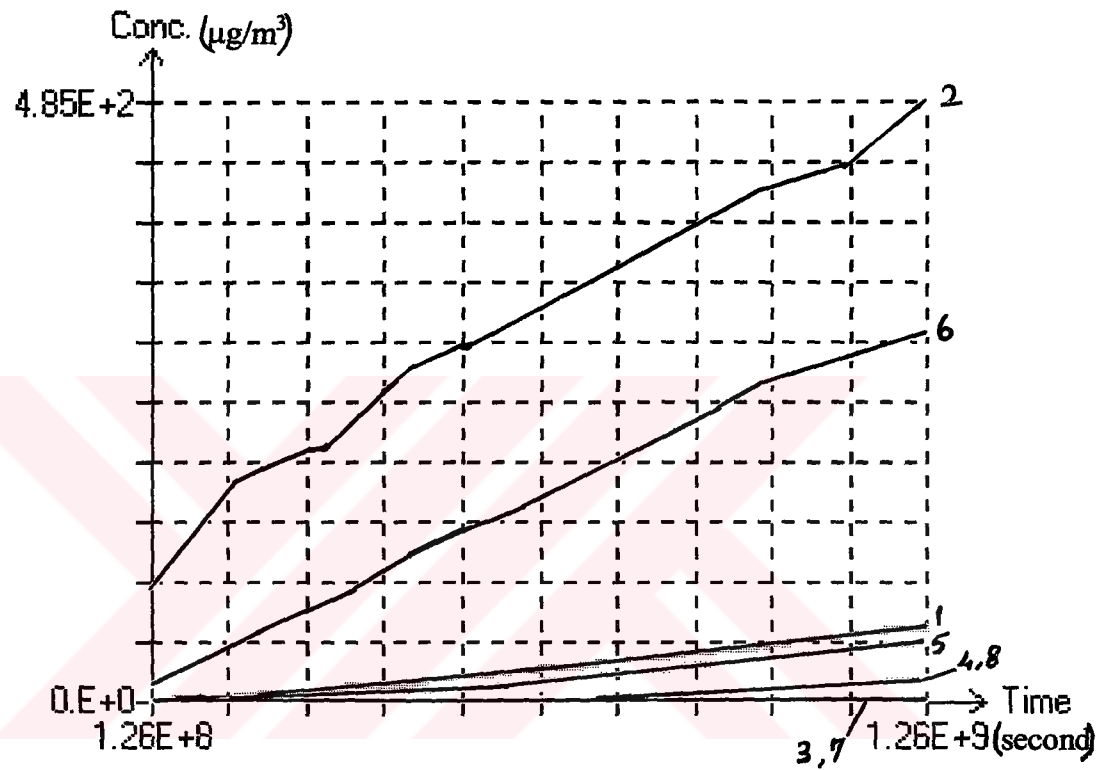Figure 5.32 represents the concentration variations at different observation wells.

The curves of equal concentration in the first layer are shown in figure 5.33.

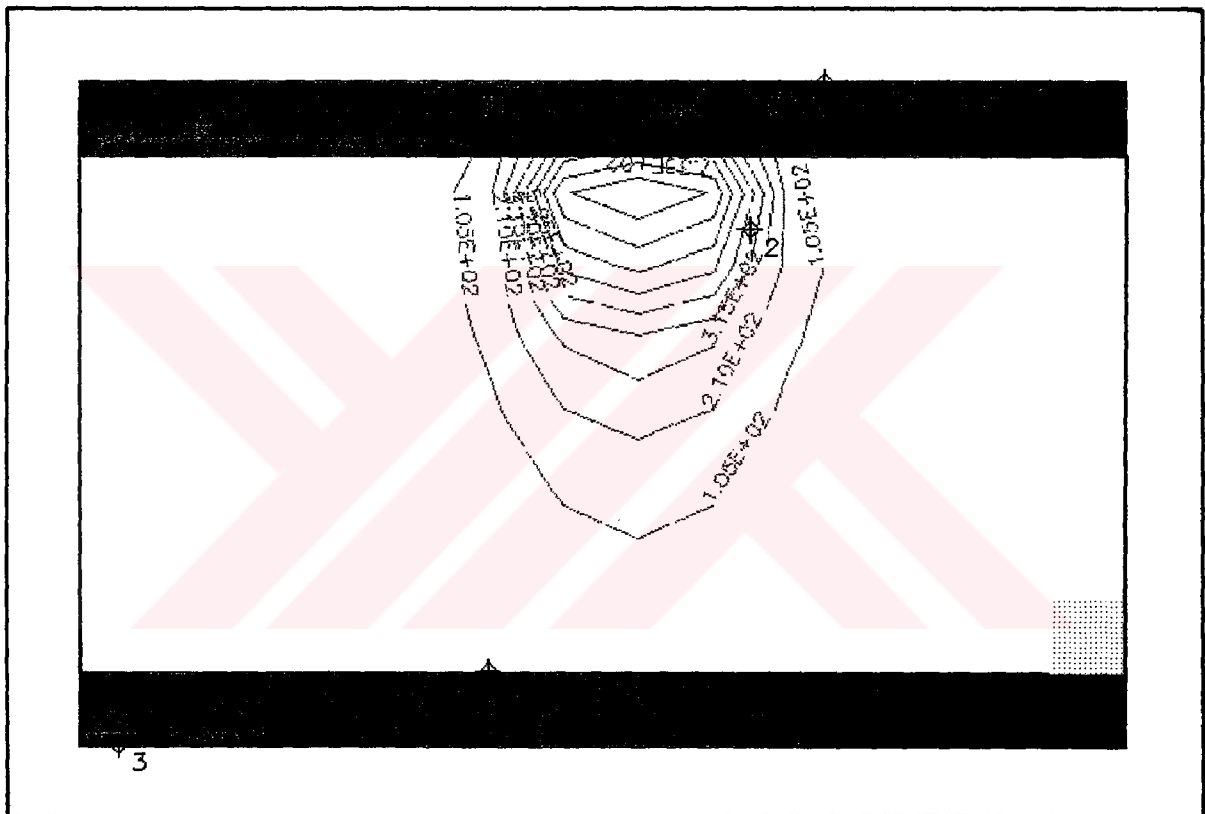Figure 5.34 shows the curves of equal concentration in the second layer.

Figure 5.31 The calculated water table elevations in the case of Model C

Figure 5.32 The concentration variations at different observation wells in the case of Model C

1, 2, 3, 4, 5, 6, 7 and 8 are numbers of observation wells.

Figure 5.33 The curves of equal concentration in the first layer for Model C

Figure 5.34 The curves of equal concentration in the second layer for Model C

5.3.4. Results obtained with Model D

The calculated water table elevations are shown in figure 5.35.

Figure 5.36 represents the concentration variations at different observation wells.

The curves of equal concentration in the first layer are shown in figure 5.37.

Figure 5.38 shows the curves of equal concentration in the second layer.

Figure 5.35 The calculated water table elevations in the case of Model D
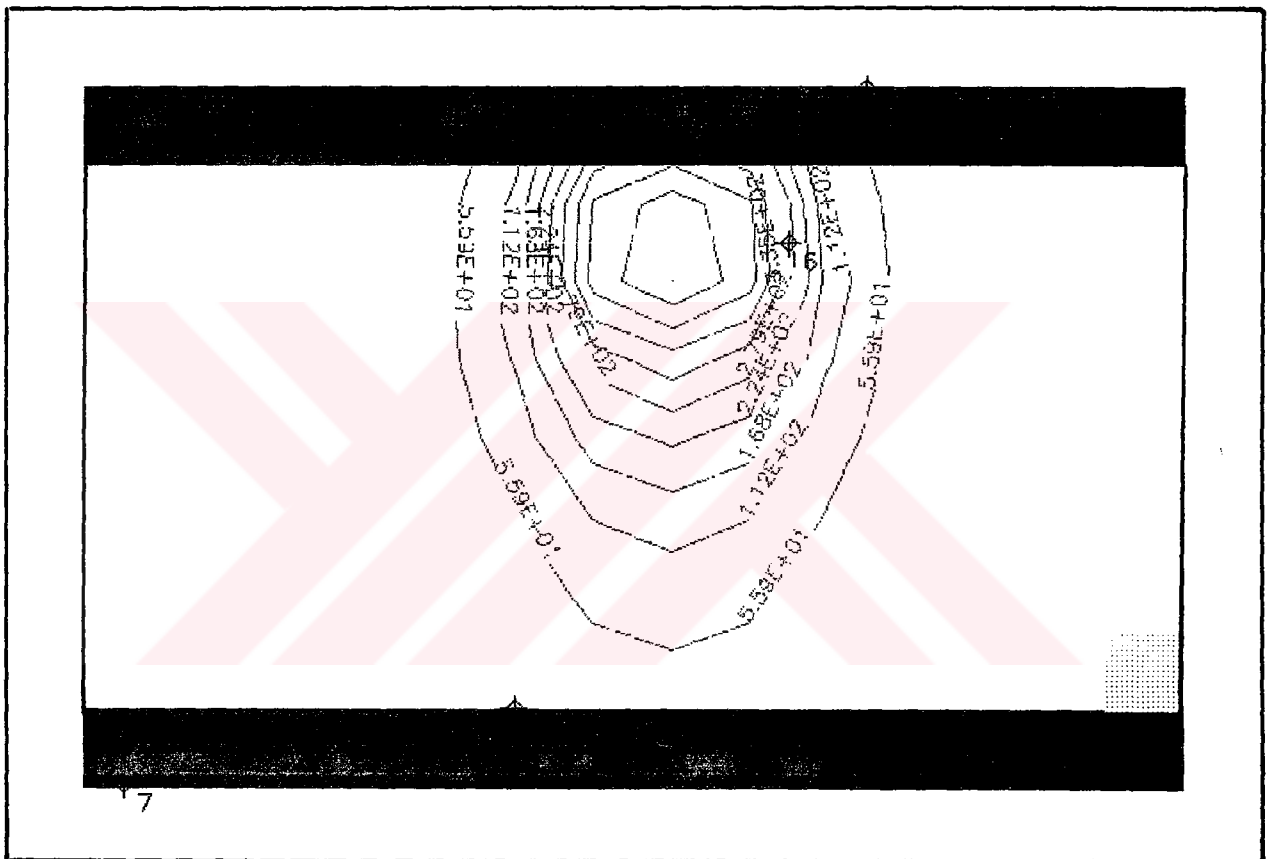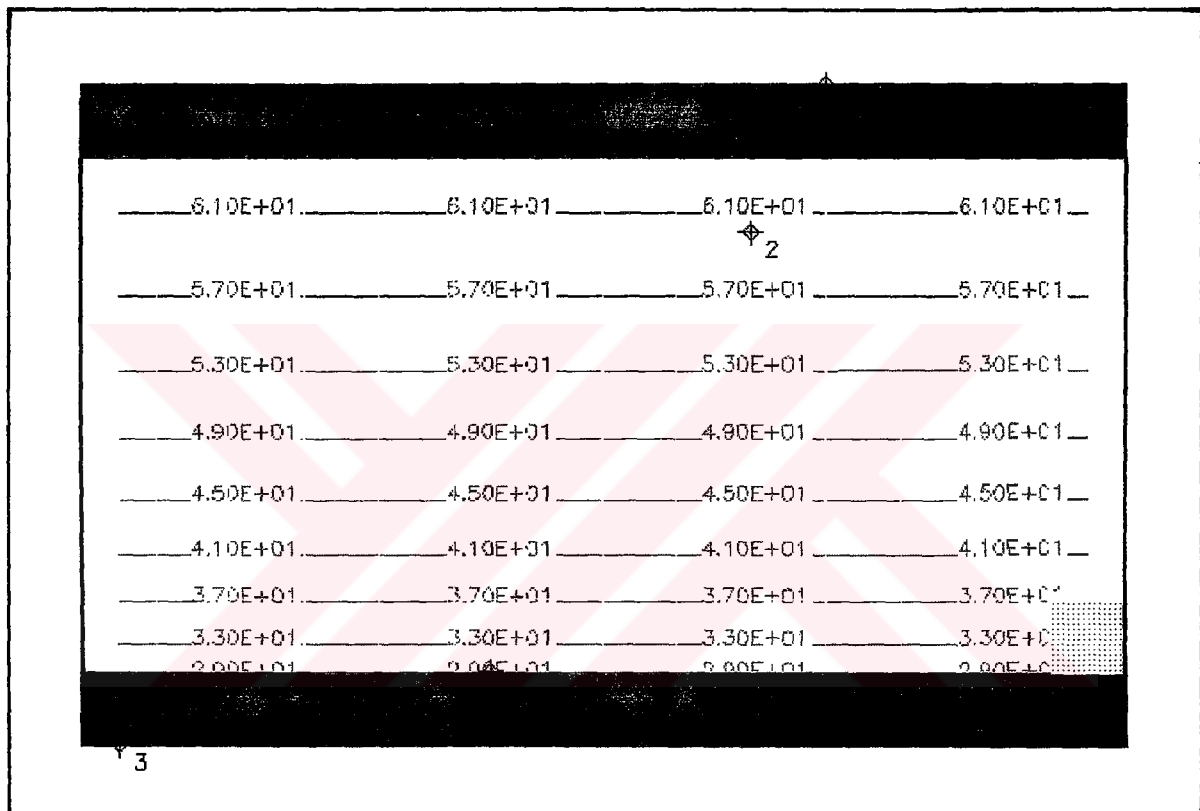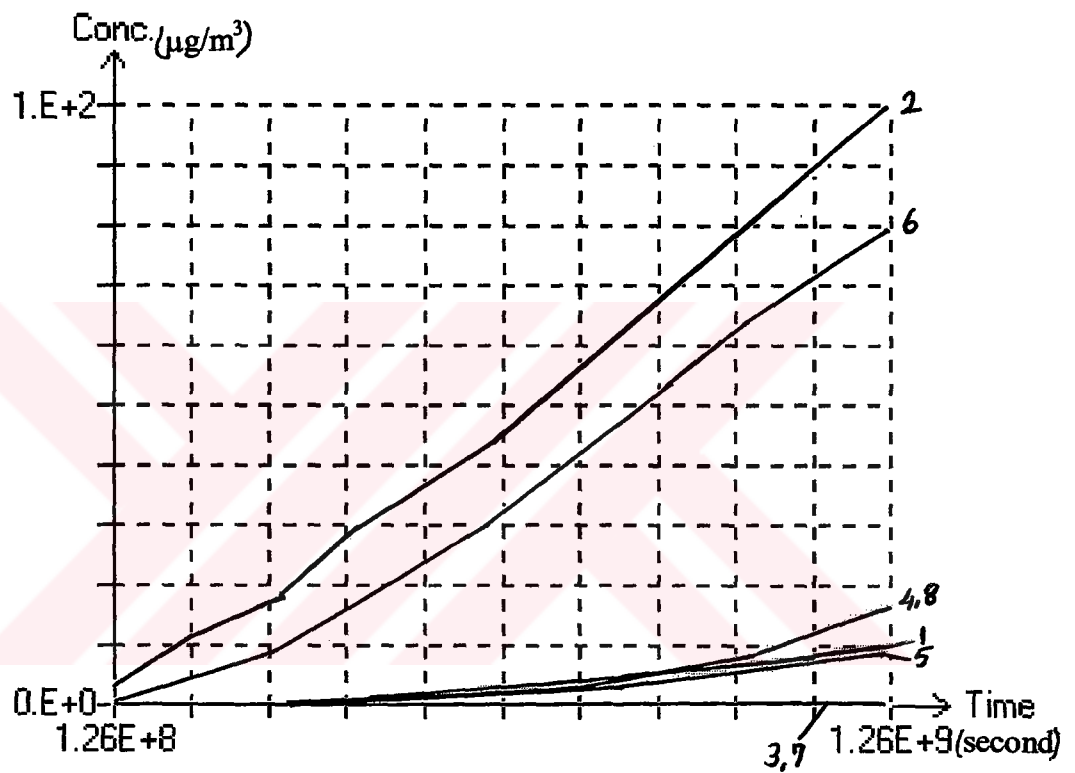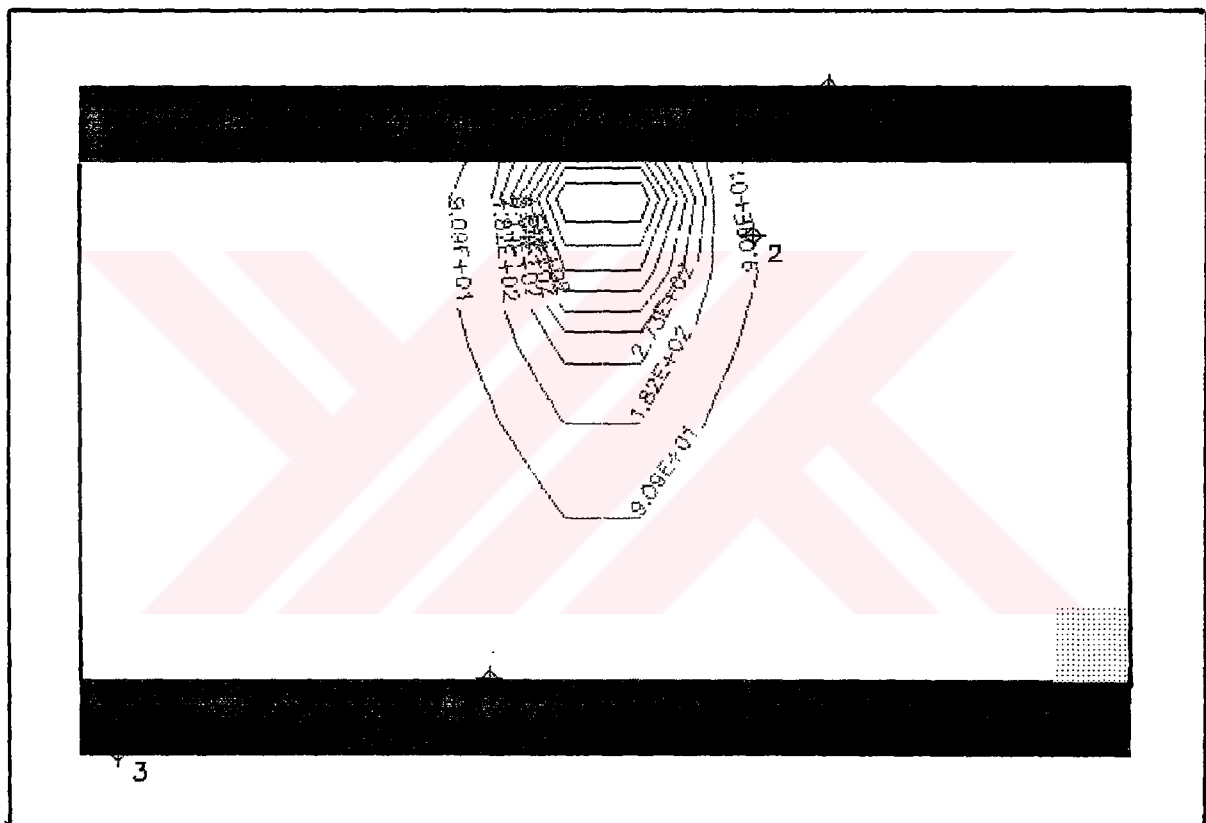
1, 2, 3, 4, 5, 6, 7 and 8 are numbers of observation wells.

Figure 5.36 The concentration variations at different observation wells in the case of Model D

**Figure 5.37** The curves of equal concentration in the first layer for Model D

Figure 5.38 The curves of equal concentration in the second layer for Model D

CHAPTER SIX

RESULTS FOR HETEROGENEOUS AQUIFER WITH HIGH PERMEABILITY

6.1 Data of the Studied Area

As shown in Figure 6.1, an aquifer system with three layers, bounded by no-flow boundaries on the North and South sides is considered. The West and East sides are bounded by rivers, which are in full hydraulic contact with the aquifer and can be considered as fixed-head boundaries. The hydraulic heads on the west and east boundaries are 18 m. and 16 m. above reference level, respectively.

	Ground Level			
▽	Unconfined	(1)	▽	8 m.
	Confined	(2)		6 m.
	Confined	(3)		6 m.
	Impervious			
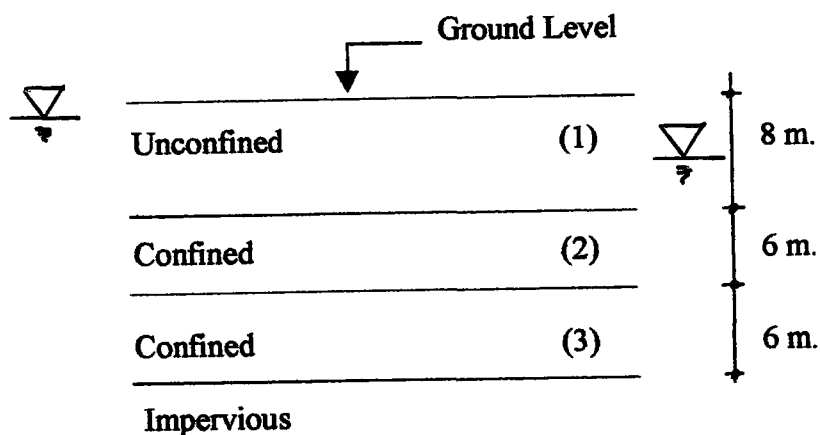
Figure 6.1 The Elevations of Layers

The aquifer system is unconfined and isotropic. The effective porosity is 20 percent. The elevation of the ground surface is 20 m. The thickness of the first,

second and third layers are 8 m. and 6 m. and 6 m., respectively. A constant recharge rate of $6*10^{-9}$ m/s is applied to the aquifer.

The pollutant is dissolved into groundwater at a rate of $1.5*10^{-4}$ µg/s/m^2. The longitudinal and transverse dispersivities of the aquifer are 10 m. and 1 m., respectively. The retardation factor is 2. In this chapter the concentration distribution is calculated after a simulation time of 4 years.

To observe the concentration distribution, 2 observation wells are located and one pumping well is placed in the studied area (figure 6.2). The pumping rate is $2*10^{-10}$ m^3/s for the first and second layers and 0.0015 m^3/s for the third layer. The observation wells are marked by (1) and (2) in the first layer, (3) and (4) in the second layer and (5) and (6) in the third layer.
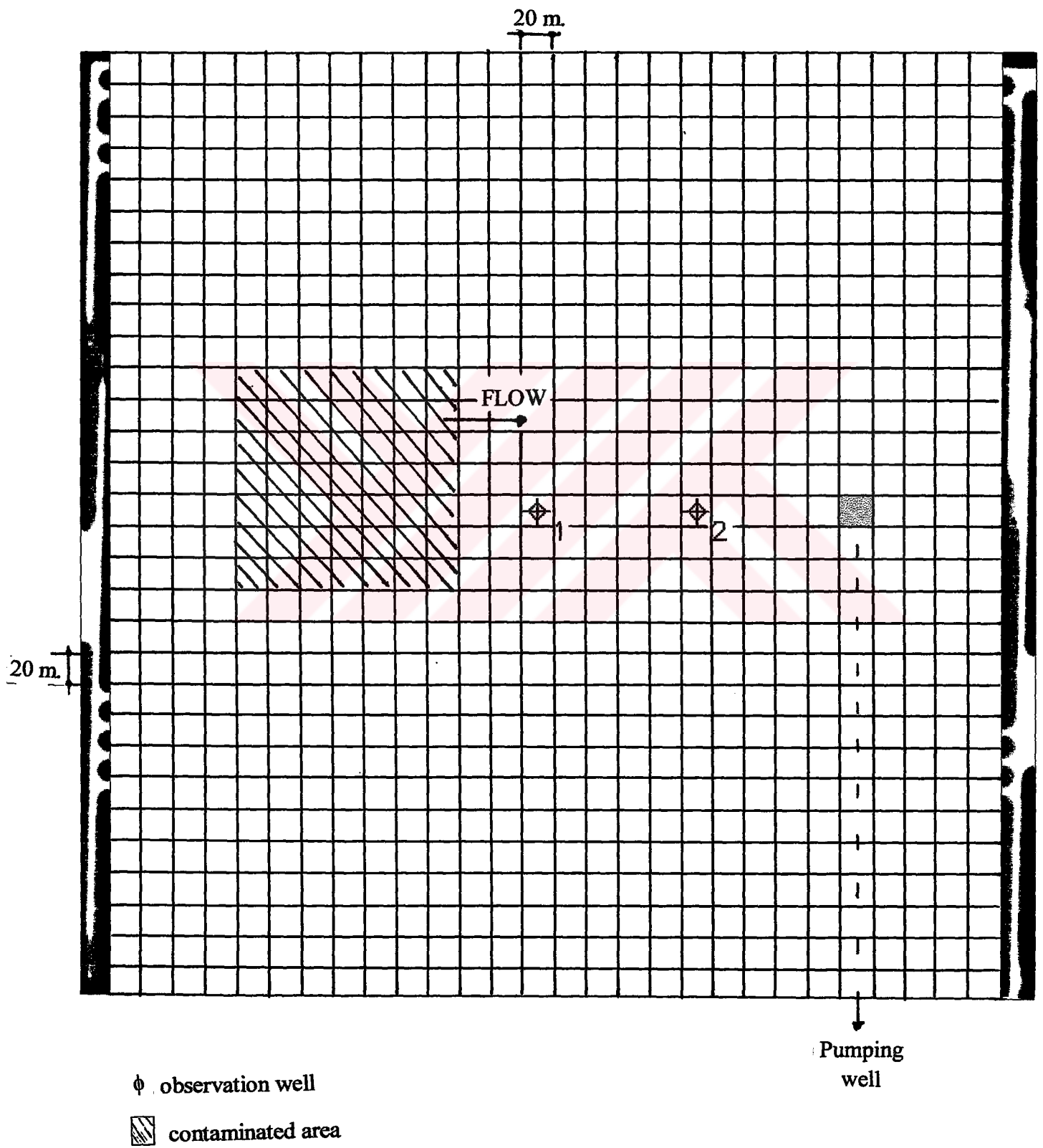
Figure 6.2 Studied area in the case of Models E, F, G, H, I

6.2. Numerical Results

6.2.1. Effects of hydraulic conductivities on the concentration variations

At Model E; the horizontal hydraulic conductivities of the first, second and third layers are 0.00032 m/s, 0.0006 m/s and 0.0006 m/s, respectively. Vertical conductivity of all layers is assumed to be 10 percent of the horizontal hydraulic conductivity.

At Model F; the horizontal conductivity is assumed to be equal to the vertical conductivity. The horizontal and vertical conductivities of the first, second and third layers are 0.00032 m/s, 0.0006 m/s and 0.0006 m/s, respectively.

6.2.1.1. Results obtained with Model E

Figure 6.3 represents the calculated water table elevations.

The concentration variations at different observation wells are given figure 6.4.

The curves of equal concentration in the first layer are shown in figure 6.5.

Figure 6.6 represents the curves of equal concentration in the second layer.

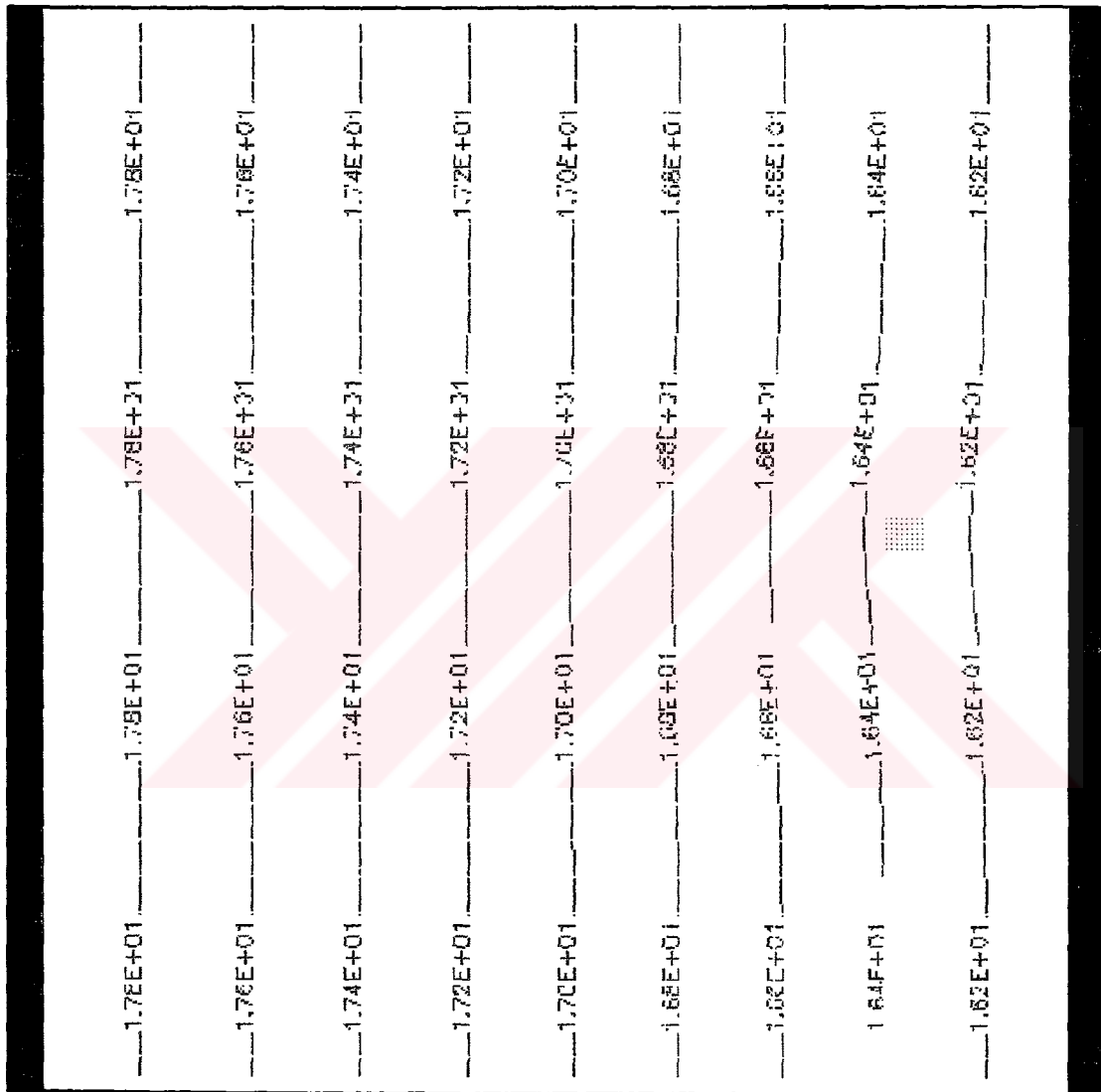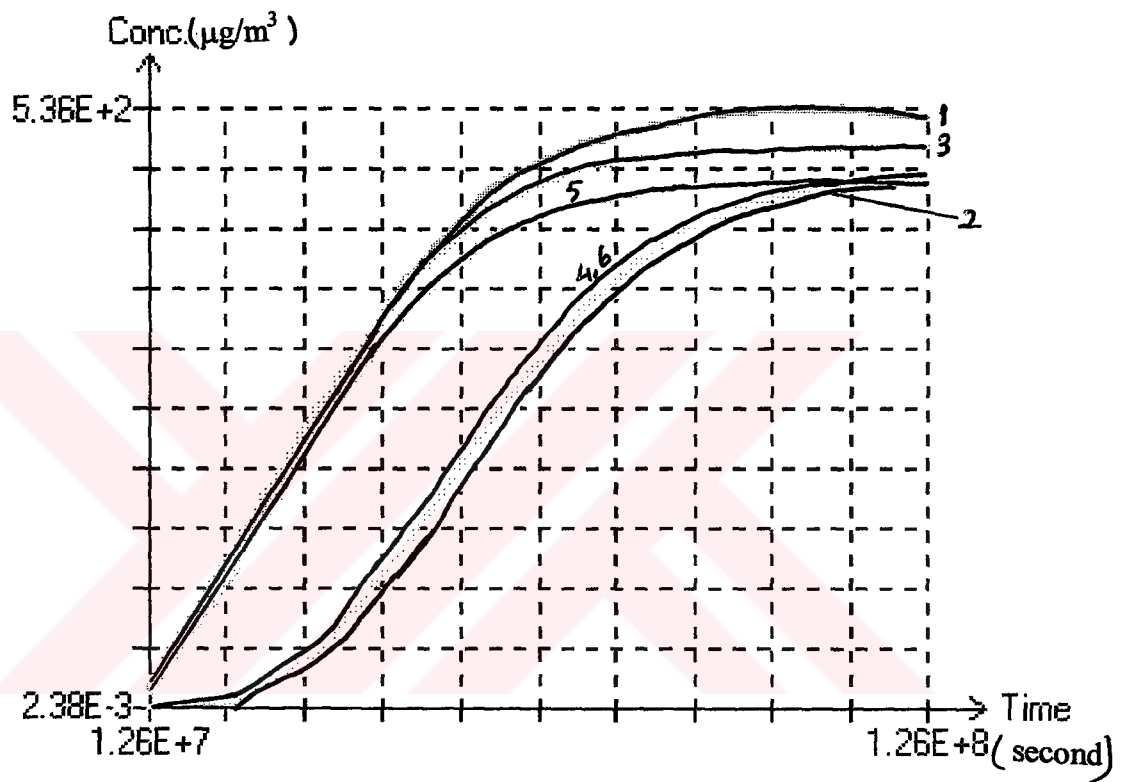Figure 6.7 shows the curves of equal concentration in the third layer.
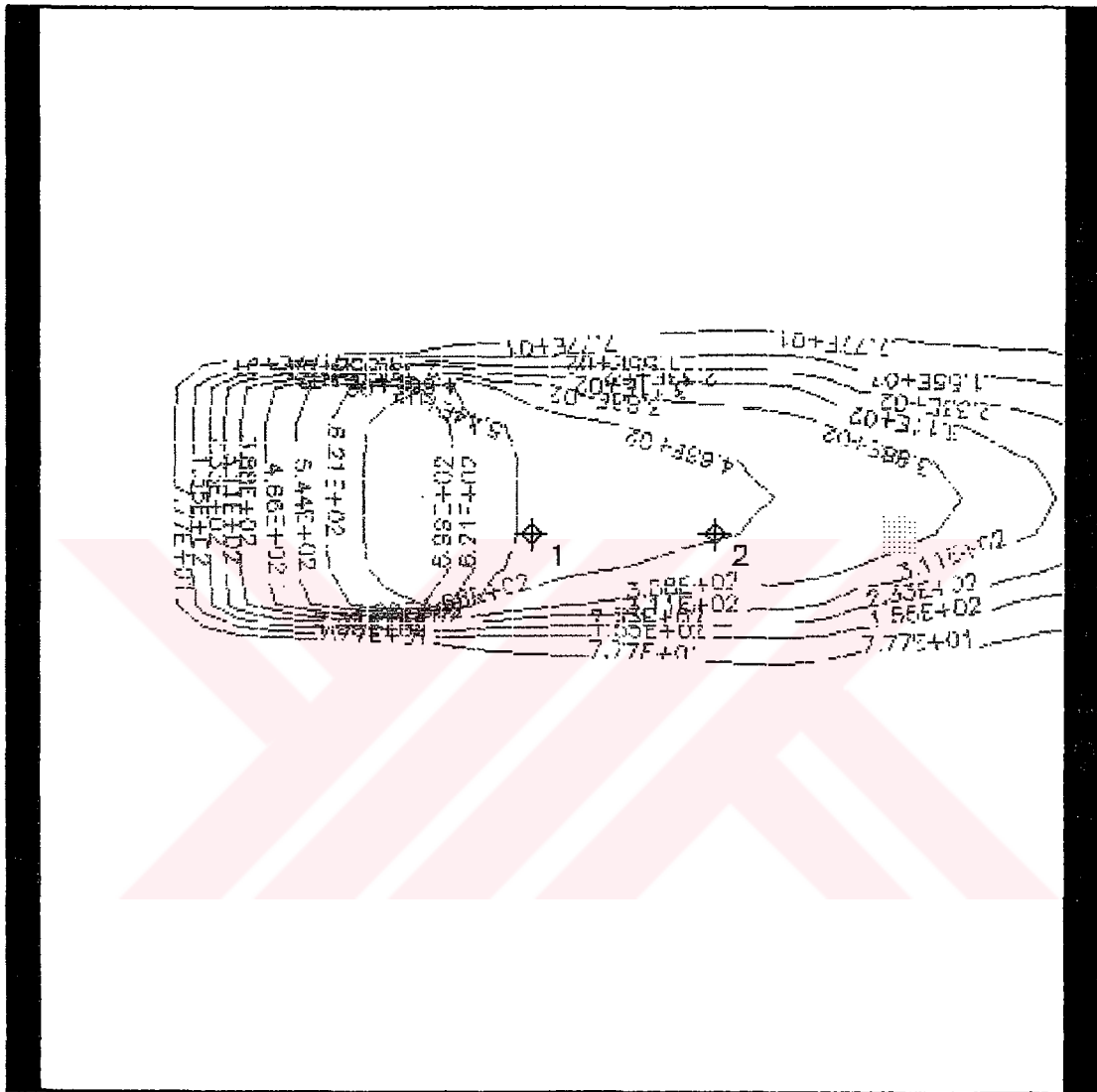
Figure 6.3 The calculated water table elevations in the case of Model E

1, 2, 3, 4, 5 and 6 are numbers of observation wells.

Figure 6.4 The concentration variations at different observation wells
in the case of Model E

Figure 6.5 The curves of equal concentration in the first layer for Model E

Figure 6.6 The curves of equal concentration in the second layer for Model E

Figure 6.7 The curves of equal concentration in the third layer for Model E

6.2.1.2. Results obtained with Model F

The calculated water table elevations are shown in figure 6.8.

Figure 6.9 represents the concentration variations at different observation wells.

The curves of equal concentration in the first layer are shown in figure 6.10.

Figure 6.11 represents the curves of equal concentration in the second layer.

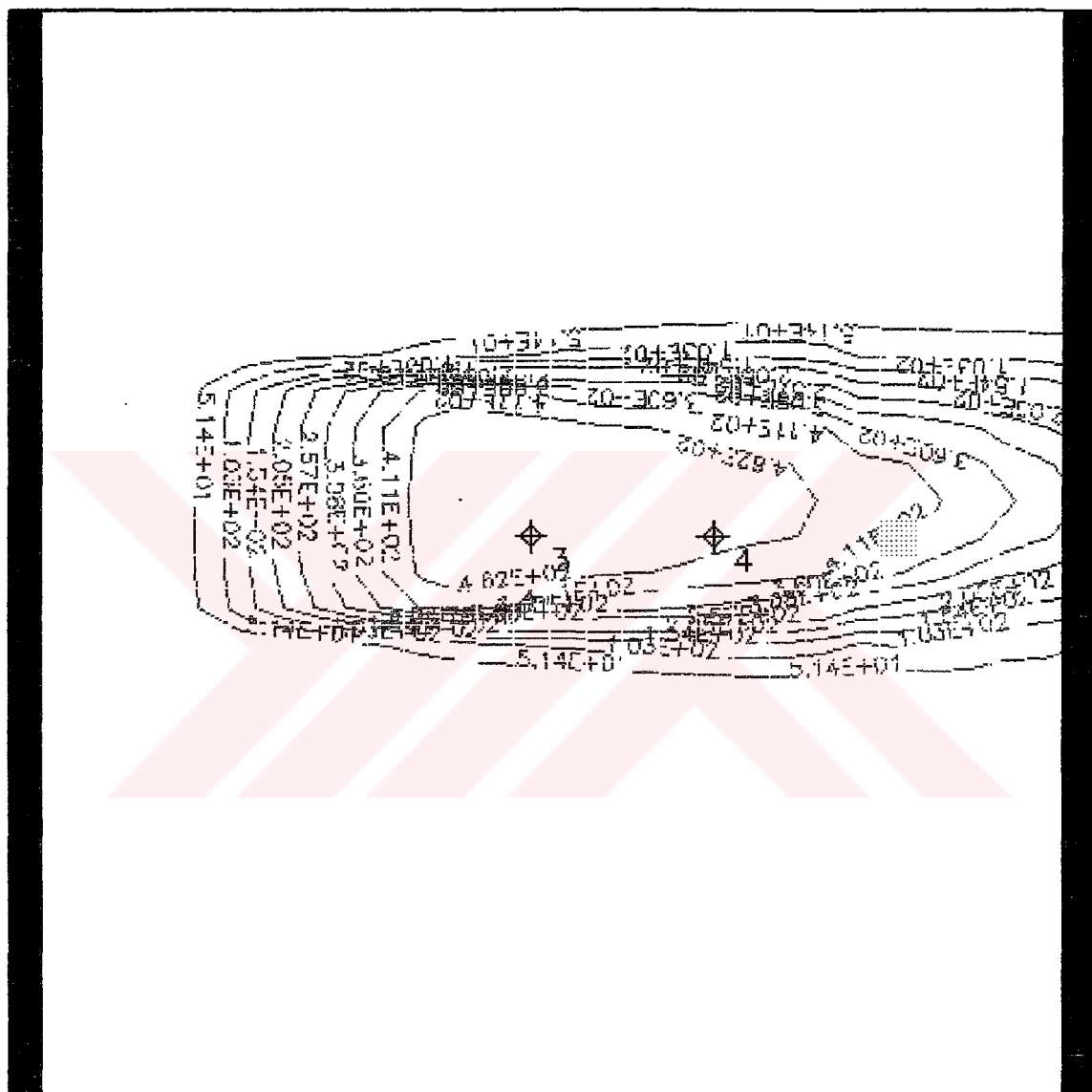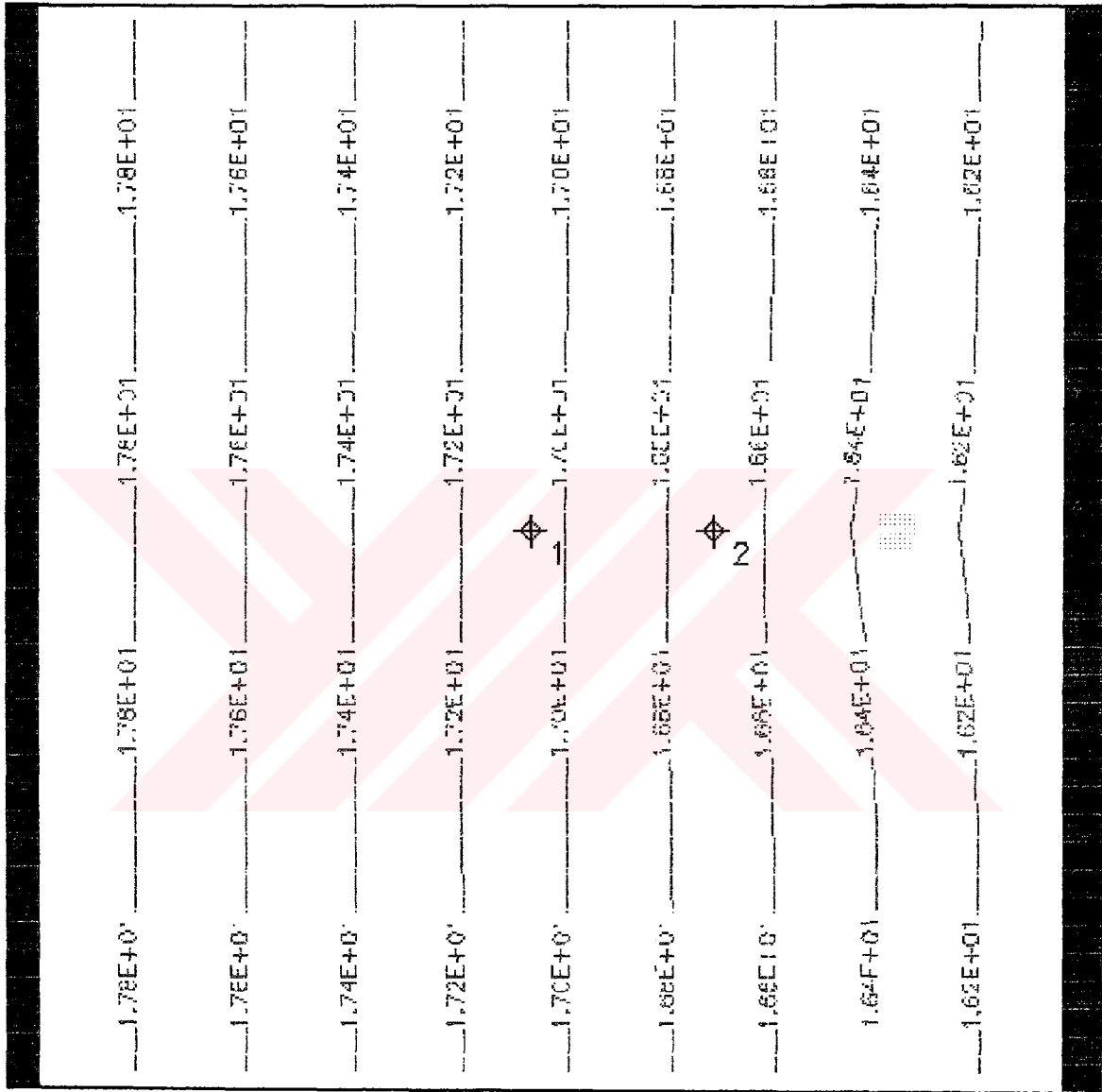Figure 6.12 shows the curves of equal concentration in the third layer.

Figure 6.8 The calculated water table elevations in the case of Model F

1, 2, 3, 4, 5 and 6 are numbers of observation wells.

Figure 6.9 The concentration variations at different observation wells in the case of Model F

Figure 6.10 The curves of equal concentration in the first layer for Model F

Figure 6.11 The curves of equal concentration in the second layer for Model F

Figure 6.12 The curves of equal concentration in the third layer for Model F

6.2.2. Effects of Different Contaminant Transport Processes

6.2.2.1. Contaminant Transport with Advection

6.2.2.1.1. Results obtained with Model G

The calculated water table elevations are shown in figure 6.13.

Figure 6.14 represents the concentration variations at different observation wells.

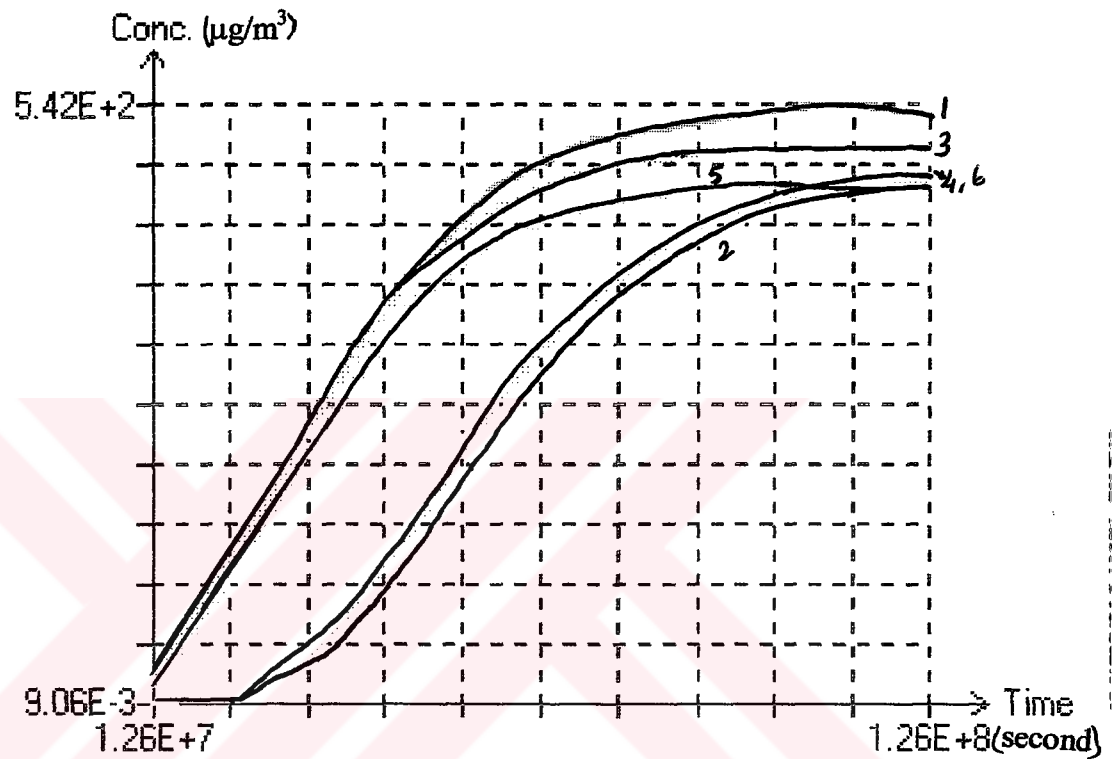The curves of equal concentration in the first layer are shown in figure 6.15.

Figure 6.16 represents the curves of equal concentration in the second layer.

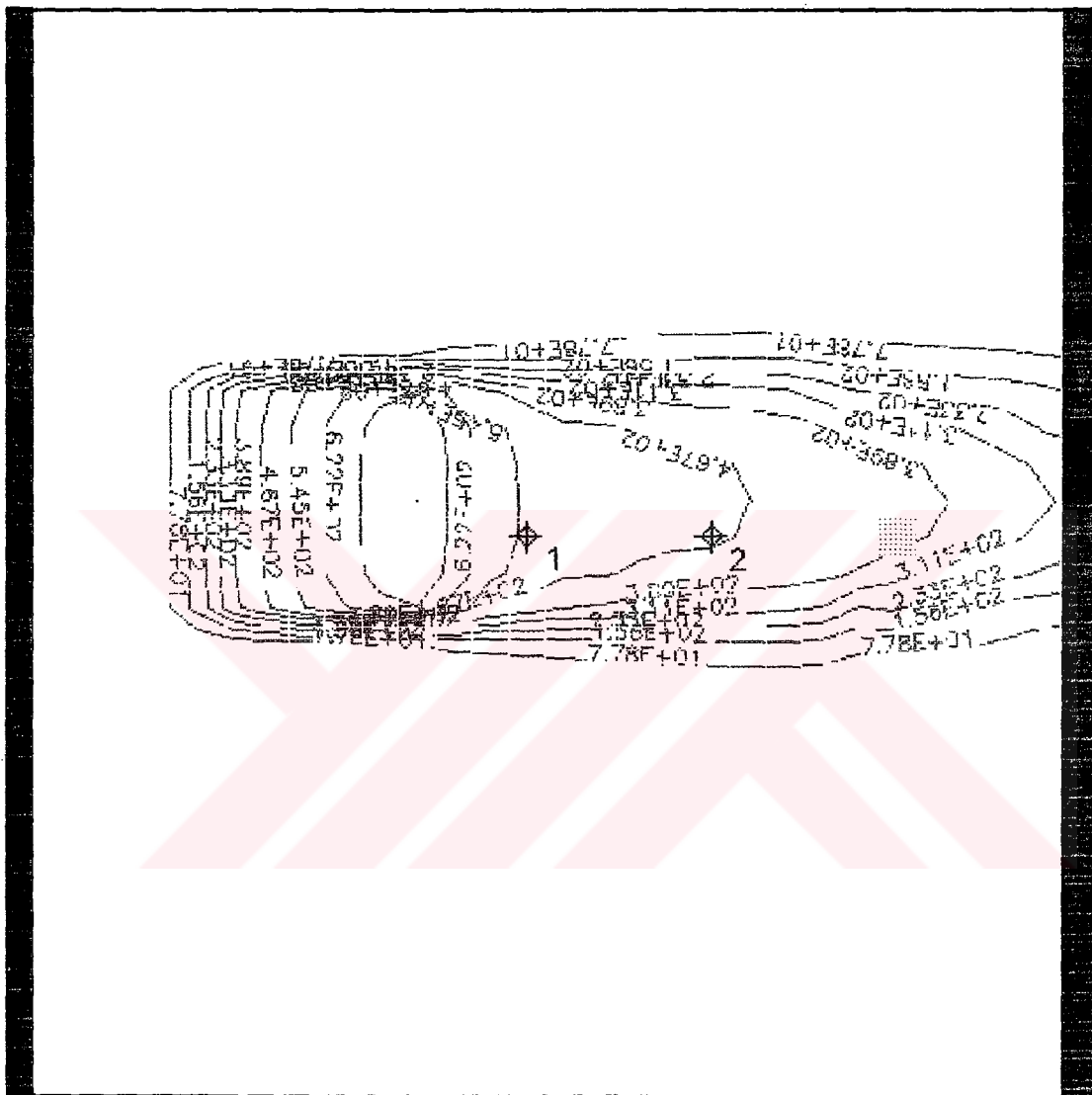Figure 6.17 shows the curves of equal concentration in the third layer.

98

Figure 6.13 The calculated water table elevations in the case of Model G
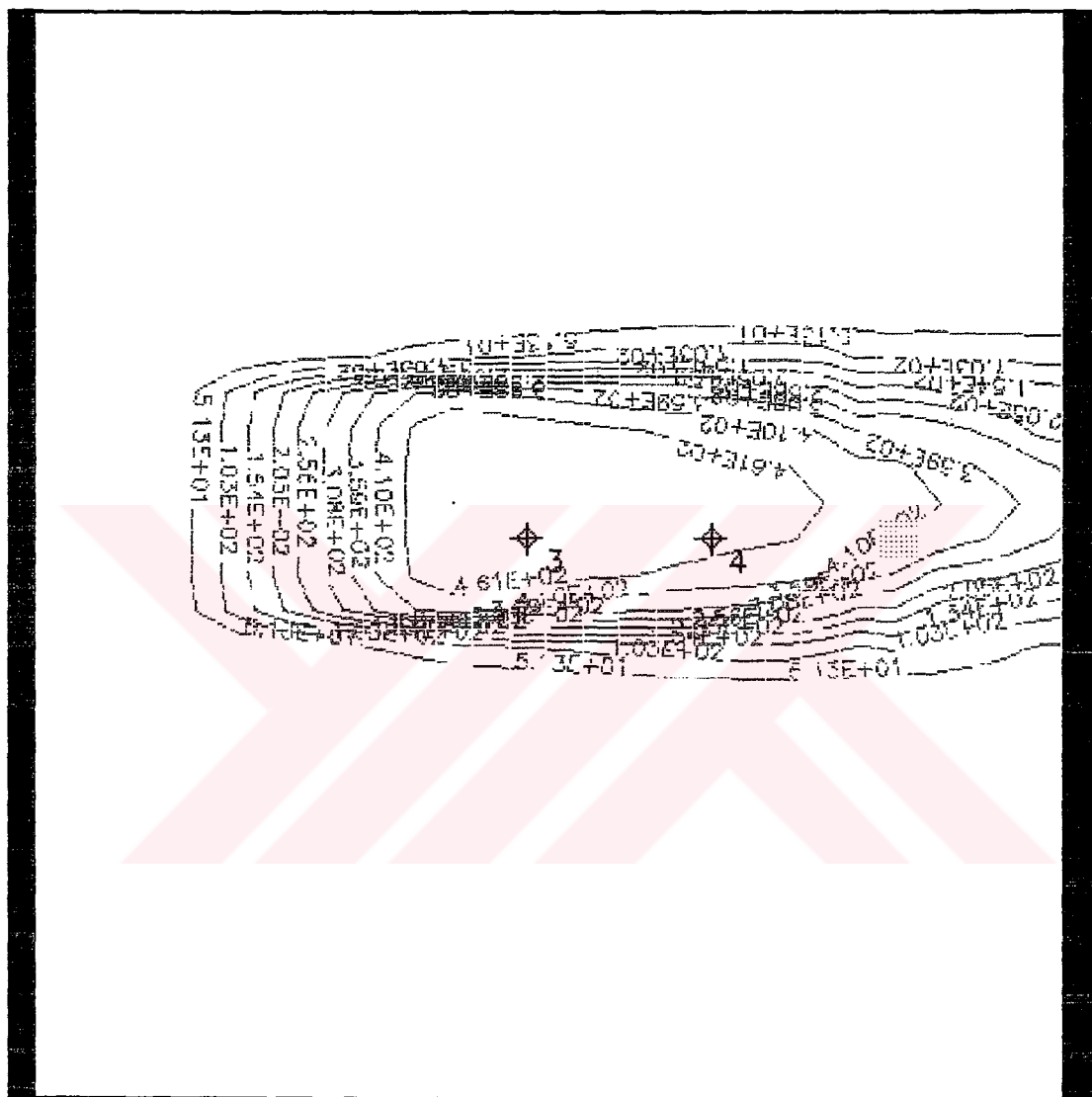
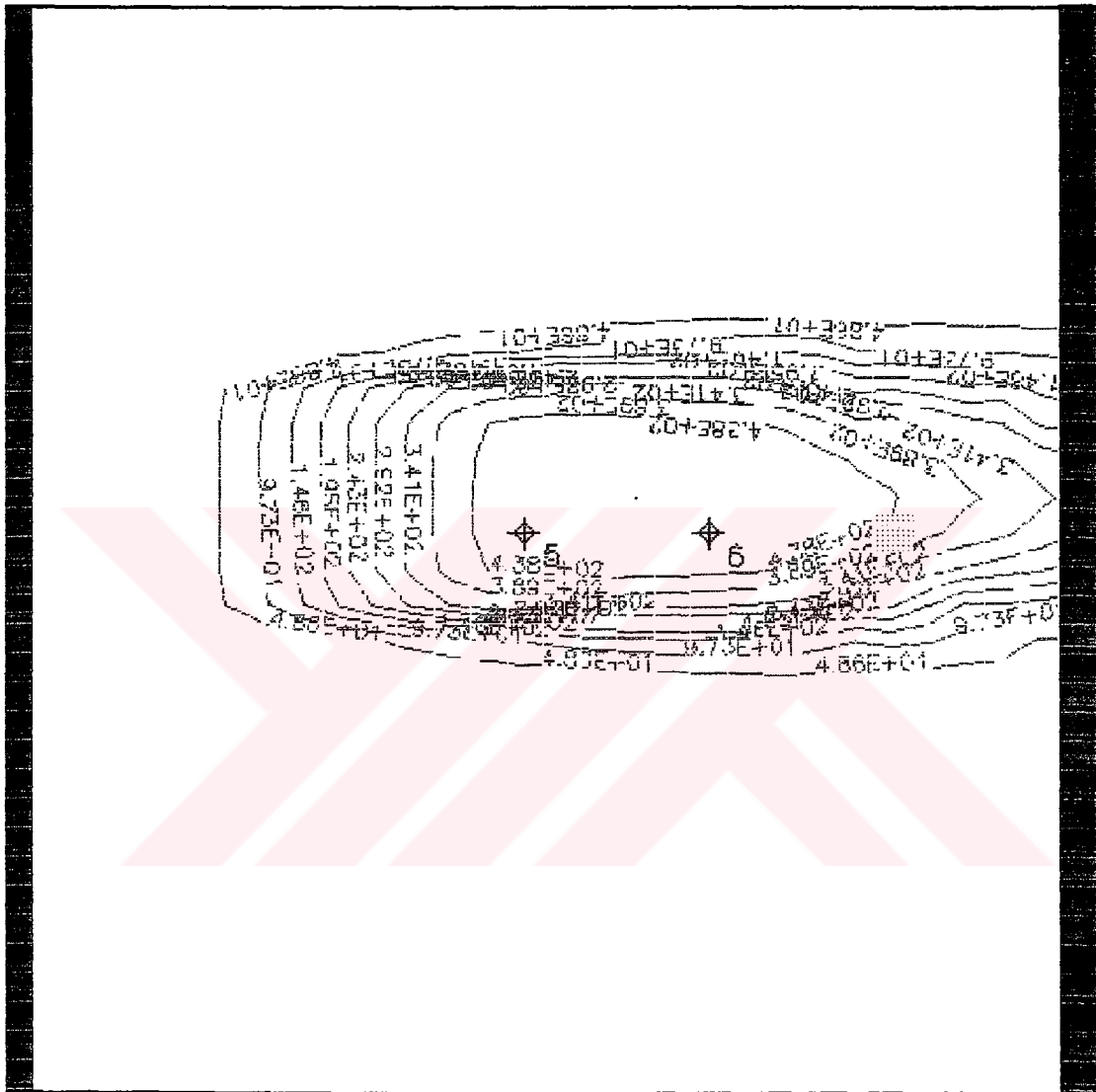1, 2, 3, 4, 5 and 6 are numbers of observation wells.

Figure 6.14 The concentration variations at different observation wells in the case of Model G

Figure 6.15 The curves of equal concentration in the first layer for Model G

Figure 6.16 The curves of equal concentration in the second layer for Model G

Figure 6.17 The curves of equal concentration in the third layer for Model G

6.2.2.2. Contaminant Transport with Advection and Dispersion
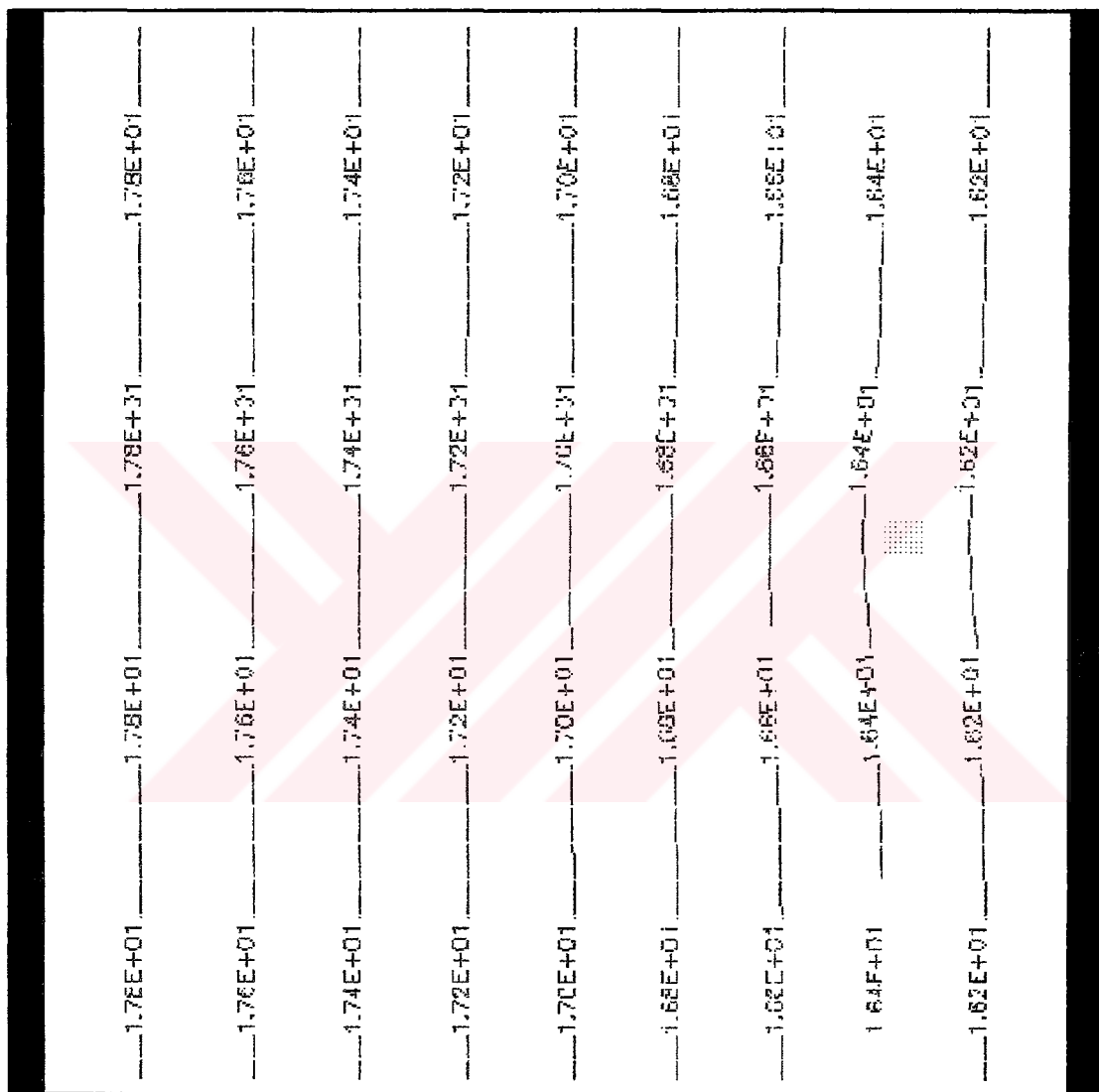
6.2.2.2.1. Results obtained with Model H

The calculated water table elevations are shown in figure 6.18.

Figure 6.19 represents the concentration variations at different observation wells.

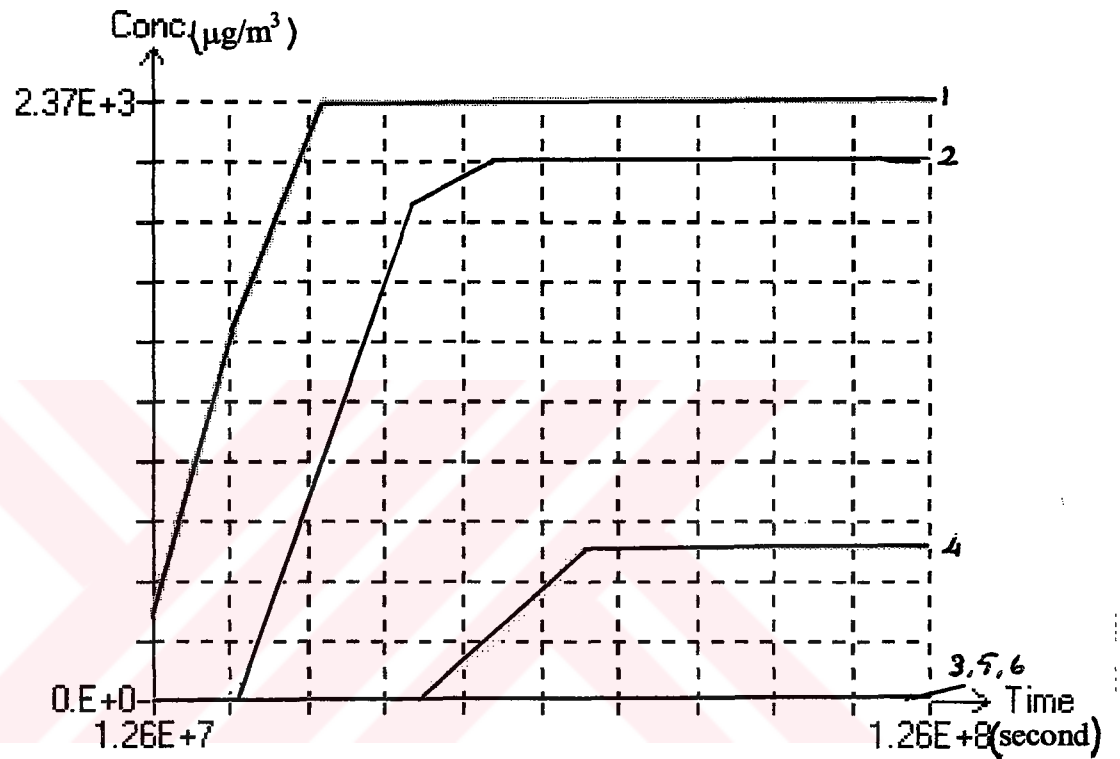The curves of equal concentration in the first layer are shown in figure 6.20.

Figure 6.21 represents the curves of equal concentration in the second layer.

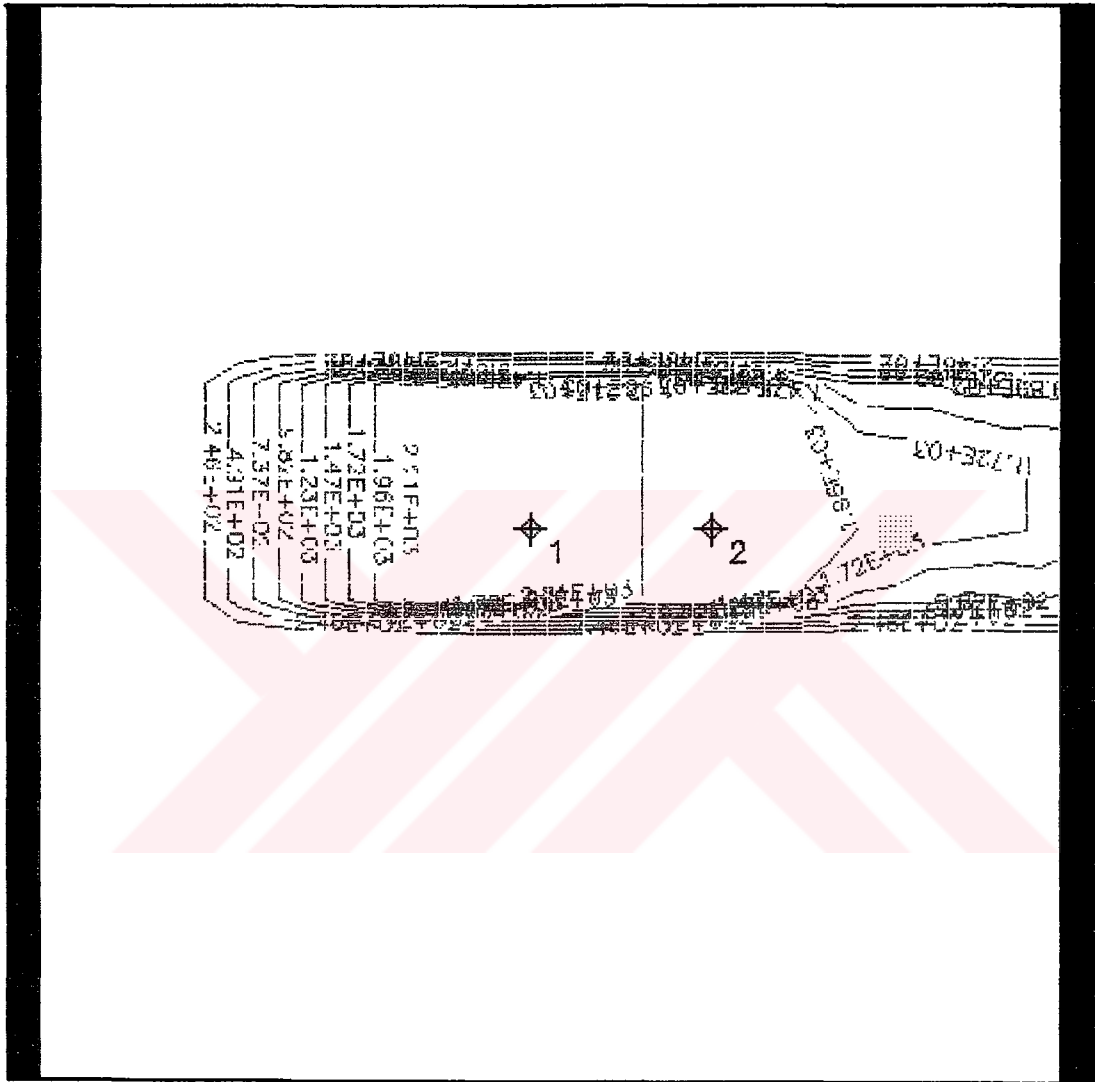Figure 6.22 shows the curves of equal concentration in the third layer.

Figure 6.18 The calculated water table elevations in the case of Model H
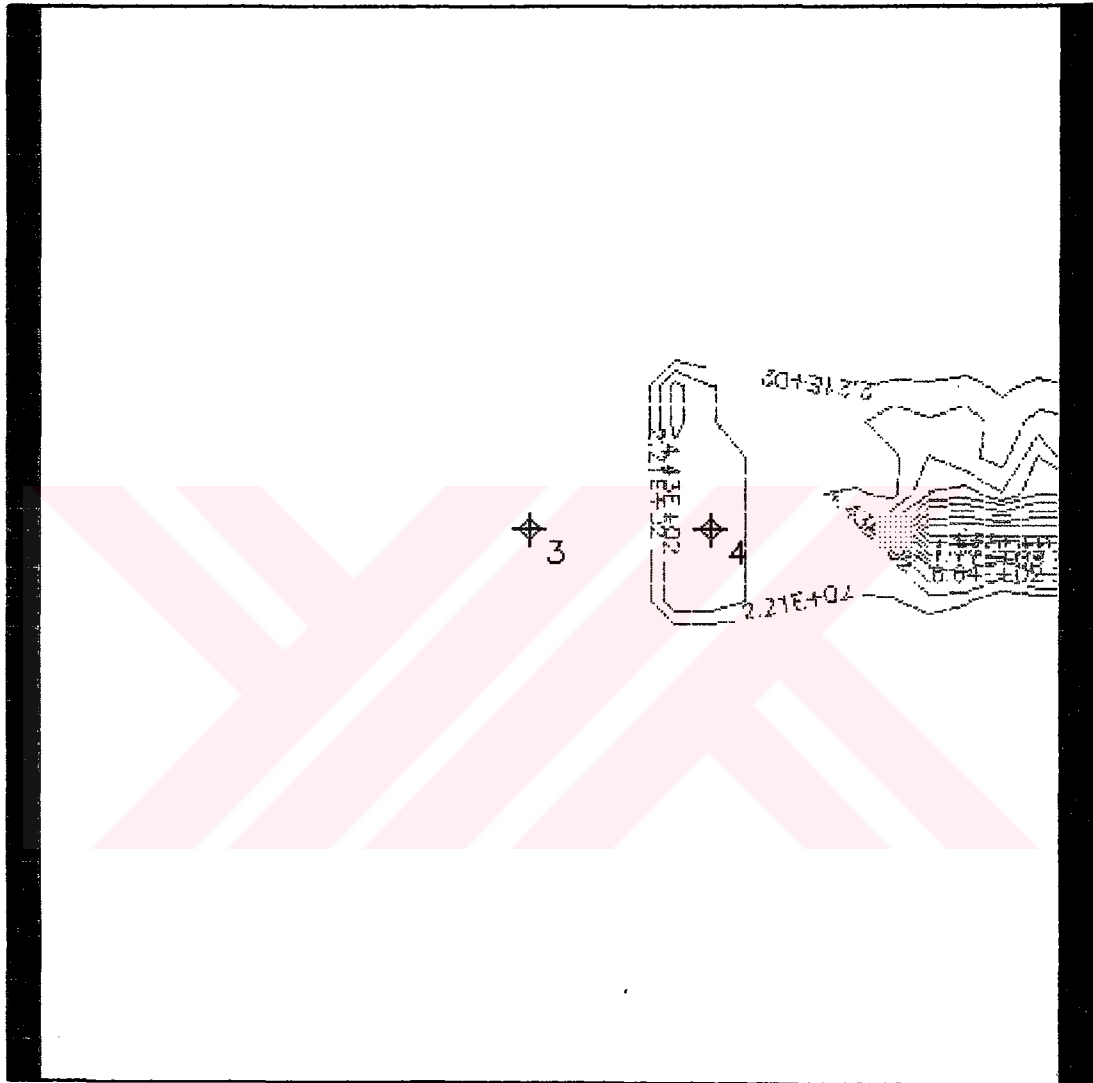
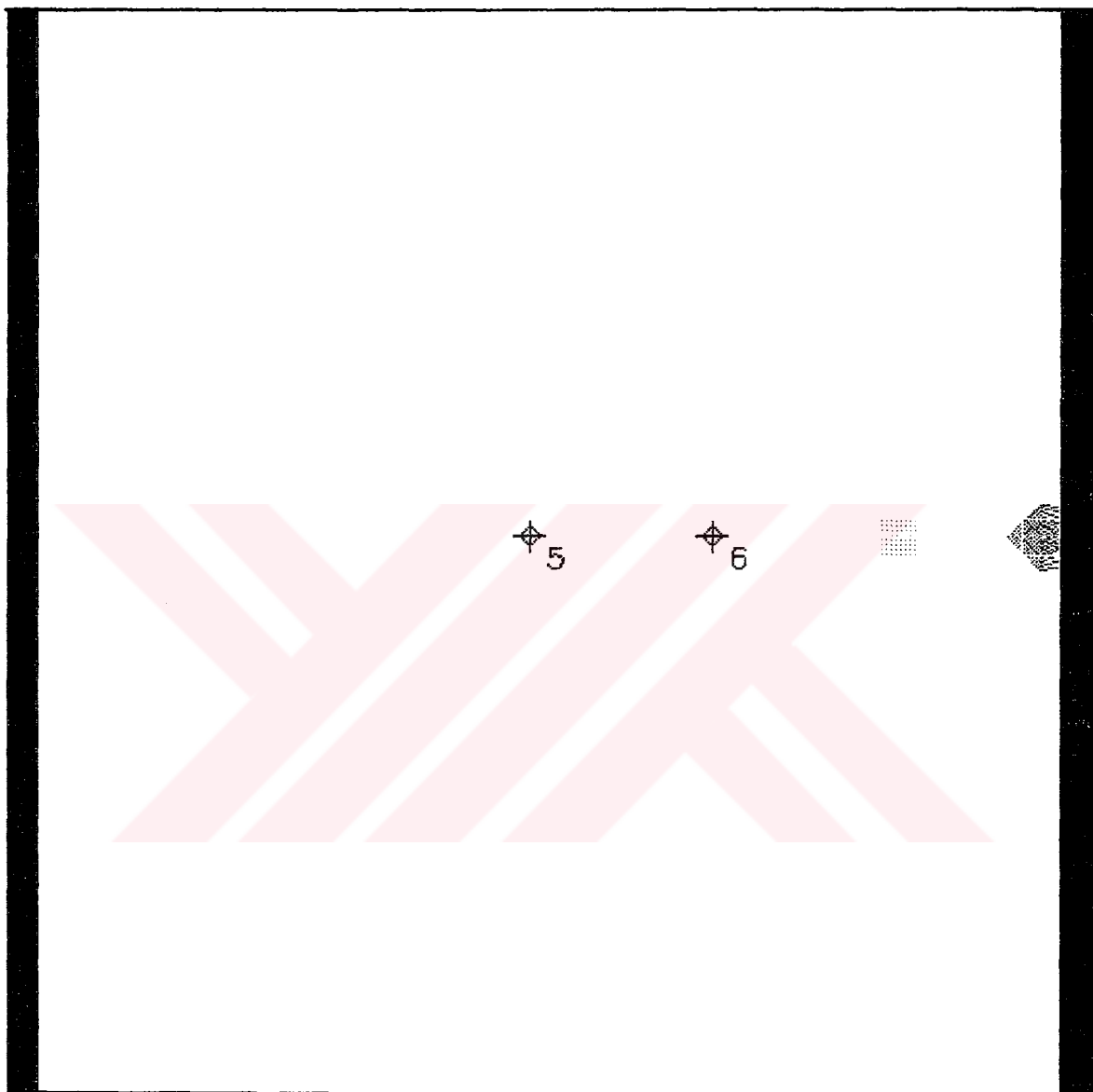1, 2, 3, 4, 5 and 6 are numbers of observation wells.

Figure 6.19 The concentration variations at different observation wells in the case of Model H

Figure 6.20 The curves of equal concentration in the first layer for Model H

Figure 6.21 The curves of equal concentration in the second layer for Model H

Figure 6.22 The curves of equal concentration in the third layer for Model H

6.2.2.3. Contaminant Transport with Advection, Dispersion and Adsorption

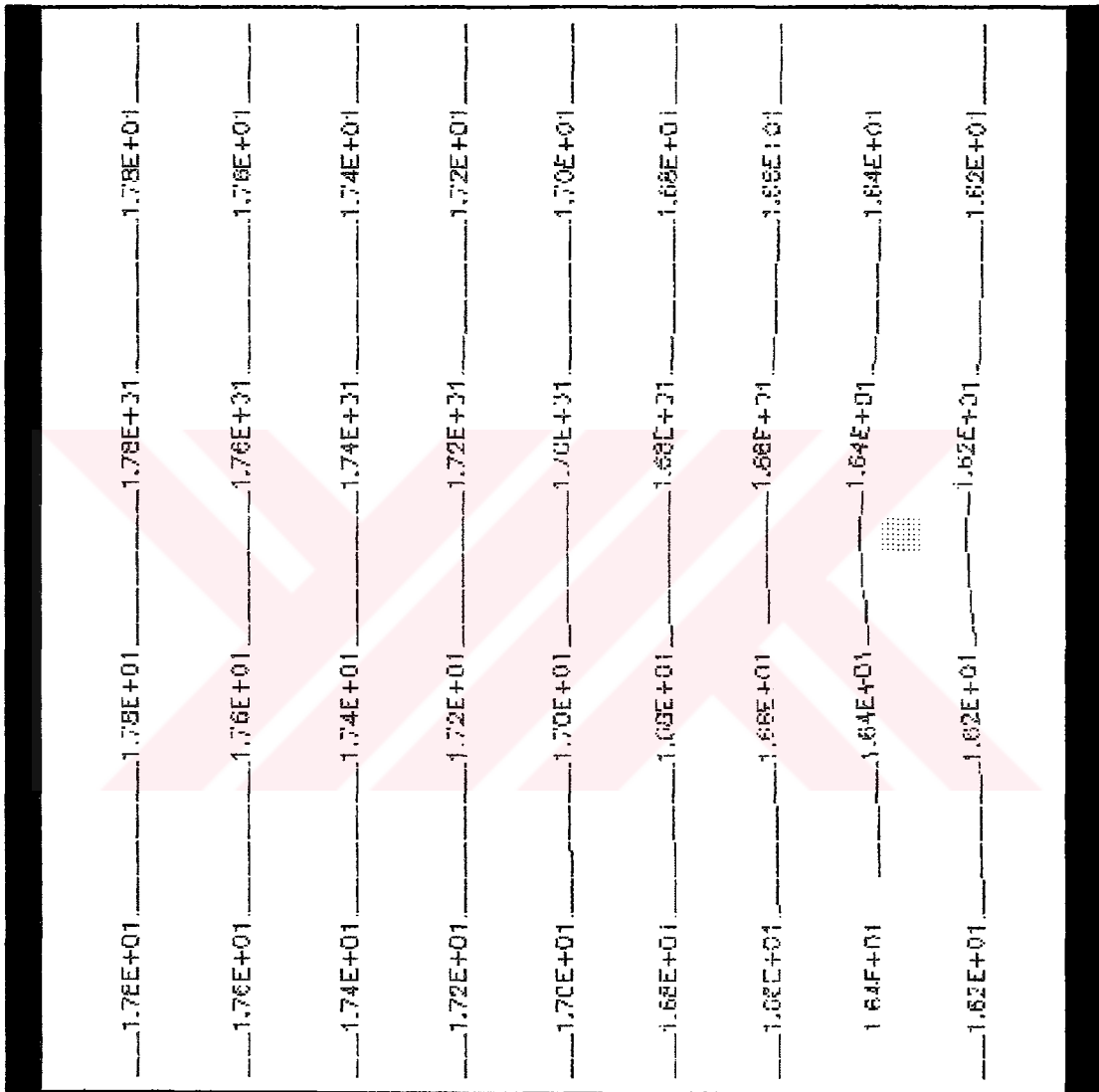### 6.2.2.3.1. Results obtained with Model I

The calculated water table elevations are shown in figure 6.23.

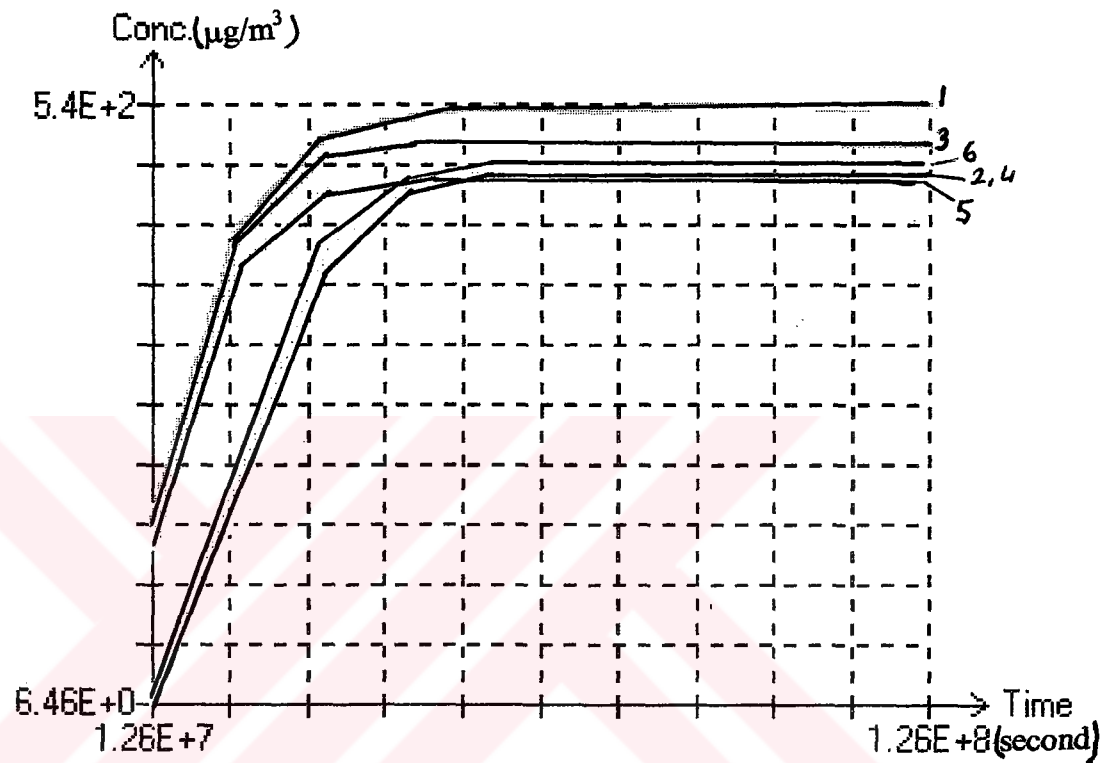Figure 6.24 represents the concentration variations at different observation wells.

The curves of equal concentration in the first layer are shown in figure 6.25.

Figure 6.26 represents the curves of equal concentration in the second layer.

Figure 6.27 shows the curves of equal concentration in the third layer.
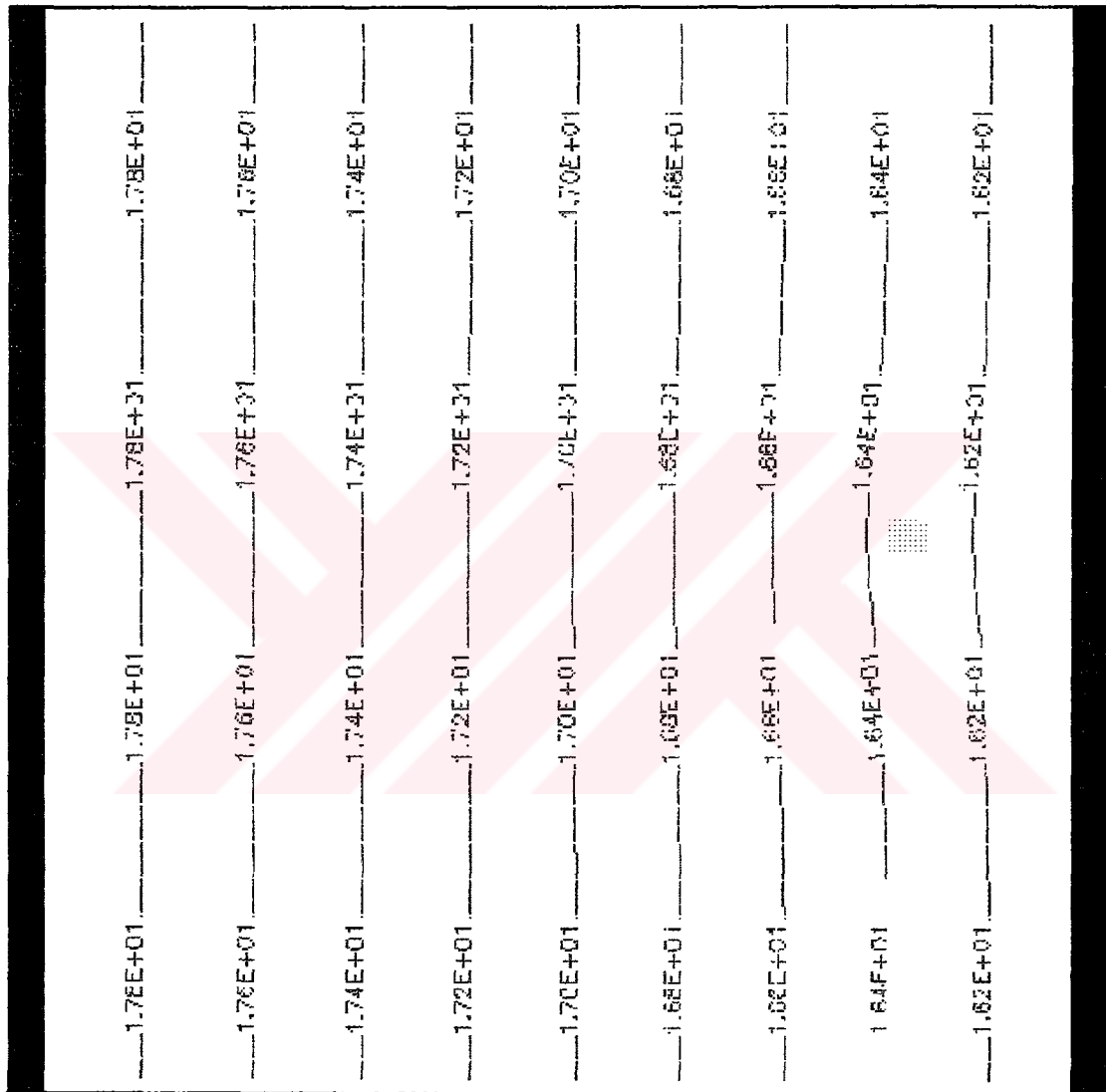
Figure 6.23 The calculated water table elevations in the case of Model I
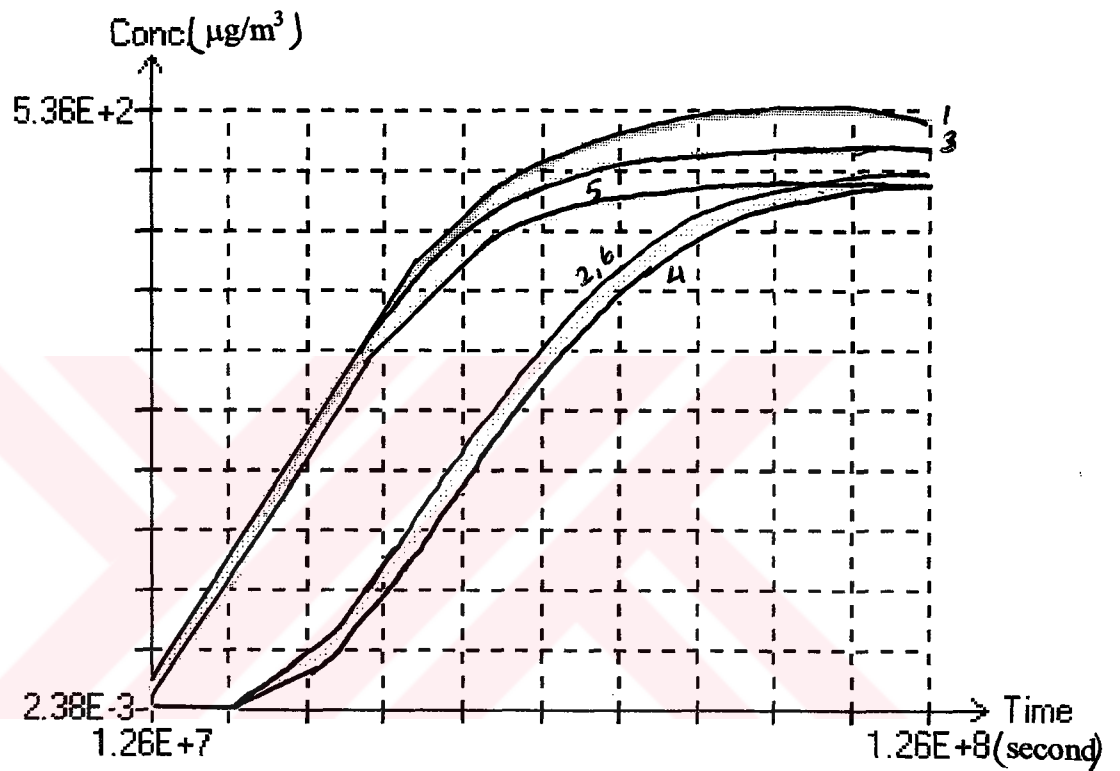
1, 2, 3, 4, 5 and 6 are numbers of observation wells.

Figure 6.24 The concentration variations at different observation wells in the case of Model I
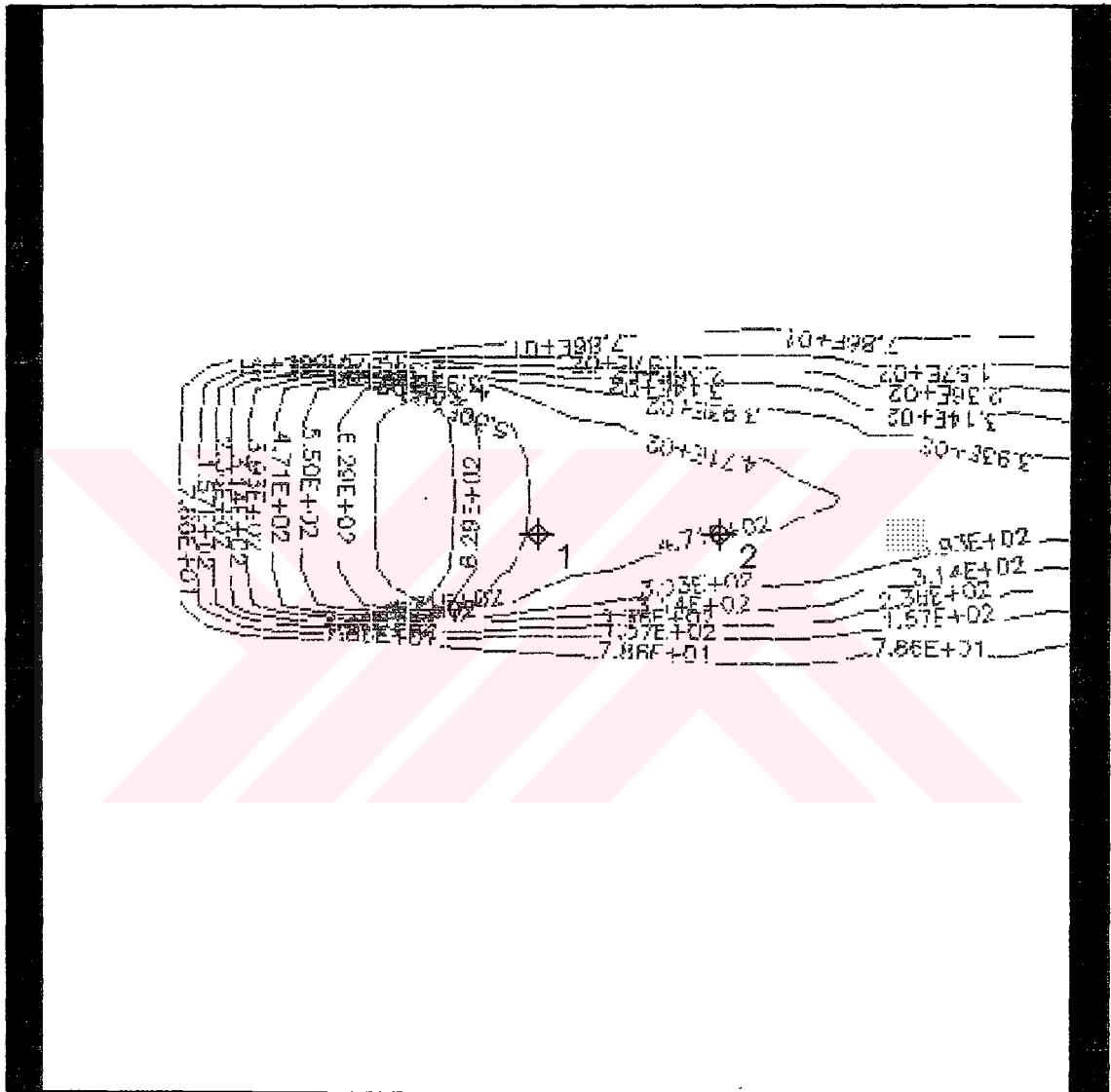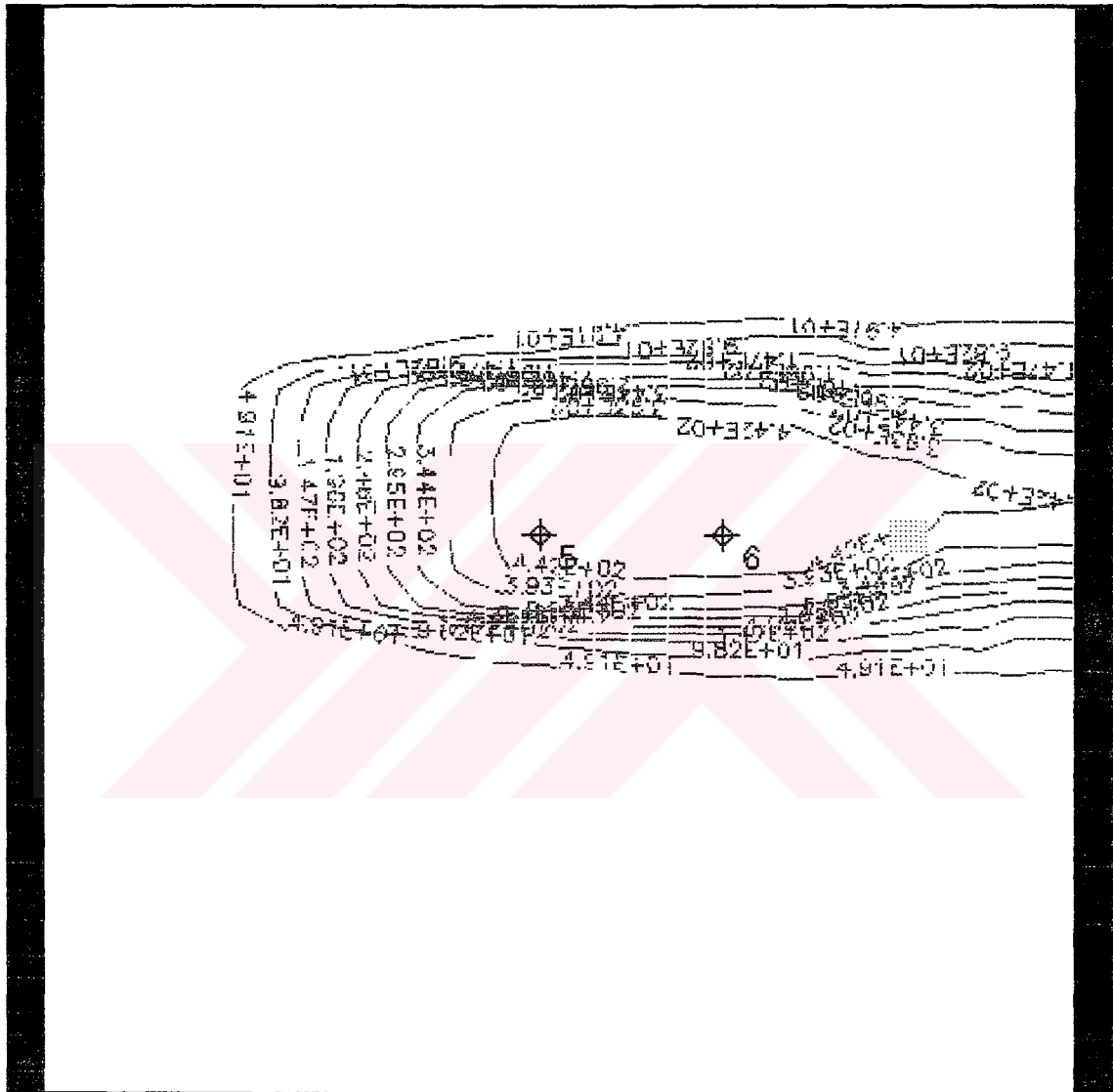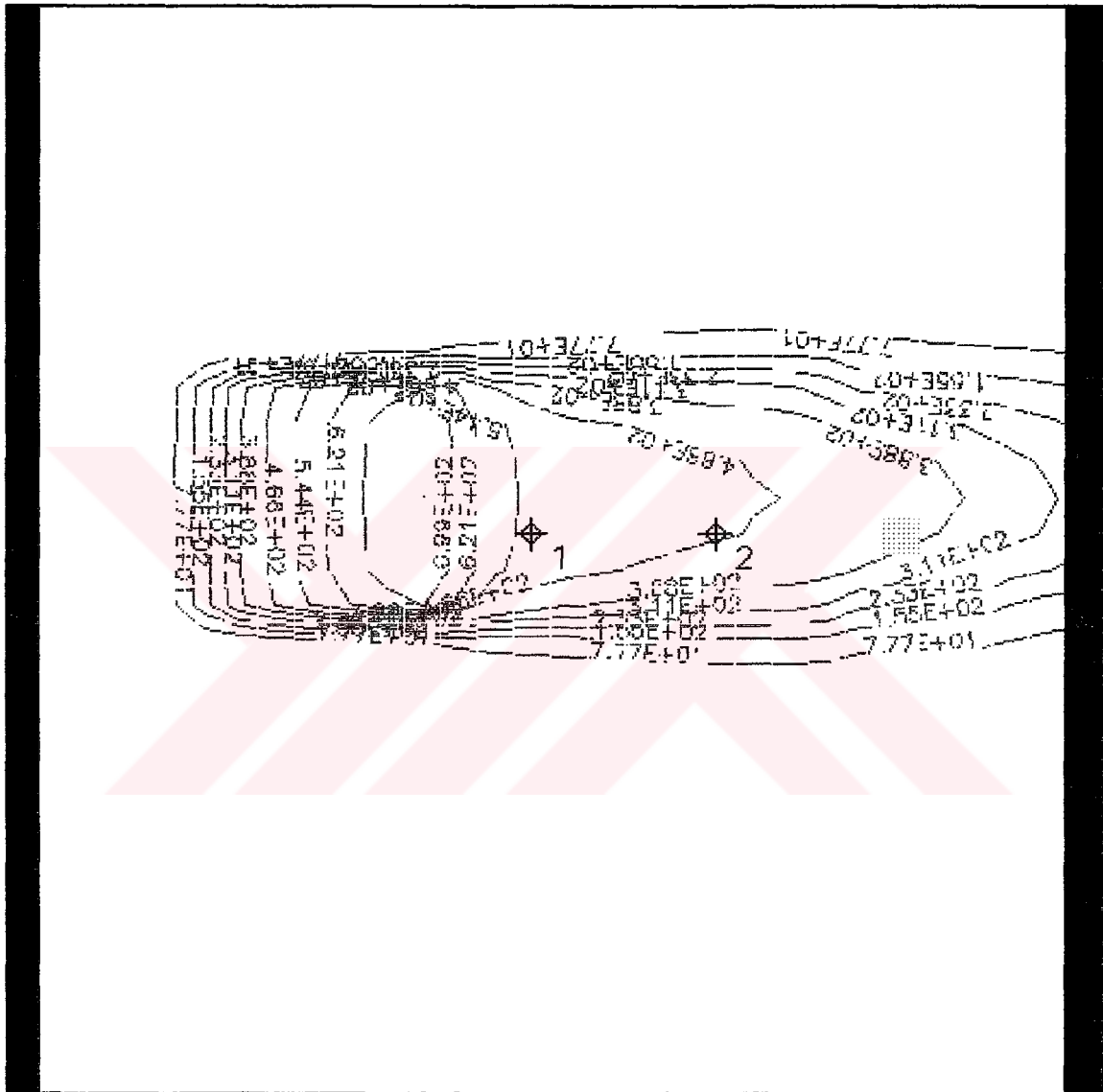
Figure 6.25 The curves of equal concentration in the first layer for Model I
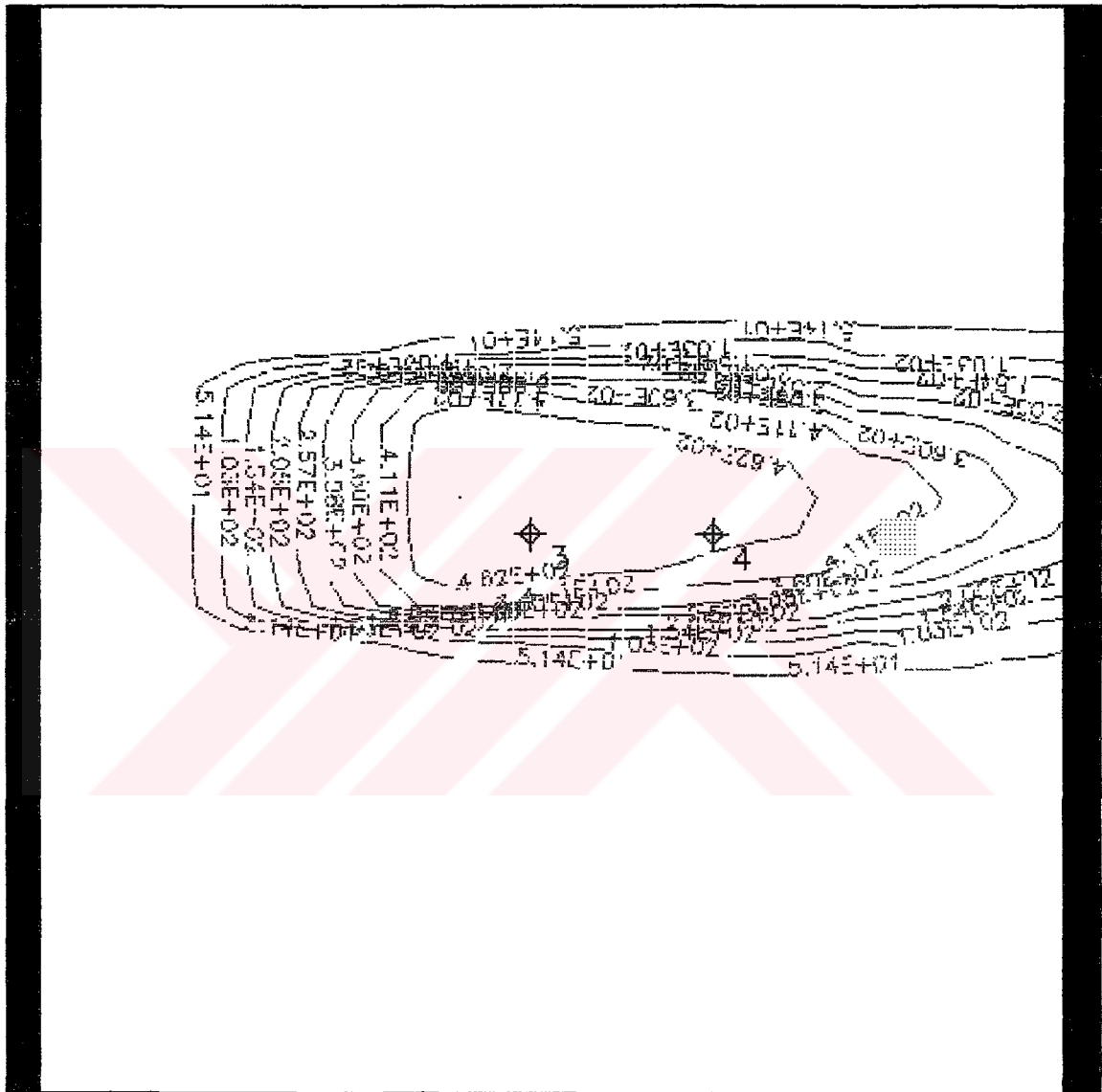
Figure 6.26 The curves of equal concentration in the second layer for Model I
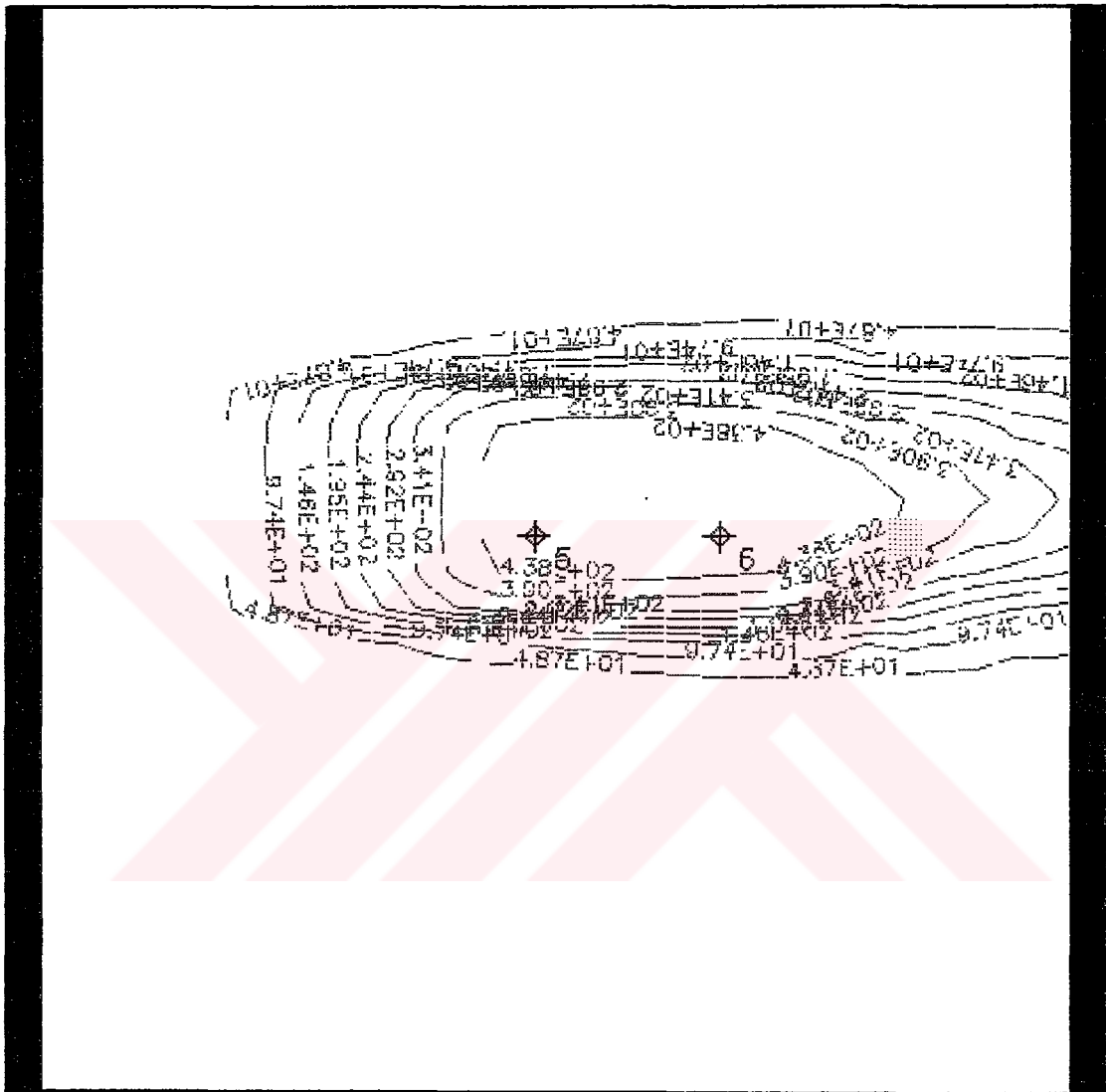
Figure 6.27 The curves of equal concentration in the third layer for Model I

CHAPTER SEVEN

COMPARISON OF RESULTS AND CONCLUSION

7.1. Comparison of the Numerical Results

In all models, the first layers are more influenced from the contamination than the lower ones, as expected.

Regions near the contaminant zone are much more affected than farther parts of the studied area.

7.1.1. Comparison of the Numerical Results for Models A, B, C, D

According to the research on computer program with time parameter 400 years, the computed concentration values vary between $3.77*10^2$ $\mu g/m^3$ and $3.49*10^3 \mu g/m^3$ at Model A.

These concentration variations change in the interval $2.76*10^2$ $\mu g/m^3$ and $2.12*10^3$ $\mu g/m^3$ at Model B which has the same data values with the Model A. The reason of this difference is the dimension of contaminated areas. The contaminated area is larger in the case of Model A.

Concentration values change in the interval $1.35*10^2$ µg/m³ and $1.35*10^3$ µg/m³ at Model C. These values are observed between $1.01*10^2$ µg/m³ and $8.21*10^2$ µg/m³ at Model D that has the same data values with the Model C. This variation is due to the largeness of the contaminant area of Model C.

When the program is executed with time parameter 40 years instead of 400 years the concentrations at Models A, B, C, D are given at table 7.1.

Models	Concentration Variations (µg/m³)
A	$7.91*10 - 1.07*10^3$
B	$5.7*10 - 1.02*10^3$
C	$5.59*10 - 7.36*10^2$
D	$4.45*10 - 4.55*10^2$

Table 7.1 The interval of the concentration values of Models A, B, C, D for a period of 40 years.

The same pattern is observed according to the magnitude of the contaminated area.

As anticipated, the outputs of Pmwin Modflow have been shown that the solute extension for 400 years is larger than that obtained for 40 years.

7.1.2. Comparison of the Numerical Results for Models E, F, G, H, I

The concentrations are observed between $4.87*10$ µg/m³ and $6.99*10^2$ µg/m³ at Model E where there is a ratio of 10 between the vertical and horizontal conductivities. At Model F this ratio is taken equal to 1, then the concentration variations are observed in the interval $4.86*10$ µg/m³ and $6.77*10^2$ µg/m³. These results are approximately equal to each other. This fact is due to the negligible influence of the vertical velocity.

The effects of contaminant transport processes examined with the Models G, H and I. In the Model G the contaminant transport mechanism is only advection. Advection and Dispersion processes is examined at Model H. In the Model I the contaminant transport processes are given with the processes of advection, dispersion and adsorption. According to the program results, the computed concentration variations are given at table 7.2.

	Advection + Dispersion + Adsorption	Advection + Dispersion	Only Advection
Concentration Values (μg/m^3)	$4.87*10 - 6.99*10^2$	$4.91*10 -$ $6.29*10^2$	$2.21*10^2 -$ $1.96*10^3$

Table 7.2. The interval of the concentration values for the different transport processes.

7.2. Conclusion

In this thesis; groundwater contamination is computed with the program PMWIN MODFLOW. In chapter 5 groundwater contamination model was applied to the Harmandalı Sanitary Landfill Area. According to the numerical results, the contamination seems not to be dangerous even after 400 years for the village Harmandalı. If one regards the numerical results for different periods, one can say Harmandalı Sanitary location is well choosen.

In chapter 6; PMWIN MODFLOW is used for a heterogeneous aquifer with high permeability. The numerical results show common effects of different processes in solute transport mechanism.

This powerfull tool of groundwater contamination analysis may be used in actual problems where complex configuration and complicated boundary conditions exist.

There are some discrepancies between the obtained numerical results and those obtained by Bilgen ÖZTUNA.

REFERENCES

Anderson, M. P. (1979). Using Models to Simulate the Movement of Contaminants through Groundwater Flow Systems. CRC Critical Rev. Environ. Control, Chemical Rubber Co.

Anderson, M. P. and Woessner, W. W. (1992). Applied Groundwater Modeling. Academic Press, San Diego, CA.

Bear, J. (1961). Some Experiments on Dispersion. J. Geophys. Res. (66(8):2455-67.)

Bear, J. (1972). Dynamics of Fluids in Porous Media. American Elsevier, New York.

Bear, J. (1979). Hydraulics of Groundwater. McGraw-Hill, New York.

Berry-Spark, K. and Barker, J. F. (1987). Nitrate Remediation of Gasoline Contaminated Ground Waters: Results of a Controlled Field Experiment. National Water Well Association / American Petroleum Institute.

Borden, R. C. and Bedient, P. B. (1986). Transport of Dissolved Hydrocarbon Influenced by Reaeration and Oxygen Limited Biodegradation: Theoretical Development. Water Resources Res.(22:1973-1982).

Bredehoeft, J. D. and Pinder, G. F. (1973). Mass Transport in Flowing Groundwater. Water Resources Res.(9:192-210).

Charbeneau, R. J. (1981). Groundwater Contaminant Transport with Adsorption and Ion Exchange Chemistry: Method of Characteristics for the Case without Dispersion. Water Resources Res.(17(3):705-713).

Charbeneau, R. J. (1982). Calculation of Pollutant Removal during Groundwater Restoration with Adsorption and Ion Exchange. Water Resources Res.(18(4):1117-1125).

Davis and College, O. (2002). Model allows better understanding of Groundwater Contamination. Journal Science, 26 April.

Domenico, P. A. and Schwartz, F. W. (1990). Physical and Chemical Hydrogeology. Wiley, New York.

Fetter, C. W. (1993). Contaminant Hydrogeology. Macmillan Publishing Co., New York.

Freeze, R. A. and Cherry, J. A. (1979). Groundwater. Prentice Hall, Englewood Cliffs, NJ.

Freyberg, D. L. (1986). A Natural Gradient Experiment on Solute Transport in a Sand Aquifer , Spatial Moments and the Advection and Dispersion of Nonreactive Tracers. Water Resources Res.(22(13):2031-2046).

Fried, J. J. (1975). Groundwater Pollution. Elsevier, Amsterdam.

Garder, A. O., Peaceman, D. W. and Pozzi, A. L. (1964). Numerical Calculation of Multidimensional Miscible Displacement by the Method of Characteristics. Soc. Pet. Eng. J. (4(1):26-36).

Güven Oktay (1983). Laboratory Investigation and Analysis of a Groundwater Contamination. Groundwater.v. 23, No.4.

Huyakorn, P. S. and Pinder, G. F. (1983). Computational Methods in Subsurface Flow. Academic Press, San Diego, CA.

LeBlanc, D. R., Garabedian, S. P., Hess, K. M., Gelhar, L. W., Quadri, R. D., Stollenwerk, K. G. and Wood, W. W. (1991). Large-scale Natural Gradient Tracer Test in Sand and Gravel, Cape Cod, Massachusetts, Experimental Design and Observed Tracer Movement. Water Resources Res.(27(5):895-910).

Mackay, D. M., Freyberg, D. L., Roberts, P. V. and Cherry, J. A. (1986). A Natural Gradient Experiment on Solute Transport in a Sand Aquifer , Approach and Overview of Plume Movement. Water Resources Res.(22(13):2017-2029).

Mclaughlin, D., Reid, L. B., Li, S. And Hyman, J. (1993). A Stochastic Method for Characterization Groundwater Contamination. Groundwater, Vol. 31, No.2.

Mercer, J. W. And Faust, C. R. (1977). The Application of Finite-Element Techniques to Immiscible Flow in Porous Media. Pentech Press, Plymouth, England (1.21-1.57).

Mercer, J. W., Skipp, D. C. and Giffin, D. (1990). Basics of Pump-and-Treat Groundwater Remediation Technology. Robert S. Kerr Environmental Research Laboratory, U.S. Environmental Protection Agency, EPA-600/8-90/003.

Nelson, R. W. (1977). Evaluating the Environmental Consequences of Groundwater Contamination. An Overview of Contaminant Arrival Distributions as General Evaluation Requirements. Water Resources Res.(14:409-415).

Ogata, A. (1970). Theory of Dispersion in a Granular Medium. U.S. Geological Survey Professional Paper 411-I.

Ogata, A., Banks, R. B. (1961). A Solution of the Differential Equation of Longitudinal Dispersion in Porous Media. U.S. Geological Survey Professional Paper 411-A, U.S. Government Printing Office, Washington, DC.

Oztuna, B. (1993). Evaluation of an Industrial Sludge Discharge Site with Respect to Mobility of Contaminants. Dokuz Eylul University; Graduate school of natural and applied science.

Pinder, G. F. and Bredehoeft, J. D. (1968). Application of the Digital Computer for Aquifer Evaluation. Water Resources Res.(4:1069-1093).

Pinder, G. F. and Cooper, H. H. (1970). A Numerical Technique for Calculating the Transient Position of the Salt Water Front. Water Resources Res.(6(3):875-882).

Pinder, G. F. (1973). A Galerkin-Finite Element Simulation of Groundwater Contamination on Long Island, New York. Water Resources Res.(9:1657-1669).

Pinder, G. F. and Gray, W. G. (1977). Finite Element Simulation in Surface and Subsurface Hydrology. Academic Press, New York.

Prickett, T. A. and Lonnquist, C. G. (1971). Selected Digital Computer Techniques for Groundwater Resource Evaluation. Illinois Water Survey Bulletin 55, Illinois State Water Survey, Urbana.

Reddell, D. L. and Sunada, D. K. (1970). Numerical Simulation of Dispersion in Groundwater Aquifers. Hydrology Paper 41, Colorado State University, Fort Collins.

Remson, I., Hornberger, G. M. and Molz, F. J. (1971). Numerical Methods in Subsurface Hydrology. Wiley-Interscience, New York.

Rifai, H. S., Bedient, P. B., Wilson J. T. , Miller, K. M. and Armstrong, J. M. (1988). Biodegradation Modeling at a Jet Fuel Spill Site. ASCE J. Environmental Engr. Div. 114:1007-1019.

Roberts, P. V., Goltz, M. N. and Mackay, D. M. (1986). A Natural Gradient Experiment on Solute Transport in a Sand Aquifer , (4) Sorption of Organic Solutes and Its Influence on Mobility. Water Resources Res.(22(13):2047-2058).

Trescott, P. C., Pinder, G. F. and Larson, S. P. (1976). Finite Difference Model for Aquifer Simulation in Two Dimensions with Results of Numerical Experiments. U.S. Geological Survey Techniques of Water Resources Investigations, Book 7, Chapter C1, Reston, VA.

Wang, H. F. and Anderson, M. P. (1982). Introduction to Groundwater Modeling, Finite Difference and Finite Element Methods. W. H. Freeman, San Francisco.

Wilson, J. L. and Liu, J. (1999). Backward tracking to find the source of pollution, in Waste-management: From Risk to Remediation. R. Bhada, ECM Press, Albuquerque, NM, 181-199.

Wilson, J. L. and Neupauer, R. M. (1999). Adjoint method for obtaining backward-in-time location and travel time probabilities of a conservative groundwater contaminant. Water Resources Research. (35(11), 3389-3398).

Wrobel, L. C. and Brebbia, C. A. (1991). Water Pollution: Modeling, Measuring and Prediction. Computational Mechanics Publications. Southampton Boston.